Regulation of flowering time by DELLA proteins in *Arabidopsis thaliana*

Dissertation

der Mathematisch-Naturwissenschaftlichen Fakultät

der Eberhard Karls Universität Tübingen

zur Erlangung des Grades eines

Doktors der Naturwissenschaften

(Dr. rer. nat.)

vorgelegt von
Vinicius Costa Galvão
Rio de Janeiro, Brasilien

Tübingen
2013

Tag der mündlichen Qualifikation:	14.05.2013
Dekan:	Prof. Dr. Wolfgang Rosenstiel
1. Berichterstatter:	Prof. Dr. Detlef Weigel
2. Berichterstatter:	Prof. Dr. Gerd Jürgens

Table of contents

Summary

The transition to flowering in plants is under multifactorial regulation. Environmental cues, such as light, temperature, and endogenous factors are integrated by a complex genetic network to ensure the correct timing of this transition. In *Arabidopsis thaliana*, the plant hormone gibberellic acid (GA) is an important endogenous element involved in the regulation of flowering under inductive long-day (LD) and non-inductive short-day (SD) photoperiod. However, important questions regarding the spatial organization of the flowering response, and the relative contribution of factors involved in the GA-mediated control of flowering such as DELLA proteins require a more detailed analysis.

In the first part of this thesis I present evidences indicating that the abundance of DELLA proteins in leaves and/or the shoot meristem is an important factor affecting flowering transition, depending on the photoperiodic conditions. Under LD, GA controls flowering by promoting the expression of the florigen *FLOWERING LOCUS T* (*FT*) and *TWIN SISTER OF FT* (*TSF*) independently of *CONSTANS* (*CO*) and *GIGANTEA* (*GI*) in the phloem companion cells of the leaf vasculature. In addition, GA positively regulates the expression of several *SQUAMOSA PROMOTER BINDING PROTEIN-LIKE* (*SPL*) transcription factors in both leaf vasculature and shoot meristem, which are themselves promoting flowering. In contrast to the spatial separation observed in LD, the control of flowering time by GA is restricted to the shoot meristem in SD. The data presented in chapter 2 integrate the well-known effect of GA on the expression of *SUPPRESSOR OF OVEREXPRESSION OF CONSTANS* (*SOC1*) and *FRUITFUL* (*FUL*) and the recently discovered age flowering pathway, which ensures flowering under SD conditions. Under SD, GA controls flowering through SPL-mediated control of *SOC1* and *FUL* expression at the shoot meristem. In agreement with a recent GA signaling model, my data suggest that in addition to the transcriptional control of *SPL* genes, GA may regulate flowering through direct SPL-DELLA interaction.

Finally, I describe a new method to map mutations in *Arabidopsis thaliana*, which relies on high coverage sequencing of polymorphic regions captured with specific probes. Using this method we were able to accurately estimate the confidence interval harboring an unknown causal mutation isolated in a suppressor screen of the strong flowering promoting gene *FT*. Interestingly, we performed mapping-by-sequencing without the use of a reference genome using only syntheny information between *Arabidopsis* and *Brassica rapa*. This method represents an interesting alternative for mapping mutations in species without a reference genome or genetic map.

Zusammenfassung

Die Bestimmung des Blühzeitpunkts in Pflanzen wird von einer Vielzahl Faktoren reguliert Umweltreize wie Licht, Temperatur und endogene Faktoren werden mit Hilfe eines komplexen genetischen Netzwerkes verarbeitet, um den richtigen Zeitpunkt dieses Überganges sicherzustellen. Das Pflanzenhormon Gibberellinsäure (GA) ist ein wichtiger endogener Faktor in *Arabidopsis thaliana*, der an der Regulation des Blühens unter induktiver Langtag- (LD) und nicht-induktiver Kurztag- (SD) Photoperiode beteiligt ist. Es ist jedoch eine detailliertere Analyse erforderlich um wichtige Fragen bezüglich der räumlichen Organisation der Blühantwort und des Beitrages anderer Faktoren der GA-vermittelten Kontrolle des Blühens wie den DELLA Proteinen zu beantworten.
Im ersten Teil dieser Arbeit präsentiere ich Hinweise darauf, dass die Menge der DELLA-Proteine in den Blättern und / oder dem Sprossmeristem ein wichtiger Faktor ist, der den Übergang zum Blühen in Abhängigkeit von den photoperiodische Bedingungen beeinflusst. Unter LD-Bedingungen, steuert GA das Blühen indem es die Expression des Florigens *FLOWERING LOCUS T* (*FT*) und *TWIN SISTER OF FT* (*TSF*) unabhängig von *CONSTANS* (*CO*) und *GIGANTEA* (*GI*) in den Geleitzellen der Blattgefäße fördert. Zudem reguliert GA auf positive Weise die Expression mehrerer *SQUAMOSA PROMOTER BINDING PROTEIN-LIKE* (*SPL*) Transkriptionsfaktoren, die selbst das Blühen induzieren, sowohl in den Blattgefäßen als auch im Sprossmeristem. Im Gegensatz zur im Langtag beobachteten räumlichen Trennung, ist die Steuerung des Blühzeitpunktes durch GA im Kurztag auf das Sprossmeristem beschränkt. Die in Kapitel 2 vorgestellten Daten verflechten den bekannten Effekt von GA auf die Expression von *SUPPRESSOR OF OVEREXPRESSION OF CONSTANS* (*SOC1*) und *FRUITFUL* (*FUL*) sowie den jüngst entdeckten altersabhängigen Blühregulationsweg, der das Blühen unter nicht-induktiven SD-Bedingungen gewährleistet. Im Kurztag steuert GA das Blühen durch SPL-vermittelten Kontrolle der *SOC1* und *FUL* Expression im Sprossmeristem. In Übereinstimmung mit dem jüngsten Modell zur GA-Signalweiterleitung legen meine Daten nahe, dass zusätzlich zur Transkriptionskontrolle der *SPL*-Gene GA das Blühen auch durch direkte SPL-DELLA Wechselwirkung regulieren kann. Zuletzt beschreibe ich eine neue Methode zur Kartierung von Mutationen in *Arabidopsis thaliana*, die darauf beruht, dass polymorphe Regionen mittels hoher Sequenziertiefe und durch spezifischen Sonden erfasst werden. Mit dieser Methode konnten wir sehr genau das Konfidenzintervall abschätzen, das eine unbekannte kausale Mutation beherbergt, die in einem Suppressor-Screen des starken blüh-induzierenden Gens *FT* isoliert wurde. Interessanterweise führten wir diese Kartierung der Sequenzen ohne die Verwendung eines Referenz-Genoms durch, nur mit Syntenie- Informationen bezüglich *Arabidopsis* und *Brassica rapa*. Diese Methode stellt eine interessante Alternative zur Kartierung von Mutationen in Spezies ohne Referenz-Genom oder genetische Karte dar.

Publications and Copyright notes

This cumulative doctoral thesis consists of the following publications:

Publication 1

Vinicius C. Galvão, Daniel Horrer, Frank Küttner, Markus Schmid

Spatial control of flowering by DELLA proteins in Arabidopsis thaliana.

Development (2012), vol. 139: 4072-4082.

Reproduced/adapted with permission of Development: dev.biologists.org. Permission sent via e-mail by Sue Chamberlain (sue@biologists.com).

Publication 2

Sha Yu*, Vinicius C. Galvão*, Yan-Chun Zhang, Daniel Horrer, Tian-Qi Zhang, Yan-Hong Hao, Yu-Qi Feng, Shui Wang, Markus Schmid, Jia-Wei Wang

Gibberellin regulates the Arabidopsis floral transition through miR156-targeted SQUAMOSA PROMOTER BINDING-LIKE transcription factors.

Plant Cell (2012), vol. 24 (8): 3320-3332.

"ASPB grants to authors whose work has been published in The Plant Cell the royalty-free right to reuse images, portions of an article, or full articles in any book, book chapter, or journal article of which the author is the author or editor".

Copyright American Society of Plant Biologists.

www.plantcell.org

Publication 3

Vinicius C. Galvão*, Karl J.V. Nordström*, Christa Lanz, Patric Sulz, Johannes Mathieu, David Posé, Markus Schmid, Detlef Weigel, Korbinian Schneeberger

Synteny-based mapping-by-sequencing enabled by targeted enrichment.

The Plant Journal (2012), vol. 71: 517-526.

Reprint with permission from The Plant Journal, Wiley Online Library through RightsLink Copyright Clearance Center. http://onlinelibrary.wiley.com

License number: 3062640188266

* denotes equal contribution

Introduction

Flowering transition in plants

Plants life can be separated into vegetative and reproductive phases. Essentially, these phases reflect the molecular identity of meristems, which are devoted to produce vegetative (leaves) or reproductive (flowers) organs. Changes in shoot meristem identity occur during the flowering transition and involve an intricate genetic network. The so called flower identity genes, such as *APETALA1* (*AP1*) and *LEAFY* (*LFY*) are activated in early stages of flowering transition to establish flower meristems. In annual and biannual plants, which experience a single reproductive transition during the life cycle, this usually is an irreversible and determinant decision for the species survival. Several studies carried out over the last decades have identified discrete but overlapping genetic programs ensuring the correct timing for reproduction. Not surprisingly, environmental cues play a critical role in the flowering time determination. Among them, light conditions (intensity, quality and daylength) and temperature (as seasonal and ambient temperature) are the most significant environmental factors involved in the control of flowering. In addition, endogenous factors as the plant hormone gibberellic acid, sugars and genes in the so-called autonomous pathway are also critical for regulating the transition to flowering.

Regulation of flowering time by light

In many plant species the transition to the reproductive stage can be greatly accelerated depending on the duration of exposure to light, or photoperiod. The photoperiod is a predictable environmental factor, which reflects seasonal changes in specific latitudes on the globe. Therefore, the flowering behavior of different species normally correlates with their geographic distribution and life history. Regarding the

photoperiodic control of flowering, plants can be separated as long-day (LD), short-day (SD) and day-neutral plants. LD plants flower when the light exposure exceeds a critical length, while SD plants bolt when plants experience shorter light exposure. Day neutral plants flower regardless of photoperiod (Thomas and Vince-Prue, 1997).

Experiments conducted in the first half of the 20th century demonstrated that light control of flowering is spatially separated in leaves, where light is perceived and translated in a molecular signal, and shoot apical meristem, where flowering is triggered and reproductive structures are produced (Knott, 1934; Naylor, 1941; Thomas and Vince-Prue, 1997). This observation led to the 'florigen hypothesis', which proposes the existence of a signal molecule produced in leaves and transported to the vegetative shoot meristem to trigger flowering (Chailakhian, 1936a; Chailakhian, 1936b).

Genetic screens identified mutants with impaired photoperiodic response in *Arabidopsis* (Redei, 1962; Koornneef et al., 1991). Due to technical limitations the molecular characterization of these mutants was not possible and the florigen identity remained obscure for decades until the advent of modern genetics and molecular biology. Simultaneously, two independent groups identified a small globular protein with a strong effect on flowering (Kardailsky et al., 1999; Kobayashi et al., 1999). *FLOWERING LOCUS T* (*FT*) encodes a 20 kDa protein similar to a phosphatidylethanolamine binding protein (PEBP) (Kardailsky et al., 1999; Kobayashi et al., 1999). So far, the importance of this domain for FT function has not been determined. Nevertheless, the role of FT in inducing flowering has been shown in several species (Kojima et al., 2002; Bohlenius et al., 2006; Lifschitz et al., 2006; Tamaki et al., 2007; Blackman et al., 2010; Pin et al., 2010; Hecht et al., 2011; Hsu et al., 2011; Navarro et al., 2011).

Constitutive expression of *FT* in *Arabidopsis*, strongly promotes flowering under both SD and LD photoperiod. In contrast, *ft* loss-of-function mutant is insensitive to

photoperiod and flowers at about the same time than wild type plants in SD (Redei, 1962; Kardailsky et al., 1999; Kobayashi et al., 1999; Wigge et al., 2005). Evidences that FT functions as a florigen come from several independent lines of observation. *FT* is specifically expressed in phloem companion cells in response to long-day conditions, while its expression at the shoot apical meristem is not observed (Takada and Goto, 2003; Wigge et al., 2005; Corbesier et al., 2007; Jaeger and Wigge, 2007). In addition, expression of immobilized but otherwise functional versions of the FT protein in phloem companion cells failed to rescue the late flowering *ft-10* mutant (Corbesier et al., 2007; Jaeger and Wigge, 2007; Mathieu et al., 2007). In contrast, its expression using a meristem specific promoter strongly induced the transition to flowering. Furthermore, the expression of the floral meristem identity gene *AP1* is delayed in *ft* mutant background under LD (Wigge et al., 2005). Together, these results suggest that FT production in leaves and transport through the vasculature to the shoot apical meristem is necessary for the transition to flowering in response to permissive photoperiod.

As proposed by the florigen hypothesis, the expression of *FT* in leaf vasculature and activity at the shoot meristem implies movement of either FT protein or RNA. To address this question, Mathieu and colleagues expressed an artificial microRNA targeting the *FT* RNA (amiR-FT) in both vegetative shoot meristem and leaf vasculature. While amiR-FT failed to repress flowering when expressed at the shoot apical meristem, expression in the vasculature resulted in a strong delay in flowering (Mathieu et al., 2007). Supporting this indirect evidence, FT protein has been found in the phloem of different species by mass spectrometry (Giavalisco et al., 2006; Lin et al., 2007; Aki et al., 2008). Recently, the membrane protein FT-INTERACTING PROTEIN 1 (FTIP1) has been proposed to directly bind FT in companion cells to assist its movement to the phloem sieve elements via the plasmodesmata (Liu et al., 2012). Contrasting the well-

supported movement of the FT protein, recent reports have shown *FT* RNA movement from leaves to the shoot meristem but evidences supporting its contribution to flowering control are not conclusive (Li et al., 2009; Lu et al., 2012).

After moving to the shoot meristem, FT interacts with the bZIP transcription factor FD to activate the expression of floral integrator genes, such as *LFY*, *SUPPRESSOR OF OVEREXPRESSION OF CONSTANS* (*SOC1*), *FRUITFUL* (*FUL*) and *AP1*, to convert the vegetative meristem to an inflorescence meristem (Samach et al., 2000; Schmid et al., 2003; Abe et al., 2005; Teper-Bamnolker and Samach, 2005; Wigge et al., 2005; Searle et al., 2006; Corbesier et al., 2007; Melzer et al., 2008; Torti et al., 2012). Experiments performed using the FT homolog in rice (Hd3a) demonstrated that Hd3a and OsFD form a ternary complex with 14-3-3 protein. In this model, after translocation through the phloem sap to the shoot meristem, Hd3a initially interacts with 14-3-3 in the cytoplasm and move to the nucleus where it interacts with OsFD in a ternary complex to activate the expression of flower meristem identity genes (Taoka et al., 2011).

Control of FT expression in response to photoperiod

Arabidopsis is a facultative LD plant, meaning that it flowers faster under this condition but still flowers under non-inductive SD photoperiod, albeit much later. Several mutants with impaired flowering response to long exposure to light have been isolated in genetic screens. Mutants like *constans* (*co*), *ft*, *gigantea* (*gi*) and *cryptocrome2* (*cry2*) are photoperiod-insensitive, and flower late under LD but at about the same time than wild type plants growing under SD (Koornneef et al., 1991; Araki and Komeda, 1993; Putterill et al., 1995; Fowler et al., 1999; Guo et al., 1999; Kardailsky et al., 1999; Kobayashi et al., 1999).

Genetic analyses have placed *CO* upstream of *FT* in a common pathway to perceive the long-day photoperiod (Kardailsky et al., 1999; Kobayashi et al., 1999). *FT* is expressed in a circadian fashion in the vasculature under LD, reaching the highest levels in the end of the light phase (Suarez-Lopez et al., 2001). In accordance with the mutant phenotype, *FT* transcripts remain at very low levels both during the day and night under SD photoperiod (Corbesier et al., 2007). Interestingly, its expression is drastically reduced in *co* background under LD, while *CO* overexpression accelerates flowering more strongly in the presence of a functional FT protein (Kardailsky et al., 1999; Kobayashi et al., 1999; Onouchi et al., 2000). In addition, microarray experiments performed using *co* mutants further supported *FT* as a target of CO under inductive photoperiod (Wigge et al., 2005). Together these results strongly indicate that CO controls *FT* expression in response to day length.

In contrast to *FT*, *CO* RNA oscillates under circadian control in a very similar way under both LD and SD photoperiod (Suarez-Lopez et al., 2001). The observation that *CO* mRNA peaks during the night in SD, and that this does not result in increased *FT* level suggested a possible light-dependent post-transcriptional control of CO protein. Indeed, transgenic plants expressing *35S:GFP:CO* presented a low fluorescence signal in darkness, whereas the exposure to light strongly induced CO accumulation (Valverde et al., 2004). Similarly, diurnal changes in CO protein abundance could only be observed in presence of light under LD, coinciding with its increased RNA level. Moreover, the treatment of *35S:GFP:CO* plants with proteasome inhibitor caused the accumulation of CO during the night, suggesting that its degradation via proteasome is necessary to reduce the protein abundance (Valverde et al., 2004). Interestingly, two different studies demonstrated that photoreceptors are important for CO accumulation and consequently *FT* expression depending on different light qualities (Yanovsky and Kay, 2002; Valverde

et al., 2004). The exposure of plants to blue light normally increases CO stability in a CRY-dependent manner, while red light reduces its stability in a PHY-dependent manner (Valverde et al., 2004). Accordingly, *cry1* and *cry2* mutants flower late and *phyB* mutant normally flower early in LD (Guo et al., 1999; Mockler et al., 1999).

Different proteins control CO stability in response to light, such as CONSTITUTIVE PHOTOMORPHOGENIC (COP1), SUPPRESSOR OF PHYA-105-1 (SPA) and FLAVIN-BINDING FACTOR 1, KELCH REPEAT, F-BOX PROTEIN (FKF1). The effect of COP1 on flowering is known for a long time. *cop1* mutants flower earlier under SD photoperiod or even when grown in complete darkness (McNellis et al., 1994). Interestingly, this phenotype is drastically suppressed in *co* background, suggesting that CO is mediating the flowering induction (McNellis et al., 1994; Jang et al., 2008; Liu et al., 2008).

COP1 encodes an E3 ubiquitin ligase with strong effects on several light-regulated mechanisms (Lau and Deng, 2012). Notably, COP1 acts as a negative regulator of several transcription factors by targeting them for degradation, with light being required to revoke its activity. Consistent with this finding, *cop1* mutants, when grown in darkness, show many characteristics typically found only in light-grown seedlings (Deng et al., 1991). Interestingly, the downstream events of most plant photoreceptors identified so far converge on COP1-mediated signaling. Despite this critical function, the mechanisms connecting light perception and COP1 signal transduction are still poorly understood. A known mechanism involves the activation of photoreceptors by light and further COP1 export from the nucleus to the cytoplasm, avoiding targeting nuclear-localized transcription factors to degradation (Vonarnim and Deng, 1994).

Two recent reports described the direct CO-COP1 interaction in plant cells to control CO abundance (Jang et al., 2008; Liu et al., 2008). These studies demonstrate

that *COP1* acts upstream of *CO* and downstream of *CRY1* and *CRY2*. The authors postulate that in darkness COP1 is localized in the nucleus, targeting CO for degradation after ubiquitination. In contrast, during the day blue light activates CRY1/2, which in turn impairs the ubiquitin ligase activity of COP1 (Jang et al., 2008; Liu et al., 2008). SPA1-4 proteins have also been shown to directly regulate COP1 ubiquitin ligase activity and CO abundance (Laubinger et al., 2006). The molecular analysis of these proteins indicates that SPA and COP1 are part of the same multimeric E3 ubiquitin ligase complex negatively regulating light signaling. Accordingly, the quadruple *spa1-4* mutant displays a similar phenotype than the *cop1* single mutant, including early flowering under SD due to increased CO accumulation (Laubinger et al., 2004; Laubinger et al., 2006). Therefore, both SPA and COP1 are necessary for the CO degradation under SD photoperiod (Laubinger et al., 2006). Until recently, the mechanism involved in the control of COP1-SPA ubiquitin ligase activity remained largely unknown. However, recent publications indicate that CRY1 and CRY2 directly bind to SPA proteins in a blue-light dependent manner to block the SPA-COP1 ubiquitin ligase activity (Lian et al., 2011; Liu et al., 2011; Zuo et al., 2011). Interestingly, CRY1 and CRY2 act differently to regulate COP1 activity. Blue light-activated CRY1 interact strongly with SPA1 and disrupt the interaction with COP1 (Lian et al., 2011; Liu et al., 2011). In contrast, CRY2-SPA1 interaction further promotes the interaction with COP1, which is believed to suppress the ubiquitin ligase activity of SPA1-COP1 complex (Zuo et al., 2011).

In contrast to CRY1 and CRY2, which promotes flowering after CO stabilization, the red light receptor PHYTOCHROME B (PHYB) acts to repress flowering presumably though CO destabilization during early exposure to light in morning hours of LD. *phyB* mutants fail to degrade CO protein in light when overexpressed from a constitutive promoter (Valverde et al., 2004). However, the red light signaling apparently works

independently of COP1 ubiquitin ligase activity (Jang et al., 2008). To date, the mechanism underlying PHYB signaling in photoperiodic flowering transition remain largely unknown.

The age flowering pathway

Despite the plasticity of vegetative growth, some traits develop in a stereotypic order, allowing the separation in juvenile and adult vegetative phase. In *Arabidopsis*, the most significant morphological differences between juvenile and adult vegetative phase occur in leaf shape, size and epidermal cell identity (Telfer et al., 1997; Kerstetter and Poethig, 1998). During the juvenile vegetative stage leaves are normally smaller, presenting reduced leaf serration and no trichomes on the abaxial side. This contrast with leaves produced at later stages, which are normally elongated, with pronounced serration and numerous trichomes on the abaxial side (Telfer et al., 1997; Poethig, 2003).

The juvenile-to-adult phase transition is strongly affected by the activity of miR156 and SQUAMOSA PROMOTER BINDING PROTEIN LIKE (SPL) proteins (Wang et al., 2009; Wu et al., 2009). *SPL* genes encode a ubiquitous family of transcription factors first identified in *Antirrhinum majus* (Klein et al., 1996*)*. Members of this family share a highly conserved DNA binding domain, which recognizes and binds to GTAC motifs in gene promoters (Klein et al., 1996; Wang et al., 2009; Yamaguchi et al., 2009). In *Arabidopsis* these proteins control several processes, such as transition to flowering, shoot maturation and leaf shape (Cardon et al., 1997; Wang et al., 2008; Shikata et al., 2009). *MIR156* constitutes a family of highly conserved microRNAs encoded by 8 loci in *Arabidopsis* (Rhoades et al., 2002; Todesco et al., 2010). After processing, mature miR156 can repress 10 of the 16 *SPL* either by transcripts cleavage and/or by translational inhibition (Gandikota et al., 2007; Guo et al., 2008).

MIR156 is highly expressed in early stages of vegetative development, and decrease gradually as plants age (Wang et al., 2009; Wu et al., 2009). Conversely, *SPL* transcript levels are low during early vegetative stages and increase during development. Molecular analyses of mutants and overexpression lines have placed *SPL* genes genetically downstream of *MIR156* (Wu and Poethig, 2006; Wang et al., 2009; Wu et al., 2009). Therefore, miR156 acts during early vegetative phase downregulating *SPL* levels. In agreement with this idea, plants overexpressing of *MIR156* and *spl9 spl15* double mutant have an extended juvenile vegetative phase. In contrast, the expression of miR156-resistent *SPL9* under its own promoter induced the premature appearance of adult traits (Wang et al., 2008; Wang et al., 2009; Wu et al., 2009).

In addition to the control of juvenile and adult traits, the SPL proteins also contribute to the transition to flowering (Cardon et al., 1997; Wang et al., 2009; Yamaguchi et al., 2009). Constitutive expression of a miR156 target mimicry (MIM156), which sequesters mature miR156 such that it is no longer available to target repression, caused precocious flowering in SD and LD, presumably due to an increase in *SPL* transcript levels (Wu et al., 2009; Todesco et al., 2010). Accordingly, the expression of miR156-resistent *SPLs* (*rSPL*) consistently accelerated the induction of flowering (Wang et al., 2008; Wang et al., 2009; Yamaguchi et al., 2009). Chromatin-immunoprecipitation (ChIP) experiments show that SPL proteins can directly bind to important flowering genes, such as the floral integrator genes *LFY*, *AP1*, *SOC1*, *FUL*, and also *MIR172* (Wang et al., 2009; Wu et al., 2009; Yamaguchi et al., 2009). More recently, SPL3 was shown to directly regulate *FT* expression in leaves in response to ambient temperature (Kim et al., 2012). Based on these results, an endogenous microRNA pathway, which ensures flowering under non-inductive SD photoperiod has been proposed (Wang et al., 2009). In this model, *SPL* levels gradually increase in response to the age-dependent

reduction of miR156. As a consequence, the expression of flower identity genes *AP1*, *LFY*, *FUL* and *SOC1* is increased at the shoot meristem to promote flowering (Wang et al., 2009).

Interestingly, miR172 accumulates in a complementary pattern to *MIR156*, low during juvenile phase and higher in adult stage (Aukerman and Sakai, 2003; Wu et al., 2009). *MIR172* was identified in an activation tagging screen as a very early flowering mutant (Aukerman and Sakai, 2003). This microRNA targets a class of flowering repressors, known as AP2-like family, encoded by 6 loci in Arabidopsis. This transcription factor family comprises *APETALA2* (*AP2*), *TARGET OF EAT* (*TOE1, TOE2* and *TOE3*), *SCHLAFMüTZE* (*SMZ*) and *SCHNARCHZAPFEN* (*SNZ*). miR172 reduces AP2-like members activity both by transcript degradation and translational inhibition (Aukerman and Sakai, 2003; Chen, 2004; Schwab et al., 2005). ChIP-chip experiments indicate that SMZ directly binds to several flowering time genes, including *FT*. In agreement, the expression of a miR172-resistent *SMZ* (*rSMZ*) strongly reduced *FT* expression and delayed flowering when expressed in the leaf vasculature (Mathieu et al., 2009). The role of the miR172 / AP2-like module in the regulation of flowering was further confirmed by genetic analysis of an AP2-like *smz snz ap2 toe1 toe2 toe3* hexuple mutant, which phenocopies *MIR172* overexpressing lines (Mathieu et al., 2009; Yant et al., 2010). Interestingly, AP2-like genes also regulate juvenile traits in *Arabidopsis* and maize (Moose and Sisco, 1994; Moose and Sisco, 1995; Moose and Sisco, 1996; Lauter et al., 2005; Wu et al., 2009).

Control of flowering by gibberellic acid

GA signaling pathway

The plant hormone gibberellic acid (GAs) has a pronounced impact on plant development. First identified in rice cultures infected with the fungus *Gibberella fujikuroi*, GA has been shown to play an important role in diverse processes such as seed germination, internode elongation, fruit formation, flower development and control of flowering time (Davies, 2004). For example, *Arabidopsis* plants treated with GA grow taller, display a light green color, flower earlier and produce siliques with fewer seeds than wild type plants (Davies, 2004). This broad spectrum of action has transformed GA into an important biotechnological tool both for improving field productivity and for industrial application.

Gibberellins encompass dozens of chemically related compounds, of which only a minor proportion, such as GA_1, GA_3, GA_4 and GA_7, are biologically active (Olszewski et al., 2002). GA is perceived by the GA receptor GIBBERELLIN INSENSITIVE DWARF1 (GID1). Structural analyses have highlighted conformation changes of GID1 after binding to bioactive GA as a key event in GA signaling (Murase et al., 2008; Shimada et al., 2008). *Arabidopsis* harbors 3 highly redundant GA receptor genes, *GID1a-c* (Ueguchi-Tanaka et al., 2005; Griffiths et al., 2006; Nakajima et al., 2006; Willige et al., 2007*)*. Recent studies have demonstrated that loss-of-function mutations for individual *GID1* genes have only a minor or no effect at all on plant development (Griffiths et al., 2006; Willige et al., 2007). However, the triple mutant displays drastic typical GA-related phenotypes, such as dwarfism, dark-green color, impaired seed germination and delayed flowering time. These plants are completely insensitive to exogenous bioactive GA treatment, confirming the importance of GID1 in GA perception (Griffiths et al., 2006; Willige et al., 2007).

The GA-induced conformational change in GID1a-c receptors constitutes the basis of the GA signaling. After binding, the bioactive GA molecule is locked in a pocket of

GID1 through its N-terminal region (Murase et al., 2008). The biological significance of the N-terminal extension switch covering the bioactive GA molecule relies on the interaction with a class of repressors, the DELLA proteins (Griffiths et al., 2006). Binding to bioactive GA creates a hydrophobic surface on the GID1-GA complex, which facilitates the interaction with the DELLA proteins. In turn, this interaction further stabilizes the GID1-GA-DELLA complex, and promotes its interaction with the F-box protein of the ubiquitin E3 ligase SCF complex. Therefore, GA binding to GID1 ultimately lead to DELLA proteins ubiquitination and degradation via proteasome (McGinnis et al., 2003; Sasaki et al., 2003; Dill et al., 2004; Fu et al., 2004).

In *Arabidopsis*, DELLA proteins were first identified in a genetic screen as a GA insensitive mutant (*gai-1*) (Koornneef et al., 1985; Silverstone et al., 1997). The gain-of-function *gai-1* mutant encodes a functional protein with a 17 amino acids deletion that removes a conserved 5 amino acids motif (DELLA) in the N-terminal region (Peng and Harberd, 1993; Peng et al., 1997). Other GA-insensitive alleles identified in wheat (*Rht*), rice (*SLR*) and maize (*D8*) also encode defective proteins lacking the DELLA domain (Fujioka et al., 1988; Ikeda et al., 2001; Pearce et al., 2011). In contrast to other species harboring a single copy gene, *Arabidopsis* encode 5 functionally redundant DELLA proteins: *GA INSENSITIVE1* (*GAI*), *REPRESSOR OF ga1-3* (*RGA*) and *RGA-LIKE1, -2 and -3* (*RGL1, -2, -3*) (Bolle, 2004). The cloning and characterization of *gai-1* and other GA-insensitive DELLA mutant indicated that the DELLA motif is critical for the interaction with the GID1 receptors and DELLA degradation in the presence of GA (Peng and Harberd, 1993; Peng et al., 1997; Dill et al., 2001; Willige et al., 2007). High GA levels induce the rapid degradation of DELLA proteins via the ubiquitin-proteasome pathway, while GA-deficient mutants present increased levels of DELLA proteins (Dill et al., 2001; Silverstone et al., 2001; Griffiths et al., 2006; Willige et al., 2007). GA-insensitive DELLA

mutants resemble to some extent dark green and dwarfed gibberellin-deficient mutants but differ from them in some aspects. First, they are genetically semi-dominant; second, they cannot be recovered by exogenous GA application; third, bioactive GA level is increased in these mutants (Koornneef et al., 1985; Dill et al., 2001). Therefore, proteins lacking the DELLA domain are insensitive to GA because they cannot interact with GID1 receptor even in the presence of high GA concentration. Together, these results suggest that the accumulation of DELLA proteins in response to GA levels mediates the biological response to this hormone.

Transcriptome experiments in *Arabidopsis* show that GA regulates a large number of genes involved in a wide range of biological processes (Willige et al., 2007; Zentella et al., 2007). Nevertheless, the analysis of the primary protein sequence indicates that the DELLA proteins do not harbor a canonical DNA binding domain typical of transcription factors (Bolle, 2004). In agreement with this data, ChIP experiments failed to consistently identify binding sites, even though binding to some GA-related targets was observed (Zentella et al., 2007). These results indicate that DELLA proteins do not act as direct transcriptional regulators but instead regulate gene expression indirectly as co-factors. A groundbreaking observation on DELLA function came from the study of *PHYTOCHROME INTERACTING FACTOR* (*PIF*) during photomorphogenesis. Two independent studies described the direct interaction between DELLA proteins and PIF transcription factors (de Lucas et al., 2008; Feng et al., 2008). Interestingly, EMSA assay demonstrated that binding to DELLA proteins impaired PIF4 capacity to binding DNA, therefore blocking its activity (de Lucas et al., 2008). Based on these findings it has been proposed that DELLA proteins regulate effector transcription factors through direct interaction (Daviere et al., 2008). In support of this model, interactions between DELLA

proteins and other transcription factors have been recently reported (Hou et al., 2010; Zhang et al., 2011; Hong et al., 2012).

GA regulation of flowering time

Early experiments performed by Anton Lang in 1956 for the first time demonstrated the effect of GA on flowering time (Lang, 1956a; Lang, 1957). Treatment of plants growing under otherwise non-inductive conditions with exogenous GA resulted in a variable flowering response depending on the species. For example, *Hyoscyamus niger* and others promptly responded to GA application, in contrast to the mild induction observed in *Daucus carota*. Flowering was not affected in response to hormone treatment in soybean growing under non-inductive LD photoperiod (Lang, 1956a; Lang, 1956b; Lang, 1957).

Most of the actual understanding of GA controlling flowering comes from mutants isolated in genetic screens in *Arabidopsis* (Koornneef and van der Veen, 1980; Koornneef et al., 1985; Jacobsen and Olszewski, 1993; Silverstone et al., 1997). The recessive loss-of-function *ga1-3* mutant impairs the first step of the GA biosynthesis pathway (Sun and Kamiya, 1994). Due to reduced levels of bioactive GA (Silverstone et al., 2001), *ga1-3* mutant display a pleiotropic phenotype, including dark green color, dwarfism and compromised flower development. Strikingly, *ga1-3* mutant completely fail to flower under SD, indicating that GA has a critical role in the induction of flowering under non-inductive photoperiodic conditions (Wilson et al., 1992). In addition, GA treatment and loss-of-function DELLA mutations strongly promoted flowering under SD conditions (Wilson et al., 1992; Silverstone et al., 1997; Cheng et al., 2004).

In contrast to the strong effect under SD, the *ga1-3* mutant displayed only a mild effect on flowering under inductive photoperiod (Wilson et al., 1992). This phenotype was

initially taken as evidence that GA does not regulate flowering under LD. However, there are several findings that suggest that GA might contribute to floral induction under LD after all. For example, the mutant *spindly* (*spy*), which is insensitive to the GA biosynthesis inhibitor paclobutrazol, flowers early under LD conditions (Jacobsen and Olszewski, 1993). The *SPY* gene encodes an O-linked N-acetylglucosamine transferase thought to regulate DELLA function through post-translational modification (Jacobsen and Olszewski, 1993; Jacobsen et al., 1996). The *spy* mutant is partially epistatic to strong GA biosynthesis mutants and dominant DELLA mutants despite the high levels of DELLA proteins found in the latter (Jacobsen and Olszewski, 1993; Silverstone et al., 2001; Silverstone et al., 2007). Moreover, the recent isolation and characterization of the triple *gid1a-c* mutant in Col-0 background further suggested a possible role of GA in the control of flowering time under LD conditions. *gid1a-c* mutant plants displayed a striking irreversible late flowering (or not flowering at all) phenotype in LD even after GA application (Griffiths et al., 2006; Willige et al., 2007). The reason for the different flowering behavior observed in *ga1-3* and *gid1a-c* backgrounds is still unclear.

Despite the detailed characterization of GA biosynthesis and signaling mutants over the last two decades, the molecular basis of the GA control of flowering remains unclear. The first gene linking GA and flowering was the floral meristem identity gene *LEAFY* (*LFY*). Induction of *LFY* expression is an important event in the transition to flowering and correct flower meristem determination (Weigel et al., 1992; Blazquez et al., 1997; Hempel et al., 1997; He et al., 2000; Benlloch et al., 2011). Plants growing under SD have a slow gradual increase in *LFY* expression compared to the faster increase under LD. The application of GA enhanced the gradual leaf *LFY* expression under SD, while GUS staining was consistently reduced in *pLFY:GUS* in *ga1-3* background (Blazquez et al., 1997; Blazquez et al., 1998). Accordingly, constitutive *LFY* expression is

sufficient to restore flowering in *ga1-3* under SD (Blazquez et al., 1998). Interestingly, ChIP-seq experiments have recently shown that LFY binds directly to some GA biosynthesis and signaling genes (Moyroud et al., 2011).

Promoter deletions identified a small GA-responsive *cis*-element in the *LFY* promoter, later confirmed as a conserved MYB transcription factor binding site (Blazquez and Weigel, 2000; Gocal et al., 2001). Interestingly, GA induces the expression of some *MYB* genes, called *GAMYB*, in *Hordeum vulgare* (Gubler et al., 1995). Likewise, the expression of *MYB33* in *Arabidopsis* was strongly promoted at the shoot meristem after GA_4 treatment under SD, similar to the induction observed for *GAMYB* in *Lolium temulentum* during flowering transition (Gocal et al., 1999; Gocal et al., 2001). *GAMYB* genes are direct targets of the miR159 family in *Arabidopsis* (Rhoades et al., 2002). Achard and colleagues have shown that GA regulates miR159 levels and suggested a possible role in regulating *GAMYB* and *LFY* to control flowering under SD (Achard et al., 2004). Together, these results indicate that *LFY* controls flowering time under SD due to the coordinated activity of miR159 and *GAMYB* in response to GA.

SOC1 has also been shown to play a role in the GA-mediated induction of flowering. Under SD, GA application strongly induces *SOC1* expression and its overexpression rescues the flowering phenotype of *ga1-3* mutant. Furthermore, the *soc1* loss-of-function mutant shows reduced sensitivity to GA application (Moon et al., 2003; Achard et al., 2004). A recent study has shown that SOC1 is binding directly to *SPL3*, *SPL4* and *SPL5* promoters and is necessary for their induction in response to GA (Jung et al., 2011). Nevertheless, how exactly GA regulates *SOC1* expression has not been solved yet. Interestingly, SPL proteins have been proposed to integrate the age flowering pathway, which ensure flowering under non-inductive condition (Wang et al., 2009;

Yamaguchi et al., 2009). This interaction adds a new player in the complex mechanism underlying the GA induction of flower under SD condition.

Aim of this work

This PhD is composed of 3 chapters addressing the following questions:

1. Elucidation the spatial separation of the GA-mediated control of flowering under different photoperiodic conditions.

2. Analysis of the contribution of individual DELLA protein during flowering transition and identification of genes involved in the regulation of flowering transition.

3. Identification new DELLA proteins targets using yeast two-hybrid screen.

4. Isolate and map an unknown mutation using a new marker targeted enrichment method.

Chapter 1

The work summarized in this chapter was originally published in:

Spatial control of flowering by DELLA proteins in *Arabidopsis thaliana.*
Vinicius C. Galvão, Daniel Horrer, Frank Küttner, Markus Schmid
Development (2012), 139: 4072-4082.

Synopsis

The hormone GA contributes to the regulation of flowering in many plant species. In *Arabidopsis*, the characterization of the strong *ga1-3* mutant, which is impaired in the first committed step of GA biosynthesis and present very low bioactive GA level, has indicated that GA affects flowering under non-inductive SD photoperiod. Based on this finding, most early studies focused on genes involved in the regulation of flowering under this condition, such as *LFY, SOC1, GAMYB* and *MIR159* (Blazquez et al., 1997; Blazquez et al., 1998; Blazquez and Weigel, 2000; Moon et al., 2003; Achard et al., 2004). Nevertheless, the isolation of new GA signaling mutant alleles, such as the early flowering *spy* and the late (or non-flowering) GA receptor triple *gid1a-c* mutant, consistently indicated that GA is also important for flowering under LD condition (Jacobsen and Olszewski, 1993; Griffiths et al., 2006; Willige et al., 2007). The first molecular evidence indicating that GA affects an important gene regulating flowering time under inductive LD photoperiod came from SD to LD shifting experiments using the *ga1-3* mutant. Hisamatsu and King showed that the sharp increase of FT expression after shifting to inductive condition in wild type plants is compromised the *ga1-3* background, indicating a possible role of GA in regulating *FT* expression (Hisamatsu and King, 2008). Despite the importance of this finding, the mechanism involved in the control of *FT* expression and if this regulation significantly contributes to flowering is still unknown.

Moreover, the fact that *ft* mutants still flower in LD contrasts with the striking non-flowering phenotype observed in the triple *gid1a-c* mutant, suggesting the existence of other genes in this pathway and/or the existence of additional regulation downstream of FT (Willige et al., 2007).

Several studies carried out during the last two decades consistently support the critical role of DELLA proteins in GA-mediated biological response. The recent discovery of the DELLA mechanisms of activity represented a landmark and has placed GA field in a new level in elucidating its biological role during plant development (Daviere et al., 2008; de Lucas et al., 2008; Feng et al., 2008). Nonetheless, the role of these proteins during flowering transition is still poorly understood. To address this question in more detail, we first investigated the contribution of DELLA proteins in the GA-mediated control of flowering under inductive photoperiod using different GA signaling mutants. Single loss-of-function DELLA mutants flowered slightly earlier than control plants, while higher order mutants presented an enhanced early flowering phenotype. In addition, mutants presenting higher DELLA accumulation, such as the dominant *gai-1* and *gid1a-c* mutants, flowered significantly later or never flowered at all, respectively. Based on these results, we concluded that DELLA proteins redundantly act as repressors of flowering and provide additional evidences supporting the role of GA in the control of flowering in LD. In agreement with this idea, several studies have indicated that the DELLA proteins act redundantly as effectors of GA signaling (Dill and Sun, 2001; Cheng et al., 2004). Nevertheless, these proteins apparently retain some functional specificity, e.g. during seed germination (Lee et al., 2002; Lee et al., 2010).

It is well known that under LD photoperiod the control of flowering can be spatially separated into processes that occur in leaves and those that take place at the shoot meristem (Kobayashi and Weigel, 2007). Due to their apparent functional redundancy in

controlling flowering time, we investigated the spatial contribution of individual DELLA proteins in this process. For this purpose, we created GA-insensitive versions of all five *Arabidopsis* DELLAs lacking 17 amino acids, including the DELLA domain (*dellaΔ17*). The expression of either wild-type or *dellaΔ17* constructs under the control of the phloem companion cell-specific *SUC2* promoter significantly delayed flowering under LD. Corroborating this result, the depletion of the endogenous levels of bioactive GA by expressing the catabolic enzyme *GA2ox8* in the vasculature also delayed flowering. In addition, *FT* expression was significantly reduced in the *gid1a-c* and *sly1-10* mutants. We next wanted to investigate if the late flowering phenotype observed in pSUC2:*dellaΔ17* occurs due to the regulation of *FT* expression. Interestingly, flowering time in the *dellaΔ17* lines was strongly anti-correlated with *FT* transcript levels. *SUC2:dellaΔ17* lines that were particularly late flowering also displayed the strongest reduction in *FT* expression. Apparently, changes in *FT* expression did not involve *CO* or *GI*, as their expression remained similar to control plants in different genetic backgrounds. In contrast to the significant effect on flowering time under LD, the expression of *dellaΔ17* constructs in the leaf vasculature have only a minor affect on flowering under SD. This result can be easily explained by the photoperiod-dependent induction of *FT*, which only occurs under LD in vasculature. Together, these results suggest that DELLA proteins regulate flowering in the vasculature specifically in under LD photoperiod through the regulation of *FT*.

FT expression is under the control of several environmental and endogenous factors (Srikanth and Schmid, 2011). Among them, several miR172-targeted AP2-like transcription factors that function as repressors of flowering have been shown to directly bind to *FT* chromatin to control its expression (Mathieu et al., 2009). Accordingly, plants lacking these genes or overexpressing *MIR172* display a drastic acceleration of flowering

under LD (Aukerman and Sakai, 2003; Mathieu et al., 2009; Yant et al., 2010). To test if the *MIR172 / AP2-like* module contributed to the induction of flowering by GA under LD, we investigated flowering time in a *35S:MIM172* line, which flowers late due to impaired miR172 function (Todesco et al., 2010). Transgenic *35S:MIM172* plants displayed reduced sensitivity to GA_3 treatment under LD at 23°C and 16°C. In agreement, miR172 levels are reduced in leaves of *SUC2:dellaΔ17* plants compared to control plants. These results indicate that GA regulates *FT* expression and flowering under LD at least partially through the *AP2-like / MIR172* module.

Using the same approach described above, we also expressed wild type and *dellaΔ17* constructs at the shoot apical meristem using the *FD* and *CLAVATA3* (*CLV3*) promoters. Strikingly, flowering time was severely affected only by *dellaΔ17* but not full length DELLA protein under LD condition, suggesting that the degradation of DELLA protein is critical for the regulation of the transition to flowering downstream of the photoperiodic signal at the shoot apical meristem. Similarly, the same transgenic lines strongly repressed flowering under SD, and frequently plants never flowered even after 6 months of vegetative growth. This observation, along with the complete suppression of flowering observed in *ga1-3* mutant, suggests that under SD GA controls flowering time mostly at the shoot apical meristem. Moreover, it indicates that GA is necessary for the transition to flowering at the shoot meristem downstream of the photoperiodic signal.

One of the first events during the induction of flowering at the shoot meristem under LD is the activation of the flowering integrator gene *SOC1* (Lee et al., 2000; Onouchi et al., 2000). In contrast to the strong induction of SOC1 expression by GA under SD, *SOC1* expression is only moderately affected by GA under LD. Therefore, it is possible that GA regulates events downstream of *SOC1* at the shoot meristem under LD. A recent study demonstrated that FD and SOC1 directly bind to the promoters of *SPL*

genes to regulate their expression (Jung et al., 2011). In turn, SPL proteins strongly induce flowering after binding to the promoters of flowering time genes (Wang et al., 2009; Yamaguchi et al., 2009). To investigate if GA affects this early event downstream of photoperiodic signal, we investigated the expression of *SPL* genes at the shoot meristem of *dellaΔ17* lines and in GA signaling mutants. Interestingly, we observed that the expression of several *SPL* genes responded strongly to GA. *SPL* mRNA was drastically reduced in transgenic plants misexpressing GA-insensitive *dellaΔ17* proteins at the meristem. Furthermore, this regulation probably occurs independently of *SOC1* and *MIR156*, since their expression remained nearly unchanged in response to GA.

In summary, our findings provide compelling evidence for the role of DELLA proteins in the regulation of flowering time in *Arabidopsis* under LD. Most importantly, this regulation triggers distinct regulatory programs taking place independently both in vasculature and shoot meristem. In stark contrast, the relation of flowering is confined to the shoot apical meristem.

Contribution

VCG and MS designed the experiments. VCG performed most of the experiments described in this work. DH phenotyped the *pSUC2:dellaΔ17* misexpression lines in LD and performed the GUS staining in transgenic *pFT:GUS pSUC2:dellaΔ17.* FK helped cloning several constructs. VCG, DH and MS analyzed the results. VCG and MS wrote the manuscript.

Chapter 2

The work summarized in this chapter was originally published in:

Gibberellin regulates the *Arabidopsis* floral transition through miR156-targeted SQUAMOSA PROMOTER BINDING-LIKE transcription factors.

Sha Yu*, Vinicius C. Galvão*, Yan-Chun Zhang, Daniel Horrer, Tian-Qi Zhang, Yan-Hong Hao, Yu-Qi Feng, Shui Wang, Markus Schmid, Jia-Wei Wang

Plant Cell (2012), 24 (8): 3320-3332.

* denotes equal contribution

Synopsis

The current model for GA signaling postulates that DELLA proteins bind to transcription factors to block their activity but do not directly bind DNA (Daviere et al., 2008; de Lucas et al., 2008; Feng et al., 2008). We therefore hypothesized that DELLA proteins could be binding to flowering-related transcription factors to regulate flowering transition.

To address this question, we performed yeast two-hybrid screens using all *Arabidopsis* DELLA proteins as baits. Among other flowering-related transcription factors, we identified SPL11 as a potential DELLA target. Direct interaction test in yeast and BiFC experiments using transient expression in *Nicotiana benthamiana* further confirmed this interaction. In addition, targeted yeast two-hybrid experiments identified interaction of DELLA proteins with SPL2, SPL9 and SPL10. The analysis of deletion constructs of SPL9 and SPL11 suggest that the interaction with the DELLA proteins is mediated thorough the C-terminal region of these SPL proteins. Interestingly, the C-terminal region of SPL9 and SPL11 contains a small leucine-rich motif that is also conserved among

several other *Arabidopsis* SPL proteins. In contrast, SPL3 and SPL5, which do not harbor this leucine-rich motif, do not interact with DELLA proteins.

In addition to the possible direct regulation by protein interaction, we want to investigate if GA affects the expression of *SPL* genes. Treatment of plants with the GA biosynthesis inhibitor paclobutrazol resulted in a reduced *SPL3* expression, whereas it had not effect on SPL9 transcript levels in SD. This finding is in agreement with the SPL expression in response to GA in LD conditions reported in the chapter 1 of this thesis and a recent report demonstrating the transcriptional regulation of *SPL* genes by GA under SD (Jung et al., 2011). Therefore, GA may not only affect SPL proteins activity by protein interaction but also through the reduction of transcript and protein abundance.

SPL and *MIR156* expression constitute the basis of an endogenous flowering pathway, which ensures flowering under non-inductive SD conditions in *Arabidopsis*. This relies on the gradual decrease in mir156 level as plants age, resulting in the slow accumulation of *SPL* transcripts, which in turn directly activate flowering time genes (Wang et al., 2009; Yamaguchi et al., 2009). Interestingly, increased DELLA accumulation either in the GA biosynthesis *ga1-3* or GA receptor *gid1a-c* mutants completely suppresses flowering in SD. Therefore, the regulation of SPL expression in response endogenous GA level and the direct interaction with DELLA proteins could explain this phenotype. To test if SPL proteins are mediating GA-mediated flowering response we used a transgenic line overexpressing *MIR156,* and therefore with reduced SPL activity. Interestingly, this line suppressed the flowering response to GA, indicating that SPL proteins are mediating GA induction of flowering. Further supporting this idea, the early flowering phenotype of pSPL9:*rSPL9* was suppressed when co-expressed with the GA-insensitive pRGA:*rgaΔ17* construct. Considering that GA apparently is not affecting *SPL9* expression, it is possible that this suppression occur due to a reduced

activity of SPL9 after binding to RGA. Together, these results indicate that DELLA protein accumulation represses flowering presumably by regulating *SPL* genes both transcriptionally and post-transcriptionally.

Previous experiments and the data presented in chapter 1 of this thesis indicate that GA regulates flowering transition under SD by regulating the expression of transcription factors at the shoot meristem (Blazquez et al., 1998; Moon et al., 2003; Achard et al., 2004). While *LFY* is apparently under control of *GAMYB* and *MIR159*, the mechanism involved in the regulation of *SOC1* is still unknown. ChIP experiments have shown that *SOC1* and *FUL* are directly regulated by *SPL9* (Wang et al., 2009). Therefore, SPL proteins could regulate *SOC1* and *FUL* expression in response to GA to control flowering. To address this question in more details, we first investigated the expression of these genes at the shoot meristem in the transgenic line *pFD:rgaΔ17* in SD. Interestingly, the expression of the dominant DELLA protein at the shoot meristem strongly suppressed the gradual increase in *SOC1* and *FUL* expression. Conversely, treatment of wild-type plants with exogenous GA_3 increased their expression. This is in agreement with the previous findings indicating that the accumulation of DELLA proteins repress SOC1 accumulation in SD (Moon et al., 2003). To test if GA controls *SOC1* and *FUL* expression through SPL activity, we used a transgenic line overexpressing *MIR156*. Indeed, the reduced *SPL* levels caused by MIR156 overexpression prevented the GA-mediated increase of *SOC1* and *FUL* transcripts. In addition, expression of *rgaΔ17* prevented the expression of *SOC1* and FUL in *rSPL9* lines. Together, these results provide strong evidence for a role of SPL proteins in regulating *SOC1* and *FUL* expression in response to GA to control flowering.

In addition to the GA control of flowering in SD, we also demonstrated that DELLA proteins control flowering under LD in the vasculature through FT. Using quantitative

expression analysis, we demonstrated that the expression of *SUC2:rgaΔ17* reduced the expression of *MIR172b*, while the expression of other known *FT* regulators such as *CO, SVP, TEM1, TEM2* and *FLC* was not affected. This finding is in agreement with the reduced sensitivity to GA treatment of *35S:MIM172* lines described in chapter 1 of this thesis.

Together, the results presented in this chapter provide important insights integrating the known mechanisms regulating flowering time in non-inductive SD photoperiod and GA signaling. In addition, it further strengthens the finding presented in chapter 1 supporting the role of *MIR172* in the regulation of *FT* expression and control of flowering under LD.

Contribution

VCG, MS and JWW designed the experiments. VCG, DH and JWW performed the yeast two-hybrid and BiFC experiments, JWW performed the Co-IP. VCG, SY, YCZ, TQZ, YHH and JWW performed expression analysis. MIR156 and rSPL9 experiments were performed by JWW.

Chapter 3

The work summarized in this chapter was originally published in:

Synteny-based mapping-by-sequencing enabled by targeted enrichment.
Vinicius C. Galvão*, Karl J.V. Nordström*, Christa Lanz, Patric Sulz, Johannes Mathieu, David Posé, Markus Schmid, Detlef Weigel, Korbinian Schneeberger
The Plant Journal (2012), 71: 517-526.
* denotes equal contribution

Synopsis

Forward genetic screens have greatly contributed to the characterization of new gene function. However, the identification of the causal mutations has in the past often been a laborious and time-consuming process (Lukowitz et al., 2000). This bottleneck can been largely overcome by the use of high-throughput sequencing methods that reduce the hands-on time required for mapping to a few working days starting from the mapping population (Schneeberger et al., 2009). This strategy relies on whole-genome sequencing of bulked segregant mapping populations and statistical estimation of a confidence interval harboring a potential causal mutation. Nevertheless, mapping-by-sequencing has been mostly applicable for model species for which a reference genome is available but not for those lacking whole genome reference sequence or with larger genomes. The current mapping-by-sequencing strategy relies on the whole genome sequencing, which provides mostly uninformative sequencing information for mapping. In this chapter we describe a new marker enrichment syntheny-based method for mapping causal mutations without use of a genetic map. This method provides an attractive alternative for mapping mutations in non-model organisms where a reference genome or a detailed genetic map is not available by comparison with closely related species.

For this proof-of-concept study we used an unknown mutant candidate identified in a genetic screen intended to identify mutants suppressing the strong FT flowering promoting activity. Approximately 10000 seeds of an early flowering line homozygous, single insertion line overexpressing *FT* in the phloem companion cells (*SUC2:FT*) in a *fd-2* mutant background (Columbia, Col-0 ecotype) were mutagenized using EMS. A late flowering candidate (96-1) was chosen among several M2 suppressors originally identified in this screen. To create a mapping population we crossed this mutant to the late flowering *fd-1* mutant in *Landsberg erecta* (L*er*-1) background. Leaves from 119 late flowering F2 individuals were pooled and used for nuclei purification and DNA extraction. In addition, leaf material was collected from F1 individuals as control for allele frequency estimation.

Capture probes were designed using Col-0, L*er*-1 and C24 genomes in order to select polymorphisms between Col-0 and a shared polymorphism in L*er*-1 and C24 within 5-10 kb intervals (Schneeberger et al., 2011). A total of 48.508 120-mer biotin-tagged RNA bait probes were designed to distinguish 24.254 marker between Col-0 and Ler-1 or Col-0 and C24. Marker-enriched libraries were created for F1 and F2 mapping populations using solution-based enrichment for marker regions (Gnirke et al., 2009). In addition, we prepared a paired-end library of the F2 segregant population using total DNA before capture.

Using conventional SHORE mapping we identified a region on chromosome 2, which harbored seven induced SNPs, as linked with the late flowering phenotype. One candidate mutation, which was predicted to disrupt a splice site of the flowering integrator gene *SOC1*, was confirmed using conventional dideoxy sequencing. We next verified that this mutation was causing the late flowering phenotype by transforming the 96-1 mutant with a construct containing an 8.2 kb *SOC1* genomic fragment. This construct

consistently rescued the late flowering phenotype of another *SOC1* allele, *soc1-2*, confirming that this is sufficient to reconstitute the *SOC1* function. Similarly, the late flowering phenotype of 96-1 mutant was rescued in T1 plants. In addition, complementation crosses with *soc1-2* further confirmed the mutation in *SOC1* in 96-1 as causal for the late flowering phenotype.

Interestingly, despite the much-reduced number of markers used for enrichment-based mapping (24.254 markers) compared to whole genome mapping-by-sequencing (461.070 markers) the resolution for both strategies were comparable. The increased number of reads supporting the markers after enrichment allowed a very similar estimation of the confidence interval in enriched and non-enriched samples. Confirming the probes capture efficiency, plastid DNA contamination was reduced from 19% in whole genome sequencing to only 0.5% after enrichment. Therefore, we demonstrated that high coverage sequencing of a reduced subset of markers is sufficient for high-resolution mapping.

We could efficiently determine a confidence interval using a reduced number of markers in a targeted enriched sample. Nonetheless, information about the genetic order of the markers was still necessary to perform this analysis. Unfortunately, such information is not yet available for other species for which often only RNA-seq or EST datasets exist. One possible solution to this problem could be in using syntheny information between closely related species to order markers contained in transcribed regions. To test whether it was possible to map a mutation using only markers contained in transcribed regions, we aligned *Arabidopsis* cDNA sequences against the publicly available *Brassica rapa* genome to order the *Arabidopsis* cDNAs based on syntheny information from *B. rapa* and to create a artificial reference genome. Using 4375 cDNAs harboring a marker, we were able to narrow down two regions in the chromosomes 4 and

5 of *B. rapa*, which are syntenic with *SOC1*-containing region of *Arabidopsis* chromosome 2. Both regions in *B. rapa* encompass a gene homologues to *AtSOC1*. Therefore, we were able to perform mapping by sequencing using an even smaller number of markers using only synteny information in a related species.

As demonstrated in our study, the use of targeted enrichment can efficiently be used to perform mapping-by-sequencing relying on the increase in coverage of a limited number of marker positions without a reference sequence or genetic map. The use of this strategy could facilitate mapping of mutations in species with large and complex genomes, substituting the costly whole genome sequencing.

Contribution

VCG, JM, MS, DW and KS planned the experiments. VCG, PS, JM performed the suppressor screen and identified the mutant candidates. VCG and PS created the mapping population. VCG, CL and PS prepared the libraries for both standard and probe-enriched sequencing. DP cloned gSOC1 rescue construct. VCG and PS performed the complementation of the mutant. KJVN and KS performed the sequencing, statistical and synteny analysis. KS and DW wrote the manuscript with contributions from VCG, KJVN and MS.

References

Abe, M., Kobayashi, Y., Yamamoto, S., Daimon, Y., Yamaguchi, A., Ikeda, Y., Ichinoki, H., Notaguchi, M., Goto, K. and Araki, T. (2005). FD, a bZIP protein mediating signals from the floral pathway integrator FT at the shoot apex. *Science* **309,** 1052-1056.

Achard, P., Herr, A., Baulcombe, D. C. and Harberd, N. P. (2004). Modulation of floral development by a gibberellin-regulated microRNA. *Development* **131,** 3357-3365.

Aki, T., Shigyo, M., Nakano, R., Yoneyama, T. and Yanagisawa, S. (2008). Nano scale proteomics revealed the presence of regulatory proteins including three FT-like proteins in phloem and xylem saps from rice. *Plant and Cell Physiology* **49,** 767-790.

Araki, T. and Komeda, Y. (1993). Analysis of the role of the late-flowering locus, Gl, in the flowering of Arabidopsis thaliana. *Plant Journal* **3,** 231-239.

Aukerman, M. J. and Sakai, H. (2003). Regulation of flowering time and floral organ identity by a microRNA and its APETALA2-like target genes. *Plant Cell* **15,** 2730-2741.

Benlloch, R., Kim, M. C., Sayou, C., Thevenon, E., Parcy, F. and Nilsson, O. (2011). Integrating long-day flowering signals: a LEAFY binding site is essential for proper photoperiodic activation of APETALA1. *Plant Journal* **67,** 1094-1102.

Blackman, B. K., Strasburg, J. L., Raduski, A. R., Michaels, S. D. and Rieseberg, L. H. (2010). The role of recently derived FT paralogs in sunflower domestication. *Current Biology* **20,** 629-635.

Blazquez, M. and Weigel, D. (2000). Integration of floral inductive signals in Arabidopsis. *Nature* **404,** 889-892.

Blazquez, M. A., Green, R., Nilsson, O., Sussman, M. R. and Weigel, D. (1998). Gibberellins promote flowering of Arabidopsis by activating the LEAFY promoter. *Plant Cell* **10,** 791-800.

Blazquez, M. A., Soowal, L. N., Lee, I. and Weigel, D. (1997). LEAFY expression and flower initiation in Arabidopsis. *Development* **124,** 3835-3844.

Bohlenius, H., Huang, T., Charbonnel-Campaa, L., Brunner, A. M., Jansson, S., Strauss, S. H. and Nilsson, O. (2006). CO/FT regulatory module controls timing of flowering and seasonal growth cessation in trees. *Science* **312,** 1040-1043.

Bolle, C. (2004). The role of GRAS proteins in plant signal transduction and development. *Planta* **218,** 683-692.

Cardon, G. H., Hohmann, S., Nettesheim, K., Saedler, H. and Huijser, P. (1997). Functional analysis of the Arabidopsis thaliana SBP-box gene SPL3: a novel gene involved in the floral transition. *Plant Journal* **12,** 367-377.

Chailakhian, M. K. (1936a). About the mechanism of the photoperiodic response. (in Russian) *Dokl. Akad. Nauk SSSR (C. R. Acad. Sci. USSR)* **1,** 85-89.

Chailakhian, M. K. (1936b). New facts supporting the hormonal theory of plant development. (in Russian). *Dokl. Akad. Nauk SSSR (C. R. Acad. Sci. USSR)* **4,** 77-81.

Chen, X. M. (2004). A microRNA as a translational repressor of APETALA2 in Arabidopsis flower development. *Science* **303,** 2022-2025.

Cheng, H., Qin, L., Lee, S., Fu, X., Richards, D. E., Cao, D., Luo, D., Harberd, N. P. and Peng, J. (2004). Gibberellin regulates Arabidopsis floral development via suppression of DELLA protein function. *Development* **131,** 1055-1064.

Corbesier, L., Vincent, C., Jang, S. H., Fornara, F., Fan, Q. Z., Searle, I., Giakountis, A., Farrona, S., Gissot, L., Turnbull, C., et al., (2007). FT protein movement contributes to long-distance signaling in floral induction of Arabidopsis. *Science* **316,** 1030-1033.

Daviere, J. M., de Lucas, M. and Prat, S. (2008). Transcriptional factor interaction: a central step in DELLA function. *Curr. Opin. Genet. Dev.* **18,** 295-303.

Davies, P. J. (2004). Plant hormones: biosynthesis, signal transduction, action! 3rd edn. Dordrecht, the Netherlands: Springer

de Lucas, M., Daviere, J. M., Rodriguez-Falcon, M., Pontin, M., Iglesias-Pedraz, J. M., Lorrain, S., Fankhauser, C., Blazquez, M. A., Titarenko, E. and Prat, S. (2008). A molecular framework for light and gibberellin control of cell elongation. *Nature* **451,** 480-484.

Deng, X. W., Caspar, T. and Quail, P. H. (1991). cop1: a regulatory locus involved in light-controlled development and gene expression in Arabidopsis. *Genes & Development* **5,** 1172-1182.

Dill, A., Jung, H. S. and Sun, T. P. (2001). The DELLA motif is essential for gibberellin-induced degradation of RGA. *Proc. Natl. Acad. Sci. USA* **98,** 14162-14167.

Dill, A. and Sun, T. (2001). Synergistic derepression of gibberellin signaling by removing RGA and GAI function in Arabidopsis thaliana. *Genetics* **159,** 777-785.

Dill, A., Thomas, S. G., Hu, J., Steber, C. M. and Sun, T. P. (2004). The Arabidopsis F-box protein SLEEPY1 targets gibberellin signaling repressors for gibberellin-induced degradation. *Plant Cell* **16,** 1392-1405.

Feng, S., Martinez, C., Gusmaroli, G., Wang, Y., Zhou, J., Wang, F., Chen, L., Yu, L., Iglesias-Pedraz, J. M., Kircher, S., et al., (2008). Coordinated regulation of Arabidopsis thaliana development by light and gibberellins. *Nature* **451,** 475-479.

Fowler, S., Lee, K., Onouchi, H., Samach, A., Richardson, K., Coupland, G. and Putterill, J. (1999). GIGANTEA: a circadian clock-controlled gene that regulates photoperiodic flowering in Arabidopsis and encodes a protein with several possible membrane-spanning domains. *EMBO Journal* **18,** 4679-4688.

Fu, X. D., Richards, D. E., Fleck, B., Xie, D. X., Burton, N. and Harberd, N. P. (2004). The Arabidopsis mutant sleepy1(gar2-1) protein promotes plant growth by increasing the affinity of the SCFSLY1 E3 ubiquitin ligase for DELLA protein substrates. *Plant Cell* **16,** 1406-1418.

Fujioka, S., Yamane, H., Spray, C. R., Katsumi, M., Phinney, B. O., Gaskin, P., Macmillan, J. and Takahashi, N. (1988). The dominant non-gibberellin-responding dwarf mutant (D8) of maize accumulates native gibberellins. *Proc. Natl. Acad. Sci. USA* **85,** 9031-9035.

Gandikota, M., Birkenbihl, R. P., Hohmann, S., Cardon, G. H., Saedler, H. and Huijser, P. (2007). The miRNA156/157 recognition element in the 3' UTR of the Arabidopsis SBP box gene SPL3 prevents early flowering by translational inhibition in seedlings. *Plant Journal* **49,** 683-693.

Giavalisco, P., Kapitza, K., Kolasa, A., Buhtz, A. and Kehr, J. (2006). Towards the proteome of Brassica napus phloem sap. *Proteomics* **6,** 896-909.

Gnirke, A., Melnikov, A., Maguire, J., Rogov, P., LeProust, E. M., Brockman, W., Fennell, T., Giannoukos, G., Fisher, S., Russ, C., et al., (2009). Solution hybrid selection with ultra-long oligonucleotides for massively parallel targeted sequencing. *Nature Biotechnology* **27,** 182-189.

Gocal, G. F., Poole, A. T., Gubler, F., Watts, R. J., Blundell, C. and King, R. W. (1999). Long-day up-regulation of a GAMYB gene during Lolium temulentum inflorescence formation. *Plant Physiology* **119,** 1271-1278.

Gocal, G. F. W., Sheldon, C. C., Gubler, F., Moritz, T., Bagnall, D. J., MacMillan, C. P., Li, S. F., Parish, R. W., Dennis, E. S., Weigel, D., et al., (2001). GAMYB-like genes, flowering, and gibberellin signaling in Arabidopsis. *Plant Physiology* **127,** 1682-1693.

Griffiths, J., Murase, K., Rieu, I., Zentella, R., Zhang, Z. L., Powers, S. J., Gong, F., Phillips, A. L., Hedden, P., Sun, T. P., et al., (2006). Genetic characterization and functional analysis of the GID1 gibberellin receptors in Arabidopsis. *Plant Cell* **18,** 3399-3414.

Gubler, F., Kalla, R., Roberts, J. K. and Jacobsen, J. V. (1995). Gibberellin-regulated expression of a myb gene in barley aleurone cells: evidence for Myb transactivation of a high-pI alpha-amylase gene promoter. *Plant Cell* **7,** 1879-1891.

Guo, A. Y., Zhu, Q. H., Gu, X. C., Ge, S., Yang, J. and Luo, J. C. (2008). Genome-wide identification and evolutionary analysis of the plant specific SBP-box transcription factor family. *Gene* **418,** 1-8.

Guo, H., Duong, H., Ma, N. and Lin, C. (1999). The Arabidopsis blue light receptor cryptochrome 2 is a nuclear protein regulated by a blue light-dependent post-transcriptional mechanism. *Plant Journal* **19,** 279-287.

He, Z., Zhu, Q., Dabi, T., Li, D., Weigel, D. and Lamb, C. (2000). Transformation of rice with the Arabidopsis floral regulator LEAFY causes early heading. *Transgenic Research* **9,** 223-227.

Hecht, V., Laurie, R. E., Vander Schoor, J. K., Ridge, S., Knowles, C. L., Liew, L. C., Sussmilch, F. C., Murfet, I. C., Macknight, R. C. and Weller, J. L. (2011). The pea GIGAS gene is a FLOWERING LOCUS T homolog necessary for graft-transmissible specification of flowering but not for responsiveness to photoperiod. *Plant Cell* **23,** 147-161.

Hempel, F. D., Weigel, D., Mandel, M. A., Ditta, G., Zambryski, P. C., Feldman, L. J. and Yanofsky, M. F. (1997). Floral determination and expression of floral regulatory genes in Arabidopsis. *Development* **124,** 3845-3853.

Hisamatsu, T. and King, R. W. (2008). The nature of floral signals in Arabidopsis. II. Roles for FLOWERING LOCUS T (FT) and gibberellin. *J. Exp. Bot.* **59,** 3821-3819.

Hong, G. J., Xue, X. Y., Mao, Y. B., Wang, L. J. and Chen, X. Y. (2012). Arabidopsis MYC2 interacts with DELLA proteins in regulating sesquiterpene synthase gene expression. *Plant Cell* **24,** 2635-2648.

Hou, X. L., Lee, L. Y. C., Xia, K. F., Yen, Y. Y. and Yu, H. (2010). DELLAs modulate jasmonate signaling via competitive binding to JAZs. *Developmental Cell* **19,** 884-894.

Hsu, C. Y., Adams, J. P., Kim, H. J., No, K., Ma, C. P., Strauss, S. H., Drnevich, J., Vandervelde, L., Ellis, J. D., Rice, B. M., et al., (2011). FLOWERING LOCUS T duplication coordinates reproductive and vegetative growth in perennial poplar. *Proc. Natl. Acad. Sci. USA* **108,** 10756-10761.

Ikeda, A., Ueguchi-Tanaka, M., Sonoda, Y., Kitano, H., Koshioka, M., Futsuhara, Y., Matsuoka, M. and Yamaguchi, J. (2001). slender rice, a constitutive gibberellin response mutant, is caused by a null mutation of the SLR1 gene, an ortholog of the height-regulating gene GAI/RGA/RHT/D8. *Plant Cell* **13,** 999-1010.

Jacobsen, S. E., Binkowski, K. A. and Olszewski, N. E. (1996). SPINDLY, a tetratricopeptide repeat protein involved in gibberellin signal transduction in Arabidopsis. *Proc. Natl. Acad. Sci. USA* **93,** 9292-9296.

Jacobsen, S. E. and Olszewski, N. E. (1993). Mutations at the SPINDLY locus of Arabidopsis alter gibberellin signal transduction. *Plant Cell* **5,** 887-896.

Jaeger, K. E. and Wigge, P. A. (2007). FT protein acts as a long-range signal in Arabidopsis. *Current Biology* **17,** 1050-1054.

Jang, S., Marchal, V., Panigrahi, K. C. S., Wenkel, S., Soppe, W., Deng, X. W., Valverde, F. and Coupland, G. (2008). Arabidopsis COP1 shapes the temporal pattern of CO accumulation conferring a photoperiodic flowering response. *EMBO Journal* **27,** 1277-1288.

Jung, J. H., Ju, Y., Seo, P. J., Lee, J. H. and Park, C. M. (2011). The SOC1-SPL module integrates photoperiod and gibberellic acid signals to control flowering time in Arabidopsis. *Plant Journal* **69,** 577-588.

Kardailsky, I., Shukla, V. K., Ahn, J. H., Dagenais, N., Christensen, S. K., Nguyen, J. T., Chory, J., Harrison, M. J. and Weigel, D. (1999). Activation tagging of the floral inducer FT. *Science* **286,** 1962-1965.

Kerstetter, R. A. and Poethig, R. S. (1998). The specification of leaf identity during shoot development. *Annual Review of Cell and Developmental Biology* **14,** 373-398.

Kim, J. J., Lee, J. H., Kim, W., Jung, H. S., Huijser, P. and Ahn, J. H. (2012). The microRNA156-SQUAMOSA PROMOTER BINDING PROTEIN-LIKE3 module regulates ambient temperature-responsive flowering via FLOWERING LOCUS T in Arabidopsis. *Plant Physiology* **159,** 461-478.

Klein, J., Saedler, H. and Huijser, P. (1996). A new family of DNA binding proteins includes putative transcriptional regulators of the Antirrhinum majus floral meristem identity gene SQUAMOSA. *Molecular & General Genetics* **250,** 7-16.

Knott, J. E. (1934). Effect of a localized photoperiod on spinach. *Proc. Am. Soc. Hortic. Sci.* **31 (Suppl.),** 152-154.

Kobayashi, Y., Kaya, H., Goto, K., Iwabuchi, M. and Araki, T. (1999). A pair of related genes with antagonistic roles in mediating flowering signals. *Science* **286,** 1960-1962.

Kobayashi, Y. and Weigel, D. (2007). Move on up, it's time for change--mobile signals controlling photoperiod-dependent flowering. *Genes & Development* **21,** 2371-2384.

Kojima, S., Takahashi, Y., Kobayashi, Y., Monna, L., Sasaki, T., Araki, T. and Yano, M. (2002). Hd3a, a rice ortholog of the Arabidopsis FT gene, promotes transition to flowering downstream of Hd1 under short-day conditions. *Plant & Cell Physiology* **43,** 1096-1105.

Koornneef, M., Elgersma, A., Hanhart, C. J., Vanloenenmartinet, E. P., Vanrijn, L. and Zeevaart, J. A. D. (1985). A gibberellin insensitive mutant of Arabidopsis thaliana. *Physiologia Plantarum* **65,** 33-39.

Koornneef, M., Hanhart, C. J. and van der Veen, J. H. (1991). A genetic and physiological analysis of late flowering mutants in Arabidopsis thaliana. *Molecular & General Genetics* **229,** 57-66.

Koornneef, M. and van der Veen, J. (1980). Induction and analysis of gibberellin sensitive mutants in Arabidopsis thaliana (L) Heynh. *Theor. Appl. Genet.* **58,** 257-263.

Lang, A. (1956a). Gibberellin and flower formation. *Naturwissenschaften* **43,** 544-544.

Lang, A. (1956b). Induction of flower formation in biennial Hyoscyamus by treatment with gibberellin. *Naturwissenschaften* **43,** 284-285.

Lang, A. (1957). The effect of gibberellin upon flower formation. *Proc. Natl. Acad. Sci. USA* **43,** 709-717.

Lau, O. S. and Deng, X. W. (2012). The photomorphogenic repressors COP1 and DET1: 20 years later. *Trends in Plant Science* **17,** 584-593.

Laubinger, S., Fittinghoff, K. and Hoecker, U. (2004). The SPA quartet: a family of WD-repeat proteins with a central role in suppression of photomorphogenesis in arabidopsis. *Plant Cell* **16,** 2293-2306.

Laubinger, S., Marchal, V., Gentilhomme, J., Wenkel, S., Adrian, J., Jang, S., Kulajta, C., Braun, H., Coupland, G. and Hoecker, U. (2006). Arabidopsis SPA proteins regulate photoperiodic flowering and interact with the floral inducer CONSTANS to regulate its stability. *Development* **133,** 3213-3222.

Lauter, N., Kampani, A., Carlson, S., Goebel, M. and Moose, S. P. (2005). microRNA172 down-regulates glossy15 to promote vegetative phase change in maize. *Proc. Natl. Acad. Sci. USA* **102,** 9412-9417.

Lee, H., Suh, S. S., Park, E., Cho, E., Ahn, J. H., Kim, S. G., Lee, J. S., Kwon, Y. M. and Lee, I. (2000). The AGAMOUS-LIKE 20 MADS domain protein integrates floral inductive pathways in Arabidopsis. *Genes & Development* **14,** 2366-2376.

Lee, K. P., Piskurewicz, U., Tureckova, V., Strnad, M. and Lopez-Molina, L. (2010). A seed coat bedding assay shows that RGL2-dependent release of abscisic acid by the endosperm controls embryo growth in Arabidopsis dormant seeds. *Proc. Natl. Acad. Sci. USA* **107,** 19108-19113.

Lee, S., Cheng, H., King, K. E., Wang, W., He, Y., Hussain, A., Lo, J., Harberd, N. P. and Peng, J. (2002). Gibberellin regulates Arabidopsis seed germination via RGL2, a GAI/RGA-like gene whose expression is up-regulated following imbibition. *Genes & Development* **16,** 646-658.

Li, C. Y., Zhang, K., Zeng, X. W., Jackson, S., Zhou, Y. and Hong, Y. G. (2009). A cis-element within FLOWERING LOCUS T mRNA Determines its mobility and facilitates trafficking of heterologous viral RNA. *Journal of Virology* **83,** 3540-3548.

Lian, H. L., He, S. B., Zhang, Y. C., Zhu, D. M., Zhang, J. Y., Jia, K. P., Sun, S. X., Li, L. and Yang, H. Q. (2011). Blue-light-dependent interaction of cryptochrome 1 with SPA1 defines a dynamic signaling mechanism. *Genes & Development* **25,** 1023-1028.

Lifschitz, E., Eviatar, T., Rozman, A., Shalit, A., Goldshmidt, A., Amsellem, Z., Alvarez, J. P. and Eshed, Y. (2006). The tomato FT ortholog triggers systemic signals that regulate growth and flowering and substitute for diverse environmental stimuli. *Proc. Natl. Acad. Sci. USA* **103,** 6398-6403.

Lin, M. K., Belanger, H., Lee, Y. J., Varkonyi-Gasic, E., Taoka, K. I., Miura, E., Xoconostle-Cazares, B., Gendler, K., Jorgensene, R. A., Phinney, B., et al., (2007). FLOWERING LOCUS

T protein may act as the long-distance florigenic signal in the cucurbits. *Plant Cell* **19,** 1488-1506.

Liu, B., Zuo, Z. C., Liu, H. T., Liu, X. M. and Lin, C. T. (2011). Arabidopsis cryptochrome 1 interacts with SPA1 to suppress COP1 activity in response to blue light. *Genes & Development* **25,** 1029-1034.

Liu, L., Liu, C., Hou, X., Xi, W., Shen, L., Tao, Z., Wang, Y. and Yu, H. (2012). FTIP1 is an essential regulator required for florigen transport. *PLoS Biol.* **10,** e1001313.

Liu, L. J., Zhang, Y. C., Li, Q. H., Sang, Y., Mao, J., Lian, H. L., Wang, L. and Yang, H. Q. (2008). COP1-mediated ubiquitination of CONSTANS is implicated in cryptochrome regulation of flowering in Arabidopsis. *Plant Cell* **20,** 292-306.

Lu, K. J., Huang, N. C., Liu, Y. S., Lu, C. A. and Yu, T. S. (2012). Long-distance movement of Arabidopsis FLOWERING LOCUS T RNA participates in systemic floral regulation. *RNA Biology* **9,** 653-662.

Lukowitz, W., Gillmor, C. S. and Scheible, W. R. (2000). Positional cloning in Arabidopsis. Why it feels good to have a genome initiative working for you. *Plant Physiology* **123,** 795-805.

Mathieu, J., Warthmann, N., Kuttner, F. and Schmid, M. (2007). Export of FT protein from phloem companion cells is sufficient for floral induction in Arabidopsis. *Current Biology* **17,** 1055-1060.

Mathieu, J., Yant, L. J., Murdter, F., Kuttner, F. and Schmid, M. (2009). Repression of flowering by the miR172 target SMZ. *PLoS Biol.* **7,** e1000148.

McGinnis, K. M., Thomas, S. G., Soule, J. D., Strader, L. C., Zale, J. M., Sun, T. P. and Steber, C. M. (2003). The Arabidopsis SLEEPY1 gene encodes a putative F-box subunit of an SCF E3 ubiquitin ligase. *Plant Cell* **15,** 1120-1130.

McNellis, T. W., von Arnim, A. G., Araki, T., Komeda, Y., Misera, S. and Deng, X. W. (1994). Genetic and molecular analysis of an allelic series of cop1 mutants suggests functional roles for the multiple protein domains. *Plant Cell* **6,** 487-500.

Melzer, S., Lens, F., Gennen, J., Vanneste, S., Rohde, A. and Beeckman, T. (2008). Flowering-time genes modulate meristem determinacy and growth form in Arabidopsis thaliana. *Nature Genetics* **40,** 1489-1492.

Mockler, T. C., Guo, H., Yang, H., Duong, H. and Lin, C. (1999). Antagonistic actions of Arabidopsis cryptochromes and phytochrome B in the regulation of floral induction. *Development* **126,** 2073-2082.

Moon, J., Suh, S.-S., Lee, H., Choi, K.-R., Hong, C. B., Paek, N.-C., Kim, S.-G. and Lee, I. (2003). The SOC1 MADS-box gene integrates vernalization and gibberellin signals for flowering in Arabidopsis. *Plant Journal* **35,** 613-623.

Moose, S. P. and Sisco, P. H. (1994). Glossy15 controls the epidermal juvenile-to-adult phase-transition in maize. *Plant Cell* **6,** 1343-1355.

Moose, S. P. and Sisco, P. H. (1995). The maize homeotic gene glossy15 is a member of the apetala2 gene family. *Journal of Cellular Biochemistry* 458-458.

Moose, S. P. and Sisco, P. H. (1996). Glossy15, an APETALA2-like gene from maize that regulates leaf epidermal cell identity. *Genes & Development* **10,** 3018-3027.

Moyroud, E., Minguet, E. G., Ott, F., Yant, L., Pose, D., Monniaux, M., Blanchet, S., Bastien, O., Thevenon, E., Weigel, D., et al., (2011). Prediction of regulatory interactions from genome sequences using a biophysical model for the Arabidopsis LEAFY transcription factor. *Plant Cell* **23,** 1293-1306.

Murase, K., Hirano, Y., Sun, T. P. and Hakoshima, T. (2008). Gibberellin-induced DELLA recognition by the gibberellin receptor GID1. *Nature* **456,** 459-463.

Nakajima, M., Shimada, A., Takashi, Y., Kim, Y. C., Park, S. H., Ueguchi-Tanaka, M., Suzuki, H., Katoh, E., Iuchi, S., Kobayashi, M., et al., (2006). Identification and characterization of Arabidopsis gibberellin receptors. *Plant Journal* **46,** 880-889.

Navarro, C., Abelenda, J. A., Cruz-Oro, E., Cuellar, C. A., Tamaki, S., Silva, J., Shimamoto, K. and Prat, S. (2011). Control of flowering and storage organ formation in potato by FLOWERING LOCUS T. *Nature* **478,** 119-132.

Naylor, A. W. (1941). Effect of nutrition and age upon rate of development of terminal staminate inflorescences of Xanthium pennsylvanicum. *Bot. Gaz.* **103,** 342-353.

Olszewski, N., Sun, T. P. and Gubler, F. (2002). Gibberellin signaling: biosynthesis, catabolism, and response pathways. *Plant Cell* **14 Suppl,** S61-80.

Onouchi, H., Igeno, M. I., Perilleux, C., Graves, K. and Coupland, G. (2000). Mutagenesis of plants overexpressing CONSTANS demonstrates novel interactions among Arabidopsis flowering-time genes. *Plant Cell* **12,** 885-900.

Pearce, S., Saville, R., Vaughan, S. P., Chandler, P. M., Wilhelm, E. P., Sparks, C. A., Al-Kaff, N., Korolev, A., Boulton, M. I., Phillips, A. L., et al., (2011). Molecular characterization of Rht-1 dwarfing genes in hexaploid wheat. *Plant Physiology* **157,** 1820-1831.

Peng, J. R., Carol, P., Richards, D. E., King, K. E., Cowling, R. J., Murphy, G. P. and Harberd, N. P. (1997). The Arabidopsis GAI gene defines a signaling pathway that negatively regulates gibberellin responses. *Genes & Development* **11,** 3194-3205.

Peng, J. R. and Harberd, N. P. (1993). Derivative alleles of the Arabidopsis gibberellin-insensitive (Gai) mutation confer a wild-type phenotype. *Plant Cell* **5,** 351-360.

Pin, P. A., Benlloch, R., Bonnet, D., Wremerth-Weich, E., Kraft, T., Gielen, J. J. and Nilsson, O. (2010). An antagonistic pair of FT homologs mediates the control of flowering time in sugar beet. *Science* **330,** 1397-1400.

Poethig, R. S. (2003). Phase change and the regulation of developmental timing in plants. *Science* **301,** 334-336.

Putterill, J., Robson, F., Lee, K., Simon, R. and Coupland, G. (1995). The CONSTANS gene of Arabidopsis promotes flowering and encodes a protein showing similarities to zinc finger transcription factors. *Cell* **80,** 847-857.

Redei, G. P. (1962). Supervital mutants of Arabidopsis. *Genetics* **47,** 443-460.

Rhoades, M. W., Reinhart, B. J., Lim, L. P., Burge, C. B., Bartel, B. and Bartel, D. P. (2002). Prediction of plant microRNA targets. *Cell* **110,** 513-520.

Samach, A., Onouchi, H., Gold, S. E., Ditta, G. S., Schwarz-Sommer, Z., Yanofsky, M. F. and Coupland, G. (2000). Distinct roles of CONSTANS target genes in reproductive development of Arabidopsis. *Science* **288,** 1613-1616.

Sasaki, A., Itoh, H., Gomi, K., Ueguchi-Tanaka, M., Ishiyama, K., Kobayashi, M., Jeong, D. H., An, G., Kitano, H., Ashikari, M., et al., (2003). Accumulation of phosphorylated repressor for gibberellin signaling in an F-box mutant. *Science* **299,** 1896-1898.

Schmid, M., Uhlenhaut, N. H., Godard, F., Demar, M., Bressan, R., Weigel, D. and Lohmann, J. U. (2003). Dissection of floral induction pathways using global expression analysis. *Development* **130,** 6001-6012.

Schneeberger, K., Ossowski, S., Lanz, C., Juul, T., Petersen, A. H., Nielsen, K. L., Jorgensen, J. E., Weigel, D. and Andersen, S. U. (2009). SHOREmap: simultaneous mapping and mutation identification by deep sequencing. *Nature Methods* **6,** 550-551.

Schneeberger, K., Ossowski, S., Ott, F., Klein, J. D., Wang, X., Lanz, C., Smith, L. M., Cao, J., Fitz, J., Warthmann, N., et al., (2011). Reference-guided assembly of four diverse Arabidopsis thaliana genomes. *Proc. Natl. Acad. Sci. USA* **108,** 10249-10254.

Schwab, R., Palatnik, J. F., Riester, M., Schommer, C., Schmid, M. and Weigel, D. (2005). Specific effects of microRNAs on the plant transcriptome. *Developmental Cell* **8,** 517-527.

Searle, I., He, Y. H., Turck, F., Vincent, C., Fornara, F., Krober, S., Amasino, R. A. and Coupland, G. (2006). The transcription factor FLC confers a flowering response to vernalization by repressing meristem competence and systemic signaling in Arabidopsis. *Genes & Development* **20,** 898-912.

Shikata, M., Koyama, T., Mitsuda, N. and Ohme-Takagi, M. (2009). Arabidopsis SBP-box genes SPL10, SPL11 and SPL2 control morphological change in association with shoot maturation in the reproductive phase. *Plant & Cell Physiology* **50,** 2133-2145.

Shimada, A., Ueguchi-Tanaka, M., Nakatsu, T., Nakajima, M., Naoe, Y., Ohmiya, H., Kato, H. and Matsuoka, M. (2008). Structural basis for gibberellin recognition by its receptor GID1. *Nature* **456,** 520-523.

Silverstone, A. L., Jung, H. S., Dill, A., Kawaide, H., Kamiya, Y. and Sun, T. P. (2001). Repressing a repressor: gibberellin-induced rapid reduction of the RGA protein in Arabidopsis. *Plant Cell* **13,** 1555-1566.

Silverstone, A. L., Mak, P. Y., Martinez, E. C. and Sun, T. P. (1997). The new RGA locus encodes a negative regulator of gibberellin response in Arabidopsis thaliana. *Genetics* **146,** 1087-1099.

Silverstone, A. L., Tseng, T. S., Swain, S. M., Dill, A., Jeong, S. Y., Olszewski, N. E. and Sun, T. P. (2007). Functional analysis of SPINDLY in gibberellin signaling in Arabidopsis. *Plant Physiology* **143,** 987-1000.

Srikanth, A. and Schmid, M. (2011). Regulation of flowering time: all roads lead to Rome. *Cell. Mol. Life Sci.* **68,** 2013-2037.

Suarez-Lopez, P., Wheatley, K., Robson, F., Onouchi, H., Valverde, F. and Coupland, G. (2001). CONSTANS mediates between the circadian clock and the control of flowering in Arabidopsis. *Nature* **410,** 1116-1120.

Sun, T. P. and Kamiya, Y. (1994). The Arabidopsis GA1 locus encodes the cyclase ent-kaurene synthetase A of gibberellin biosynthesis. *Plant Cell* **6,** 1509-1518.

Takada, S. and Goto, K. (2003). Terminal flower2, an Arabidopsis homolog of heterochromatin protein1, counteracts the activation of flowering locus T by constans in the vascular tissues of leaves to regulate flowering time. *Plant Cell* **15,** 2856-2865.

Tamaki, S., Matsuo, S., Wong, H. L., Yokoi, S. and Shimamoto, K. (2007). Hd3a protein is a mobile flowering signal in rice. *Science* **316,** 1033-1036.

Taoka, K., Ohki, I., Tsuji, H., Furuita, K., Hayashi, K., Yanase, T., Yamaguchi, M., Nakashima, C., Purwestri, Y. A., Tamaki, S., et al., (2011). 14-3-3 proteins act as intracellular receptors for rice Hd3a florigen. *Nature* **476,** 332-335.

Telfer, A., Bollman, K. M. and Poethig, R. S. (1997). Phase change and the regulation of trichome distribution in Arabidopsis thaliana. *Development* **124,** 645-654.

Teper-Bamnolker, P. and Samach, A. (2005). The flowering integrator FT regulates SEPALLATA3 and FRUITFULL accumulation in Arabidopsis leaves. *Plant Cell* **17,** 2661-2675.

Thomas, B. and Vince-Prue, D. (1997). Photoperiodism in plants 2nd edn.: Academic Press.

Todesco, M., Rubio-Somoza, I., Paz-Ares, J. and Weigel, D. (2010). A collection of target mimics for comprehensive analysis of microRNA function in Arabidopsis thaliana. *PLoS Genet.* **6,** e1001031.

Torti, S., Fornara, F., Vincent, C., Andres, F., Nordstrom, K., Gobel, U., Knoll, D., Schoof, H. and Coupland, G. (2012). Analysis of the Arabidopsis shoot meristem transcriptome during floral transition identifies distinct regulatory patterns and a leucine-rich repeat protein that promotes flowering. *Plant Cell* **24,** 444-462.

Ueguchi-Tanaka, M., Ashikari, M., Nakajima, M., Itoh, H., Katoh, E., Kobayashi, M., Chow, T. Y., Hsing, Y. I., Kitano, H., Yamaguchi, I., et al., (2005). GIBBERELLIN INSENSITIVE DWARF1 encodes a soluble receptor for gibberellin. *Nature* **437,** 693-698.

Valverde, F., Mouradov, A., Soppe, W., Ravenscroft, D., Samach, A. and Coupland, G. (2004). Photoreceptor regulation of CONSTANS protein in photoperiodic flowering. *Science* **303,** 1003-1006.

Vonarnim, A. G. and Deng, X. W. (1994). Light inactivation of Arabidopsis photomorphogenic repressor cop1 involves a cell-specific regulation of its nucleocytoplasmic partitioning. *Cell* **79,** 1035-1045.

Wang, J. W., Czech, B. and Weigel, D. (2009). miR156-regulated SPL transcription factors define an endogenous flowering pathway in Arabidopsis thaliana. *Cell* **138,** 738-749.

Wang, J. W., Schwab, R., Czech, B., Mica, E. and Weigel, D. (2008). Dual effects of miR156-targeted SPL genes and CYP78A5/KLUH on plastochron length and organ size in Arabidopsis thaliana. *Plant Cell* **20,** 1231-1243.

Weigel, D., Alvarez, J., Smyth, D. R., Yanofsky, M. F. and Meyerowitz, E. M. (1992). LEAFY controls floral meristem identity in Arabidopsis. *Cell* **69,** 843-859.

Wigge, P. A., Kim, M. C., Jaeger, K. E., Busch, W., Schmid, M., Lohmann, J. U. and Weigel, D. (2005). Integration of spatial and temporal information during floral induction in Arabidopsis. *Science* **309,** 1056-1059.

Willige, B. C., Ghosh, S., Nill, C., Zourelidou, M., Dohmann, E. M., Maier, A. and Schwechheimer, C. (2007). The DELLA domain of GA INSENSITIVE mediates the interaction with the GA INSENSITIVE DWARF1A gibberellin receptor of Arabidopsis. *Plant Cell* **19,** 1209-1220.

Wilson, R. N., Heckman, J. W. and Sommerville, C. R. (1992). Gibberellin is required for flowering in Arabidopsis thaliana under short days *Plant Physiology* **100,** 403-408.

Wu, G., Park, M. Y., Conway, S. R., Wang, J. W., Weigel, D. and Poethig, R. S. (2009). The sequential action of miR156 and miR172 regulates developmental timing in Arabidopsis. *Cell* **138,** 750-759.

Wu, G. and Poethig, R. S. (2006). Temporal regulation of shoot development in Arabidopsis thaliana by miR156 and its target SPL3. *Development* **133,** 3539-3547.

Yamaguchi, A., Wu, M. F., Yang, L., Wu, G., Poethig, R. S. and Wagner, D. (2009). The MicroRNA-regulated SBP-Box transcription factor SPL3 is a direct upstream activator of LEAFY, FRUITFULL, and APETALA1. *Developmental Cell* **17,** 268-278.

Yanovsky, M. J. and Kay, S. A. (2002). Molecular basis of seasonal time measurement in Arabidopsis. *Nature* **419,** 308-312.

Yant, L., Mathieu, J., Dinh, T. T., Ott, F., Lanz, C., Wollmann, H., Chen, X. and Schmid, M. (2010). Orchestration of the floral transition and floral development in Arabidopsis by the bifunctional transcription factor APETALA2. *Plant Cell* **22,** 2156-2170.

Zentella, R., Zhang, Z. L., Park, M., Thomas, S. G., Endo, A., Murase, K., Fleet, C. M., Jikumaru, Y., Nambara, E., Kamiya, Y., et al., (2007). Global analysis of DELLA direct targets in early gibberellin signaling in Arabidopsis. *Plant Cell* **19,** 3037-3057.

Zhang, Z. L., Ogawa, M., Fleet, C. M., Zentella, R., Hu, J. H., Heo, J. O., Lim, J., Kamiya, Y., Yamaguchi, S. and Sun, T. P. (2011). SCARECROW-LIKE 3 promotes gibberellin signaling by antagonizing master growth repressor DELLA in Arabidopsis. *Proc. Natl. Acad. Sci. USA* **108,** 2160-2165.

Zuo, Z. C., Liu, H. T., Liu, B., Liu, X. M. and Lin, C. T. (2011). Blue Light-Dependent Interaction of CRY2 with SPA1 Regulates COP1 activity and Floral Initiation in Arabidopsis. *Current Biology* **21,** 841-847.

Acknowledgements

This thesis is dedicated to my grandfather, Nelson dos Santos Galvão.

To my mom and brother, which supported and encouraged me no matter what. All this work would never be possible without you.

To all my family in Brazil, mainly those who have been so supportive from the very beginning: Christa Vörckel, Indira Vörckel, Vania Baptista, Jose Antonio Costa e Ligia Costa.

To my amazing girlfriend Adriana for all support, sacrifice and for believing that all would be possible, no matter the distance! Thanks for being always with me!

I would like to thank my supervisor, Dr. Markus Schmid, for the great opportunity to work in his group and for all guidance during these years. It was not only a really great work experience but also a very nice life experience.

To the flowering time group, former and current members, a BIG THANKS!!

My former students Daniel Horrer, Johanna Weirich and Patric Sulz for all nice moments and for the help! I've learned a lot with you guys!

And a special thanks to the 'cloning machine' Frank Küttner! Not only for all the help and teaching but also for being such a nice and patient guy!

To the members of my PhD committee, Prof. Dr. Detlef Weigel, Prof. Dr. Gerd Jürgens and Prof. Dr. Christine Dreyer for discussions, ideas and support.

To all nice people I've met during these years in weigelworld! I really enjoyed having really nice moments with you all! A special thanks to Carmen Pizarro, David Pose, Diep, Eshita Sharma, Felipao Felipes, Francelli Kulcheski, Nacho Rubio, Jathish Ponnu, Johannes Kaut, Luis Toledo, Maricris Zaidem, Natalia Camomili, Pablo Manavella, Subhashini Muralidhanran, Tobias Langneker, Vanessa Tragante and Yasushi Kobaiashi.

To all my unforgettable friends in Brazil! Aline, Anderson, Caca, Gabriel, Jaburanga, Leandrez, Leandrinho, Moises, Talita, Vitor Hugo etc. I'm really looking forward to meeting you soon!

Curriculum Vitae

Personal information

Date of birth: 10.12.1981
Place of birth: Niterói, Brazil.

Education

2002 – 2005 Bachelor in Biological Sciences, Genetics
Federal University of Rio de Janeiro, Rio de Janeiro, Brazil.

2006 – 2008 Master of Sciences, Genetics
Federal University of Rio de Janeiro, Rio de Janeiro, Brazil.

2008 - 2013 Ph.D., Molecular Biology
Max Planck Institute for Developmental Biology, Tübingen, Germany

Publications

Teixeira, F.K., Menezes-Benavete, L., **Galvão, V.C.,** Margis-Pinheiro, M. (2005). Multigene families encode the major enzymes of antioxidant metabolism in Eucalyptus grandis L.. *Genetics and Molecular Biology,* 28 (4): 529-538.

Teixeira, F.K., Menezes-Benavete, L., **Galvão, V.C.,** Margis, R., Margis-Pinheiro, M. (2006). Rice ascorbate peroxidase isoforms localized in different subcellular compartments. *Planta,* 224:300-314.

Mangeon, A., Magioli, C., Menezes-Salgueiro, A.D., Jorge, V.C., Oliveira, C. **Galvão, V.C.,** Margis, R., Engler, G., Sachetto-Martins, G. (2009). AtGRP5, a vacuole-located glycine-rich protein involved in cell elongation. *Planta,* 230: 253-265.

Galvão, V.C.*, Nordström, K.J.V.*, Lanz, C., Sulz, P., Mathieu, J., Posé, D., Schmid, M., Weigel, D., Schneeberger, K. (2012). Synteny-based mapping-by-sequencing enabled by targeted enrichment. *The Plant Journal,* 71 (3): 517-526.

Galvão, V.C., Horrer, D., Kütnner, F., Schmid, M. (2012). Spatial control of flowering by DELLA proteins in *Arabidopsis thaliana*. *Development* (2012), 139: 4072-4082.

Yu, S.*, Galvão, V.C.*, Zhang, Y.C., Horrer, D., Zhang, T.Q., Hao, Y.H., Feng, Q.Y., Wang, W., Schmid, M., Wang, J.W. (2012). Gibberellin controls Arabidopsis floral transition through miR156-targeted SPL transcription factors. *Plant Cell* (2012), 24 (8): 3320-3332.

Manuscripts in Preparation

Galvão, V.C., Cardeal, V., Sachetto-Martins, G. Complete survey and expression analysis of glycine-rich proteins (GRP) in *Arabidopsis* and rice.

Richter, R., **Galvão, V.C.,** Kaufmann, K., Schmid, M., Schwechheimer, C. DELLA regulation of *GNC* and *GNL/CGA1* through APETALA1 controls floral development and flowering time in *Arabidopsis thaliana.*

* denotes equal contribution

Appendix

the plant journal

SEB Society for Experimental Biology

The Plant Journal (2012) **71**, 517–526 doi: 10.1111/j.1365-313X.2012.04993.x

TECHNICAL ADVANCE

Synteny-based mapping-by-sequencing enabled by targeted enrichment

Vinicius C. Galvão[1,†], Karl J.V. Nordström[2,†], Christa Lanz[1], Patric Sulz[1], Johannes Mathieu[1,‡], David Posé[1], Markus Schmid[1], Detlef Weigel[1,*] and Korbinian Schneeberger[1,2,*]

[1]*Max Planck Institute for Developmental Biology, 72076 Tübingen, Germany, and*

[2]*Max Planck Institute for Plant Breeding Research, 50829 Cologne, Germany*

Received 31 October 2011; revised 10 February 2012; accepted 5 March 2012; published online 14 May 2012.

*For correspondence (e-mail weigel@weigelworld.org or schneeberger@mpipz.mpg.de).

†These authors contributed equally to this work.

‡Present Address: Boyce Thompson Institute for Plant Research, Tower Road, Ithaca, NY 14853-1801, USA.

SUMMARY

Mapping-by-sequencing, as implemented in SHOREmap ('SHOREmapping'), is greatly accelerating the identification of causal mutations. The original SHOREmap approach based on resequencing of bulked segregants required a highly accurate and complete reference sequence. However, current whole-genome or transcriptome assemblies from next-generation sequencing data of non-model organisms do not produce chromosome-length scaffolds. We have therefore developed a method that exploits synteny with a related genome for genetic mapping. We first demonstrate how mapping-by-sequencing can be performed using a reduced number of markers, and how the associated decrease in the number of markers can be compensated for by enrichment of marker sequences. As proof of concept, we apply this method to *Arabidopsis thaliana* gene models ordered by synteny with the genome sequence of the distant relative *Brassica rapa*, whose genome has several large-scale rearrangements relative to *A. thaliana*. Our approach provides an alternative method for high-resolution genetic mapping in species that lack finished genome reference sequences or for which only RNA-seq assemblies are available. Finally, for improved identification of causal mutations by fine-mapping, we introduce a new likelihood ratio test statistic, transforming local allele frequency estimations into a confidence interval similar to conventional mapping intervals.

Keywords: SHOREmapping, mapping-by-sequencing, genetics, targeted enrichment sequencing, whole-genome sequencing, technical advance.

INTRODUCTION

Forward genetic screens remain one of the most powerful tools for characterization of gene function in genetically tractable organisms. Before the arrival of next-generation sequencing technologies, identification of sequence variation causing mutant phenotypes typically began with genome-wide mapping, followed by further fine-mapping and identification of the causal mutation by sequencing candidate genes and complementation with transgenes. Recently, we streamlined this laborious and time-intense procedure by introduction of SHOREmap, a method that relies on whole-genome resequencing and the principles of bulked segregant analysis (Michelmore *et al.*, 1991; Schneeberger *et al.*, 2009a). This one-step method combines mutation mapping and identification, and thus reduces the actual workload from establishment of mapping populations to candidate validation to a few days. Similar strategies, subsequently introduced in *A. thaliana* and later in various other systems, have demonstrated the general applicability of mapping-by-sequencing (Bigelow *et al.*, 2009; Blumenstiel *et al.*, 2009; Nijman *et al.*, 2010; Zuryn *et al.*, 2010; Austin *et al.*, 2011). So far, mapping-by-sequencing has been performed only in model species with medium-sized genomes and a reference genome sequence, although genetic screens and mutant populations are available for several other species, including many crops. Two difficulties have so far hampered the application of whole-genome resequencing

technologies to these species. First, their genome sizes are usually large, substantially increasing the costs of whole-genome resequencing. Second, and probably more important, without a high-quality reference genome, one cannot perform mapping-by-sequencing by aligning short reads against a reference sequence.

A successful way to reduce genome complexity is enzymatic digestion of genomic DNA followed by high-throughput sequencing of restriction-associated regions (Baird *et al.*, 2008). Short reads derived from these regions are grouped by clustering and then mined for polymorphisms. This method has been further improved by incorporation of paired-end reads and avoidance of repetitive regions by using a methylation-sensitive restriction enzyme (Willing *et al.*, 2011; Etter *et al.*, 2011; Elshire *et al.*, 2011). As the clustering is performed solely on sequence similarities between the short reads, this method not only reduces complexity but has also been suggested for mapping-by-sequencing without a reference sequence (Baird *et al.*, 2008). Marker density and sequencing requirements can be adjusted by selection and combination of restriction enzymes that have recognition sites of varying abundance (Willing *et al.*, 2011). Hence, the complexity reduction relies on the presence and distribution of restriction sites generating a non-random reduction that is specific to the combination of genome and restriction enzyme(s). Incorporation of existing genetic maps is difficult as only those markers that reside near the restriction sites can be genotyped, and linkage information between accessible markers needs to be established for each setting separately. This can be further complicated by a low polymorphism rate, which is the case in cultivated crop species, leading to an increased proportion of restriction sites that are non-informative but still require sequencing. Alternatively, targeted enrichment sequencing methods can reduce genome complexity, with a focus on predefined regions of the genome (Turner *et al.*, 2009; Gnirke *et al.*, 2009). This requires prior knowledge about the genome sequence, but allows selection of known marker regions and candidate genes.

To demonstrate the feasibility of mapping-by-sequencing based on sequencing data that do not include the entire genome, we enriched genomic DNA at selected sequence-based markers and used it for mapping-by-sequencing. As all complexity reduction methods are likely to exclude the causal mutation from the sequence library, simultaneous identification of causal variations is ordinarily not possible, and more tedious fine-mapping approaches are required. To minimize the workload of fine-mapping, we introduce a likelihood ratio test method that translates marker-wise estimates of local allele frequencies from pooled genomic data into confidence mapping intervals similar to conventional mapping intervals. These intervals serve as a probabilistic alternative to arbitrary definition of mapping intervals through visual inspection only (Schneeberger *et al.*, 2009a; Austin *et al.*, 2011).

Such enrichment sequencing libraries do not require full-length reference sequences and can be designed from incomplete assemblies such as exon sequences only, commonly referred to as exome enrichment sequencing (Gnirke *et al.*, 2009). Although it suffices for resequencing and variation mining, unordered RNA-seq assemblies do not support genetic mapping. We therefore demonstrate how gene models can be ordered by homology with related species, and how such synteny-based ordering of genic sequences can provide alignment targets for the resequencing step of mapping-by-sequencing. This scenario mimics the present situation for many species, for which complete reference sequences are missing but partial genome information is available, e.g. EST libraries or RNA-seq assemblies, that can be mapped via synteny to related species (Mayer *et al.*, 2011).

RESULTS AND DISCUSSION

Genetic screen, enrichment design and resequencing

To improve on the original SHOREmap approach (Schneeberger *et al.*, 2009a), we made use of a recessive flowering time mutant. A late-flowering line was obtained from a suppressor screen for factors that affect the activity of *FLOWERING LOCUS T (FT)*, the major output of the photoperiod pathway (Kardailsky *et al.*, 1999; Kobayashi *et al.*, 1999) (see Experimental procedures). An early-flowering *SUC2::FT fd-2* line, which expresses *FT* from the phloem companion cell-specific *SUC2* promoter in the *fd-2* mutant background (Figure 1), was mutagenized using ethyl methanesulfonate (EMS). Suppressors of the early flowering phenotype were identified in the M_2 generation. Among 25 M_2 plants, we found six recessive mutants that flowered late, but were not characterized by increased expression of the floral repressor *FLOWERING LOCUS C* (*FLC*). Integrity and expression of the transgene were confirmed by dideoxy sequencing and quantitative RT-PCR, indicating that the late flowering was caused by the EMS-induced mutation.

To create a mapping population, we crossed one of the suppressor lines, 96-1, to the *fd-1* mutant (Abe *et al.*, 2005), which is in the Landsberg *erecta* (L*er*) background. The offspring were allowed to self-fertilize, resulting in a F_2 mapping population of Col-0/L*er* recombinants. Leaves of 119 late-flowering F_2 individuals were pooled, and genomic DNA was prepared. In addition, we extracted DNA from pooled F_1 individuals to serve as a control for resequencing-based allele estimates. Illumina paired-end sequencing libraries were prepared for both DNA samples.

Using whole-genome assemblies of the common laboratory strains L*er*-1 and C24 of *A. thaliana* (Schneeberger *et al.*, 2011), we searched for SNP markers with a preferred

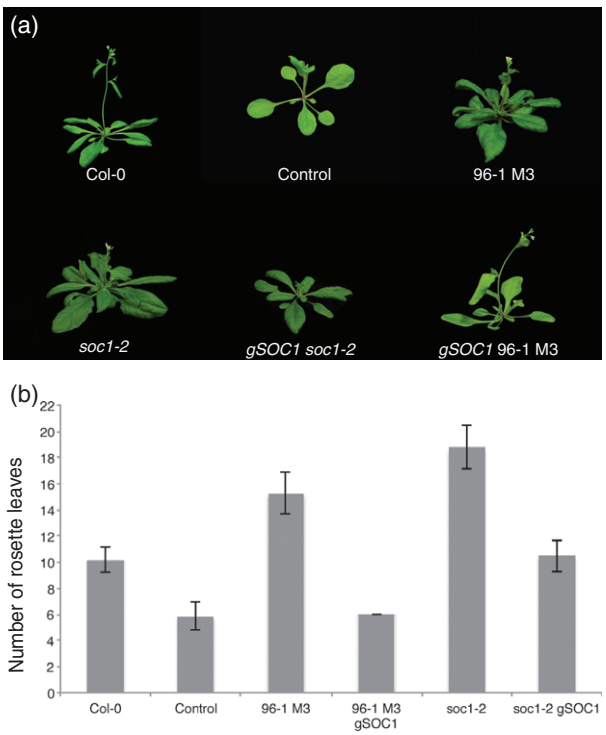

Figure 1. Mutant isolation and phenotypic rescue using g*SOC1* construct.
(a) Wild-type Col-0 plants flower much later than the *SUC2::FT fd-2* line. The 96-1 *SUC2::FT fd-2* line flowers late compared to the control plants, and this late flowering was completely rescued by the g*SOC1* construct. The loss-of-function *soc1-2* mutant shows delayed flowering, and expression of g*SOC1* efficiently rescues its phenotype.
(b) Flowering time measured by the number of rosette leaves. Error bars indicate 2× the standard error of the mean (SEM).

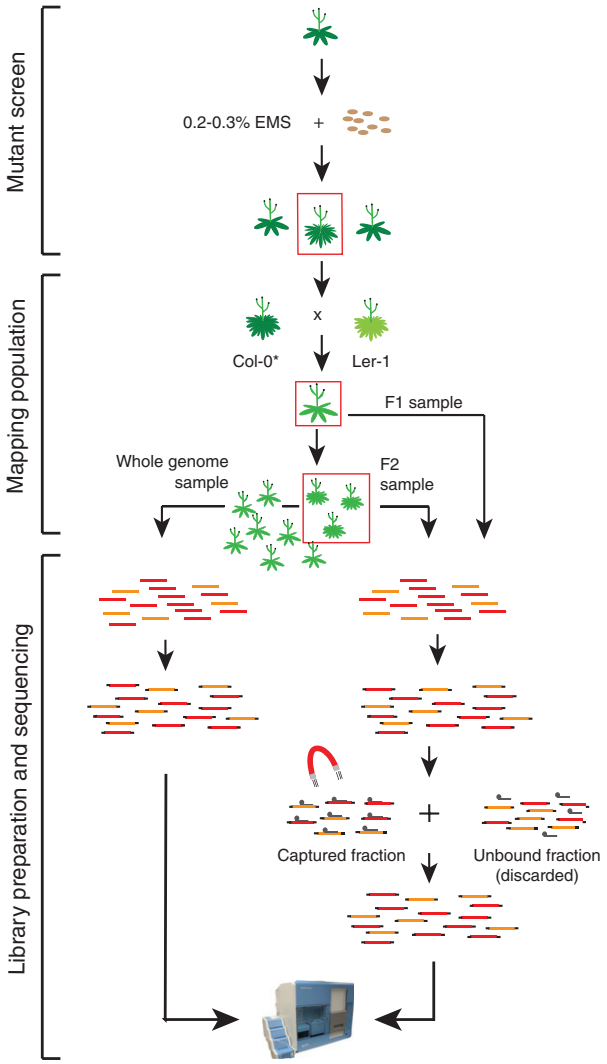

Figure 2. Overview of sequencing experiments.
After the mutant screen and generation of a mapping population, two DNA extracts were prepared for sequencing. The DNA of bulked segregants was pooled and used for standard paired-end library preparation (whole-genome sample). In an independent step, the same DNA was used for preparation of a targeted enrichment library (F_2 sample). In addition, we also performed targeted enrichment on the DNA of F_1 individuals (F_1 sample).

physical distance of 5–10 kb between each other. To ensure generic application of these markers, we only selected those for which L*er*-1 and C24 shared an identical allele, resulting in a map with 24 254 markers distinguishing the alleles of Col-0 from L*er*-1 or those of Col-0 from C24, respectively. Both alleles of all markers were used to generate an Agilent SureSelect target enrichment sequencing library (http://www.agilent.com) consisting of 48 508 120 bp bait sequences (see Table S1 and Experimental procedures).

We performed solution-based enrichment to isolate genomic DNA corresponding to the region represented by the 24 254 markers (Figure 2). Marker-enriched libraries were prepared for both the F_2 population and the F_1 control sample, together with a conventional library using total genomic DNA of the F_2 mapping population before enrichment. Paired-end 101 bp reads were generated for each library in a single lane of an Illumina GAIIx instrument (http://www.illumina.com). Sequencing resulted in 36.2 (whole-genome sample), 39.8 (F_2 sample) and 41.5 (F_1 sample) million read pairs. After read filtering and trimming, high-quality reads were aligned against a reference sequence using SHORE and GenomeMapper (Ossowski *et al.*, 2008; Schneeberger *et al.*, 2009b) (see Experimental procedures).

A splice site-affecting mutation of *SOC1* is causal for late flowering

Using the whole-genome sample, we performed conventional SHOREmapping based on 461 070 SNP markers to identify the mutation causing late flowering (Schneeberger *et al.*, 2011). Figure 3 displays the new output of SHOREmap, including the *r* value (brown line) introduced with the original SHOREmap approach, and the marker-wise Col-0 allele frequency estimates (AFEs) along chromosome 2

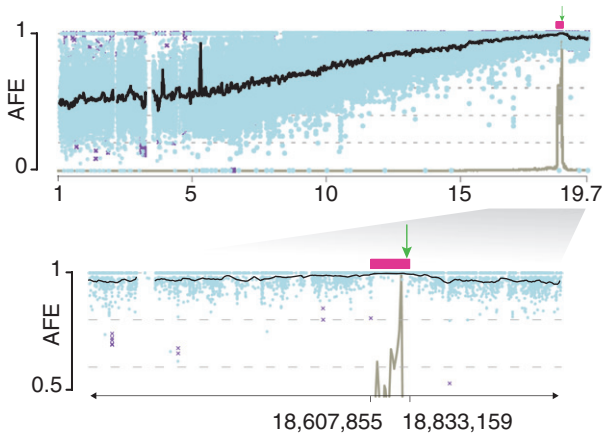

Figure 3. Allele frequency estimations using *A. thaliana* as the reference.
The plot shows a modified version of the SHOREmap output for the whole-genome sample. Light blue dots indicate allele frequency estimates from single markers. The black line shows the allele frequency estimates summarized in a 50 kb sliding window for simplified interpretation of the data. Purple crosses represent markers that were excluded in the outlier removal step. Pink bars indicate the 99% confidence mapping interval, and the exact physical borders are given below. Brown line shows the r-value introduced with the first SHOREmap approach. Green arrows are not part of SHOREmap output, and indicate the position of the causal change in the *SOC1* mutant. The analysis included the complete reference sequence as the alignment target and 461 070 markers for allele frequency estimations.

(light blue dots) (Figure S1 for all chromosomes). AFEs are the percentage of reads supporting one of the parental alleles (see Experimental procedures). Both *r* values and AFEs reveal an allele frequency bias in the parental allele frequencies on the lower arm of chromosome 2, reflecting phenotypic selection for the mutated parental genome only.

Access to the entire reference genome sequence and whole-genome sequencing information allows simultaneous identification of causal candidate mutations (Schneeberger *et al.*, 2009a). The point estimator of the original SHOREmap approach peaked at 18 792 986 bp on chromosome 2 (Figure 3). Within a statistically assessed interval from 18 607 855 to 18 833 159 bp on chromosome 2 (see below), we found seven mutations, of which two were predicted to affect transcribed sequences (Arabidopsis Genome Initiative 2000). One of the affected genes, *SOC1*/At2g45660, is known for its late-flowering mutant phenotype (Onouchi *et al.*, 2000; Lee *et al.*, 2000). The mutation affects a splice site and was confirmed by dideoxy sequencing. To verify that this mutation caused the late-flowering phenotype, we engineered a transgene containing an 8.2 kb *SOC1* genomic fragment (g*SOC1*). This transgene was sufficient to completely rescue the late flowering of a strong *soc1-2* null mutant (Figure 1). Similarly, flowering time was restored in 96-1 M_3 mutant lines transformed with this SOC1 rescue construct (Figure 1). In addition, a complementation cross with *soc1-2* confirmed that the lesion in *SOC1* is responsible for the late-flowering phenotype.

Along chromosome 2, the increases or decreases in AFEs around the causal mutation were not monotonic, as expected in mapping populations for a single Mendelian trait. This suggests that there is a considerable difference between real allele frequencies and AFEs. This variation makes it very difficult to clearly define the start and end position of a region of interest by visual inspection only (Schneeberger *et al.*, 2009a; Austin *et al.*, 2011).

Mapping intervals at specified confidence levels

The size of the final SHOREmap interval is important for candidate selection or deciding on fine-mapping strategies. The original point estimator implemented in SHOREmap predicted one position that was used to rank candidate mutations based on the distance between mutation and peak, but did not accurately delineate the borders of a mapping interval. To improve delineation of the final mapping interval, we developed a statistical test for SHOREmap that uses AFEs to derive an interval that harbors the causal change at a specified confidence level.

To define an effective statistical model, we first analyzed the factors that may contribute to variation in AFEs. The F_1 sample, which has an equimolar mixture of both parental alleles, allows evaluation of the nature of the difference between real allele frequency and AFEs, as all differences between the AFE and 0.5 are random or technical in nature, rather than biological. In particular, we analyzed three factors affecting the precision of AFEs: random sampling, sequencing errors and mis-alignments.

As the number of alignments is finite, random sampling is one of the factors that influences AFEs. In addition to the number of chromosomes in the pool, the impact of random sampling depends on the number of alignments per marker, with higher coverage supporting more accurate AFEs, as indicated by the reduced variation after enrichment. As the inter-marker distances were generally larger than the insert sizes of the sequencing library, AFEs are independent, and the effect of random sampling is best described by a binomial distribution (Figure S2). As the distribution of observed AFEs is considerably broader than expected under random sampling only, we conclude that other effects influence AFEs as well, such as sequencing errors and mis-alignments (Figure S2).

To quantify the impact of sequencing errors, we assessed the number of bases aligned to markers that did not support any of the parental alleles. Using alignments against the complete reference genome sequence, we found that 0.06, 0.09 and 0.14% of the aligned bases did not match any of the parental alleles for the F_1, F_2 and whole-genome samples, respectively. Assuming an equal transition error between all four nucleotides, we have detected only two-thirds of all sequencing errors, and therefore we estimate the error

probability in our data to be between 0.09 and 0.21% after quality filtering using SHORE (Ossowski *et al.*, 2008). Although this is much lower than usually expected for next-generation sequencing data, we conclude that sequencing errors do act as a minor contributor to AFE variation.

Mis-alignments often result from sequence reads derived from regions that are absent from the reference genome sequence. For example, transposons, local duplications or any kind of copy-number variation may account for sequence reads aligning to regions that do not represent their origin. Mis-alignments heavily influence AFEs at such loci. As these are preferentially local effects, we implemented a local outlier removal step. AFEs for each marker were then compared to the distribution of AFEs at surrounding markers. Markers with a significant probability of not being drawn from this distribution were marked as outliers, and are not considered further (see Experimental procedures).

Using outlier-adjusted marker sets only, we defined a likelihood model that includes variation in allele frequencies introduced by random sampling and sequencing errors with even transition rates (see Experimental procedures). This model allows a probabilistic comparison of the allele frequencies for any given set of markers to the estimated frequency of the causal mutation.

To accelerate subsequent computations of confidence intervals, we implemented rapid identification of a seed region (similar to rough mapping intervals) that was used to guide subsequent confidence interval calculations. This seed region is defined as the window whose frequency estimate is closest to the expected target frequency. Misphenotyped plants introduce unexpected changes to the expected frequency. If desired, SHOREmap can automatically adjust for this by estimating the frequency in the window identified by the initial peak finding and using this value as the expected frequency for confidence interval calculation. For more precise calculation of a confidence mapping interval, the initial seed region is then expanded to include as many markers as possible under the constraint that the probability of a log-likelihood ratio test between the optimal and expected frequency does not exceed the pre-defined confidence level of 0.99 (see Experimental procedures). Chromosomes without a skew in AFEs are also tested, but do not produce a valid window.

Applying this algorithm to the whole-genome sample and the complete set of 461 070 markers yielded a confidence interval spanning from 18 607 855 to 18 833 159 bp on chromosome 2, including the causal mutation (Figure 3). Our method requires *ab initio* definition of the window sizes for outlier removal and seed region. Our algorithm is stable for changes in both, but may need to be adjusted for different datasets (Figures S3 and S4). This adjustment is straightforward applying the approximated recombination frequency and marker density for any given sample. The sliding windows for outlier removal should pool include a large number of recombination events in the, and the window for the seed regions should be smaller than the approximated size for the targeted homozygous region, although slight over- or under-estimation will not hamper the calculation (Figures S3 and S4).

Targeted enrichment can compensate for a reduced number of markers

Unfinished assemblies can complicate practical application of SHOREmapping. Nevertheless, as the genetic mapping step in the process of mapping-by-sequencing relies on markers only, unfinished or gene space-focused assemblies still have the potential to support mapping-by-sequencing. However, limited access to the reference genome sequence reduces the number of markers that can be accessed, thus limiting the power for identifying causal regions. Along the same lines, the large genome size of many species makes whole-genome sequencing costly, and lower fold sequencing can further reduce the mapping power. However, targeted enrichment sequencing can substantially increase the coverage at marker loci without the need for a full-length reference sequence.

Although the regions targeted by our enrichment procedure were only 120 bp, increased sequence coverage of short-read alignments of the F_2 sample extended beyond the targets (Figure 4a). This most likely reflects the insert size of the sequencing library, with a mean clone length of 182 bp, as both ends of enriched molecules were sequenced (Figure 4b). Organelle contamination before enrichment was estimated to be as high as 19%; it was reduced to 0.5% after enrichment. Without enrichment, only 3% of the read pairs with at least one mapped read aligned against 24 254 marker positions; with enrichment, this increased to 62%, with 88% of the read pairs aligning with the regions targeted by enrichment, as assessed using alignments against the complete reference genome sequence (Table 1).

The increased coverage at the markers allowed more accurate assessment of the allele frequencies (Figures 4c and S5 for all chromosomes). When comparing the confidence interval analyses of the whole-genome sample (using 461 070 markers and the complete reference sequence as the alignment target) with analysis of the enriched F_2 sample (using 24 254 markers and their surrounding 800 bp as the alignment target), the confidence intervals were surprisingly similar (Figures 3 and 4). Their sizes are 225.3 and 212.7 kb for the whole genome sample and the enriched F_2 sample, respectively. The causal mutation was very close to the edge of the confidence interval, probably reflecting unequal recombination rates on either side of the mutation. The relatively high number of reads per marker for the F_2 sample allows an ad hoc approximation of the homozygous region that is well matched by our confidence interval calculation

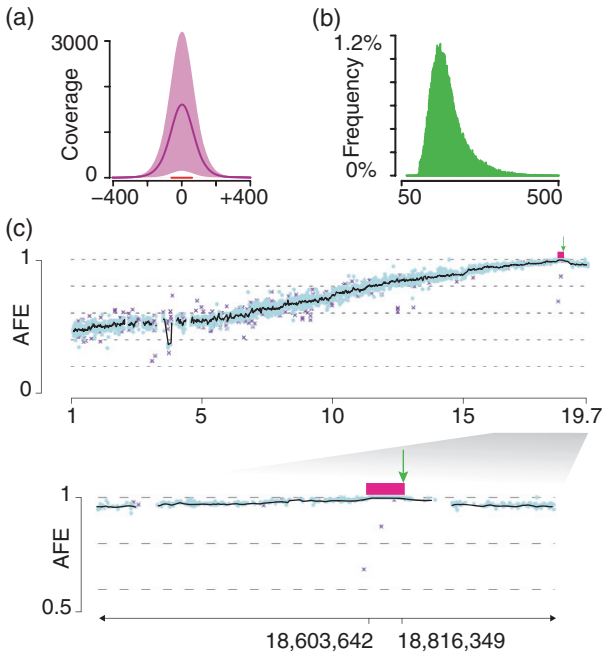

Figure 4. Targeted enrichment sequencing results.
(a) Median of position-wise short read coverage values around the regions targeted within the enrichment assay (dark purple). Plots are centered on the 120 bp bait regions (red). The light purple region includes the coverage values of 95% of all enriched regions.
(b) Size distribution of the DNA sequencing insert of the F_2 sample.
(c) Allele frequency estimation of the F_2 sample aligned against the set of 24 254 markers. Symbols/colors are defined in the legend to Figure 3.

(Figure 4). Although such an approximation is not possible using the marker-wise AFEs of the whole-genome sample, the confidence intervals calculated for these data differ only marginally.

SHOREmapping using sequencing data from an enrichment library can thus be performed on a lower number of markers and still result in similar outcomes to whole-genome analysis. This may be explained by the drastic increase of reads per marker (Table 1), compensating for the smaller number of markers and the loss of informative reads aligned to them. However, this effect is limited by the actual allele frequency; once the coverage is sufficiently high to assess the marker-wise allele frequency accurately, an increase in the number of reads will not improve the results. Instead, marker density (and recombination) will determine mapping resolution.

SHOREmapping-by-synteny

As shown above, partial assembly information can be used for mapping-by-sequencing. We utilized only small parts of the reference sequence for design of an enrichment assay and subsequent mapping-by-sequencing. However, the genetic order of these sequences was known, which would not be the case if relying only on RNA-seq assemblies or EST information.

For a proof-of-principle study, we sorted *A. thaliana* ESTs according to their synteny relationships in a relative, *Brassica rapa*. Although *B. rapa* is from the same family, its genome is distinguished from that of *A. thaliana* by several large-scale rearrangements and segmental duplications (Wang *et al.*, 2011). We limited our analysis to markers for which enrichment baits were completely in exons, simulating an exome enrichment experiment (Turner *et al.*, 2009). Consequently, we only used markers derived from transcribed regions.

We used tBLASTx to align 78 096 publically available Arabidopsis cDNAs (ftp://ftp.arabidopsis.org/home/tair/Sequences/ATH_cDNA_EST_sequences_FASTA/ATH_cDNA_sequences_20101108.fas) to the reference genome sequence of *B. rapa*, which diverged from the Arabidopsis lineage at least 30 million years ago (Beilstein *et al.*, 2010). Using the order of cDNAs suggested by the alignment locations of reliable best tBLASTx hits (*E*-value cut-off 1e-05), we built a pseudo reference sequence of 25 819 non-overlapping *A. thaliana* cDNAs. This sequence includes 4375 cDNAs harboring markers that were included in the enrichment design. Although the *B. rapa* and *A. thaliana* genomes are largely syntenic, there are several small-scale rearrangements that interfere with syntenic regions (Wang *et al.*, 2011), and even in syntenic regions, the order of *A. thaliana* cDNAs cannot be expected to be perfect.

Performing mapping-by-sequencing using the enriched F_2 sample and the pseudo reference from the ordered cDNAs revealed multiple regions enriched for the mutant allele on *B. rapa* chromosomes. The *Brassica* lineage underwent a genome triplication after the split from Arabidopsis, followed by extensive reduction in gene number (O'Neill

Table 1 Read pairs at marker regions

	Whole genome	F_2	F_1
Number of markers	461 070	24 254	24 254
Read pairs aligned	26 931 203 (100)	39 350 643 (100)	41 127 254 (100)
Read pairs aligned to targeted regions	n/a	34 576 458 (87.9)	36 344 814 (88.4)
Read pairs aligned to marker	6 650 334 (24.7)	24 406 324 (62.0)	25 676 615 (62.4)
Mean number of reads per marker	14.4	1006.3	1058.7

Reads of all samples were aligned against the reference sequence and scored for overlapping markers and their regions (absolute counts, percentage in parentheses). F_2 and F_1 samples are enriched for 24 254 markers. n/a, not applicable.

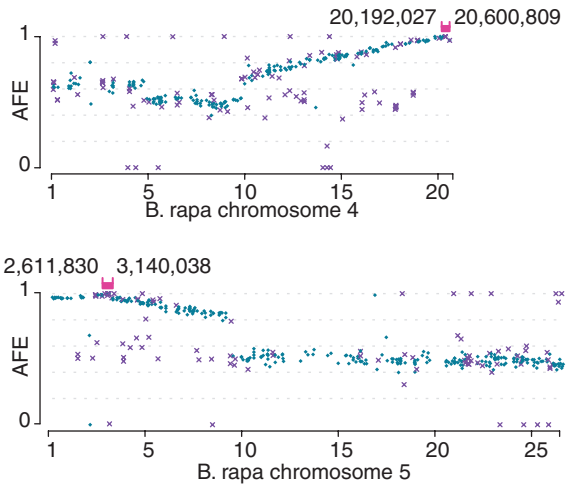

Figure 5. Synteny-based allele frequency estimations using cDNAs as alignment targets.
Allele frequency estimations (AFEs) for the F_2 sample assessed at 4375 marker loci. Short reads were aligned against 25 819 *A. thaliana* cDNAs arranged according to their best BLAST hit against the reference sequence of *B. rapa*. The *x* axis represents the physical map of *B. rapa*. Symbols/colors are defined in the legend to Figure 3.

and Bancroft, 2000). The causal mutation was mapped to two regions on *B. rapa* chromosomes 4 and 5, which are syntenic with *A. thaliana* chromosome 2 (Wang *et al.*, 2011). The likelihood ratio test statistic resulted in confidence intervals spanning 409 and 528 kb, respectively (Figure 5, S6). This region of *A. thaliana* chromosome 2 is partially syntenic with a third region on *B. rapa* chromosome 2. However, because it is incomplete, it cannot yield a valid interval. Determining confidence intervals is confounded by differences in the length of the physical intervals in the two species and differences in microsynteny. However, these intervals are remarkably small and can serve as starting points for further fine-mapping.

To validate our results and to show that these markers enclose the causal region, we aligned the markers that define the borders of the mapping intervals to the *A. thaliana* reference sequence. Both intervals encompassed the causal mutation. The physical distances between these marker pairs in *A. thaliana* are 144 and 181 kb, respectively. These surprisingly small intervals, which are smaller than the ones calculated using the *A. thaliana* reference sequence, result from low marker density, as not all markers are represented in each of the three syntenic regions. Thus, we were able to perform mapping-by-sequencing using synteny information only. We conclude that mapping-by-sequencing is possible in species without a full-length reference sequence and high-density genetic maps, as long as a reasonably syntenic reference genome from a not-too distant relative is available. We note that genomes in the Brassicaceae are particularly variable, and that genomes in many other families, such as the Solanaceae, are much more syntenic (Wu and Tanksley, 2010).

CONCLUSIONS

To date, mapping-by-sequencing has relied on almost complete reference genome sequences and whole-genome resequencing. Using whole-genome sequencing data for a bulked segregant F_2 mapping population, we have shown that alignment against a subset of marker sequences is sufficient for mapping-by-sequencing at a resolution comparable to whole-genome analyses. The drastic increase in read coverage at markers achieved by enrichment more than compensated for the almost 20-fold smaller number of markers.

RNA-seq assemblies or EST libraries cannot be used for mapping-by-sequencing on their own, because they lack genetic order. However, the genetic order can be imputed through homology with related species for which full-length reference sequences are available (Mayer *et al.*, 2011). Syntenic regions will yield a similar order of marker sequences. In our proof-of-principle study, we sorted 25 819 *A. thaliana* cDNAs according to the genomic position of homologs in *B. rapa*, and used 4375 markers for mapping-by-sequencing. The region under investigation is triplicated within the *B. rapa* genome, and markers were sorted to all three syntenic regions. Nevertheless, despite this complication, we easily identified a confidence interval that can be used for targeted fine-mapping. We emphasize that this mapping exercise did not involve the *A. thaliana* genetic map at any stage. The levels of synteny are much higher for many monocot species or other dicot families, such as the Solanaceae, suggesting that SHOREmapping-by-synteny is a promising approach (Mayer *et al.*, 2011).

Similar enrichment sequencing methods, such as genome representation reduction by digestion with restriction endonucleases, are promising and inexpensive alternatives to hybridization-based methods. However, it is less straightforward to combine them with established marker sets (Baird *et al.*, 2008). Further, targeted enrichment sequencing allows simultaneous analysis of candidate regions and gene sets, which is not possible when using genome digestion (Mokry *et al.*, 2011). However, without any knowledge about candidate genes, reducing genome complexity comes at the cost of not being able to simultaneously identify the causal mutation, as it is unlikely to be included in the targeted portion of the genome. Additional fine-mapping approaches beyond *in silico* efforts are therefore required. To minimize the workload for this laborious process, the size of the candidate interval must be as small as possible, without risking exclusion of the causal region. So far, candidate intervals have been arbitrarily selected based on ad hoc interpretation of allele frequency maps (Schneeberger *et al.*, 2009a; Austin *et al.*, 2011). We have introduced likelihood ratio tests that support conversion of local allele frequency

estimates into confidence mapping intervals. This method is robust against outliers and can self-adjust for occasional mis-phenotyping.

Alternatively, with low-fold coverage whole-genome sequencing of bulked segregant mapping populations, all markers, not only those targeted by enrichment or those near restriction sites, contribute to the interval detection. Combining such markers in sliding windows can compensate for the lack of deep sequence information (Nijman *et al.*, 2010). However, some crosses suffer from low marker density because of recent shared ancestry, reducing the information obtained by whole-genome sequencing. Thus, even in species with small or medium-sized genomes, marker enrichment can be advantageous. This is particularly evident when selection of the mapping population was based on a trait with complex genetics. Higher read coverage is required to effectively counteract the variation introduced by random sampling and to more precisely estimate local allele frequency differences. Sequencing of pooled populations under artificial selection has been successfully performed in yeast and *Drosophila* (Ehrenreich *et al.*, 2010; Turner *et al.*, 2011; Parts *et al.*, 2011). This requires very large numbers of individuals and generations. This has not yet been attempted in plants, but, as sequencing costs fall further, the savings could be invested in growing and phenotyping much larger panels of plants.

EXPERIMENTAL PROCEDURES

Plant material and growth conditions

The *fd-1*, *fd-2* and *soc1-2* mutant lines are described in Table S2. The T-DNA insertion lines were confirmed by PCR-based genotyping using specific oligonucleotides (Table S3). Except for the M_1 and M_2 populations, which were grown in the greenhouse, plants were grown in growth chambers in a controlled environment (23°C, 65% relative humidity). Plants were raised on soil under a mixture of Cool White and Gro-Lux Wide Spectrum fluorescent lights (Sylvania, http://www.sylvania-lighting.com/), with a fluence rate of 125–175 μmol m^{-2} sec^{-1} and long-day photoperiods (16 h light/8 h dark).

Mutant isolation

A *SUC2::FT* construct (Mathieu *et al.*, 2007) was transformed into the *fd-2* mutant obtained from the SALK T-DNA insertion collection (Table S2) to create a single-insertion, non-segregant early-flowering line (*SUC2::FT fd-2*). Seeds from this line were mutagenized using 0.2/0.3% ethyl methanesulfonate (EMS) for 16 h as described previously. Approximately 10 000 M_1 plants were grown on soil supplemented with glufosinate (BASTA) in the greenhouse (Weigel, D., and Glazebrook, J.,). M_2 seeds were collected from pools of approximately 50 M_1 individuals. M_2 plants were screened in the greenhouse, and six mutants for which late flowering was later confirmed in the M_3 generation were used for further analysis.

Complementation

The *SUC2::FT* construct (pJM69) has been described previously (Mathieu *et al.*, 2007). The 8.2 kb genomic *SOC1* (At2g45660) rescue construct, encompassing approximately 4.5 kb promoter, all exons and introns, and approximately 1.2 kb downstream sequence, was amplified from genomic Col-0 DNA using Phusion polymerase (New England Biolabs, www.neb.com) and oligos G-27271 and G-27272 (Table S3). The amplified fragment was purified using the Wizard SV Gel and PCR Clean-Up System (Promega, http://www.promega.com/) and ligated into TOPO vector (Invitrogen, http://www.invitrogen.com/) to create pDP29. The entry vector was digested using *Pvu*II (Fermentas, http://www.fermentas.com/), and the fragment containing g*SOC1* and the Gateway recombination sites was purified and subsequently recombined into a Gateway-compatible pGREEN-IIS binary vector (pFK205, providing resistance against kanamycin), resulting in a vector suitable for plant transformation (pPS01).

For plant transformation, constructs were introduced into *Agrobacterium tumefaciens* strain ASE by electroporation, and plated on LB medium supplemented with appropriated antibiotics. Plants were transformed by the floral-dip method (Clough and Bent, 1998). Transgenic plants were selected using 0.1% BASTA (www.bayer.com) directly on soil or with 50 μg ml kanamycin in half-strength Murashige & Skoog medium (Sigma-Aldrich, http://www.sigmaaldrich.com/).

Agilent bait design

We identified SNPs in conserved regions from whole-genome assemblies of L*er*-1 and C24 (Schneeberger *et al.*, 2011) (see Table S4 for all criteria). This ensured that the focal SNPs were accessible through short read alignments. It also prevented misalignments that would affect AFEs. Both alleles in 24 254 regions were used as input for Agilent's bait design file (https://earray.chem.agilent.com/earray/).

Library preparation and Illumina sequencing

Genomic DNA was extracted using a DNeasy plant mini kit (Qiagen, http://www.qiagen.com/) and resuspended in TE buffer (Tris 10mM EDTA 1mM pH 8.0). For preparation of paired-end DNA libraries, 1000 ng genomic DNA were fragmented to a mean length of 200 bp using a Covaris S2 instrument (Covaris, www.covarisinc.com). The pre-hybridization library was prepared using the NEB Next DNA Sample Prep Reagent Set 1 (New England Biolabs), according to the instructions provided with the SureSelect Target Enrichment System for Illumina paired-end sequencing library, version 2.0.1 (Agilent). PE Adapter Oligo Mix was ligated to the fragmented DNA, and the pre-hybridization library was amplified using PCR primers PE 1.0 and 2.0 from the PE DNA Sample Prep Kit (Illumina). Enrichment of DNA at target marker positions was performed using the SureSelect Target Enrichment System for Illumina Paired-End Sequencing Library according to the manufacturer's instructions. After enrichment, the post-hybridization library was amplified using Phusion high-fidelity DNA polymerase (New England Biolabs) and SureSelect GA primers in a reaction comprising 12 PCR cycles. Sequencing was performed on an Illumina GAIIx instrument with 2 × 101 bp paired-end reads.

Short-read mapping and consensus calling

Raw short read sequencing data were quality-filtered and trimmed using SHORE (Ossowski *et al.*, 2008). Resequencing was performed with the GenomeMapper alignment tool (Schneeberger *et al.*, 2009b) and SHORE as the consensus calling program (Ossowski *et al.*, 2008). Depending on the application, we used either the complete reference sequence (whole-genome sample) or the 800 bp surrounding all or some of the SNP markers selected for the enrichment design (F_1 and F_2 sample) as the alignment target. Experiments were performed with default parameter settings,

except that *shore consensus* was run with the additional parameter, v, to retain the intermediate data required for SHOREmap.

Calculation of allele frequency estimations (AFEs)

AFEs were calculated at marker positions as the number of alignments supporting the mutant parental allele divided by the sum of alignments supporting either of the parental alleles. Sliding-window AFE calculations combined all alignments for both alleles at all markers in a sliding window, and AFEs were based on these counts. 10 kb sliding windows were calculated every 10 kb.

Model for allele frequency estimations

The mostly heterozygous nature of mapping populations allows observation of both parental alleles at most marker locations. For each marker, the percentages of alignments represent the two parental alleles are termed $p_{1,\mathrm{obs}}$ and $p_{2,\mathrm{obs}}$, respectively. Misplaced alignments can skew these observations from the underlying parental allele frequency. In order to remove such artifacts, we introduced outlier filtering by estimating the mean AFE in 200 kb windows centered on each marker. The tested marker itself was excluded from these calculations. Each marker that had a probability (after adjustment for multiple testing) below 0.05 of being sampled from an allele frequency similar to the mean AFE of the respecitive window was discarded. In addition, sequencing errors may introduce reads supporting the two remaining (non-existing) alleles. The observed percentage of such reads compared to all reads aligned to a marker is termed $\varepsilon_{\mathrm{obs}}$. As sequencing errors also cause transitions between the two parental alleles, only two-thirds of the sequencing errors support the non-parental alleles. It has been shown that Illumina sequencing errors are biased, but, as this effect is minor, we assume equal sequencing error transition rates between all nucleotides (Ossowski *et al.*, 2008). Altogether, we define the observed frequencies, $p_{1,\mathrm{obs}}$, $p_{2,\mathrm{obs}}$ and $\varepsilon_{\mathrm{obs}}$, as functions of the true frequency of the parent P_1 and the total error probability ε:

$$\begin{aligned} p_{1,\mathrm{obs}}(P_1,\varepsilon) &= P_1\left(1-\frac{4\varepsilon}{3}\right)+\frac{\varepsilon}{3} \\ p_{2,\mathrm{obs}}(P_1,\varepsilon) &= 1-P_1\left(1-\frac{4\varepsilon}{3}\right)+\varepsilon \\ \varepsilon_{\mathrm{obs}}(P_1,\varepsilon) &= \frac{2\varepsilon}{3} \end{aligned} \quad (1)$$

A major effect influencing observed marker frequencies is random sampling. This can be modeled using a likelihood function consisting of the probability of sampling the observed counts of reads given P_1 and ε. Observed read counts for marker i are indicated by $x_i = (P_{1,\mathrm{count}}, P_{2,\mathrm{count}}, \varepsilon_{\mathrm{count}})$, and $\mathrm{Mult}(p_i|x_i)$ indicates the probability of observing the probabilities p_i given x_i and a multinomial distribution. Then, the likelihood function describing the likeliness L of allele frequencies for a given window can written be as:

$$L(P_1,\varepsilon|x_1\ldots x_n)=\prod_{i=1}^{n}\mathrm{Mult}\left(p_{1,\mathrm{obs}}(P_1,\varepsilon),p_{2,\mathrm{obs}}(P_1,\varepsilon),\varepsilon_{\mathrm{obs}}(P_1,\varepsilon)|x_i\right) \quad (2)$$

Using equation (2) and the known estimate of the multinomial distribution, it is possible to calculate the most likely frequency of P_1 for every arbitrary set of markers and observed allele frequencies.

Confidence interval calculation

For the set of 50 kb windows evenly spaced by 10 kb, the underlying allele frequencies were estimated, and the window with the frequency closest to the target frequency was selected as starting point for the interval estimation. If this procedure resulted in multiple candidate windows, the middle window was selected. The initial interval consisted of ten markers centered on the marker closest to the mean position of the markers in the selected window.

We then applied a maximum-likelihood estimator to estimate the ε parameter for the given interval while keeping P_1 fixed at the expected frequency. The likelihood-value was then calculated and used as a null hypothesis in a likelihood ratio test. This was contrasted to the likelihood-value when both P_1 and ε were estimated. Assuming that the quota was χ^2-distributed with one degree of freedom allowed calculation of the *P*-value for rejection of the null hypothesis. The initial interval was iteratively extended up- and downstream to include as many markers as possible under the constraint that the rejection probability cannot exceed the confidence value. The extension was performed by first adding a set of markers up- and downstream to bypass smaller local dips introduced, for instance, by markers with reads mapped to multiple loci. Afterwards, one marker at a time was added to refine the borders of the interval. Finally, heuristic optimizations were used to find the largest valid interval and to further extend the window. Table S5 shows the command line calls for SHOREmap.

ACKNOWLEDGEMENTS

The authors would like to thank Benjamin Stich (Max Planck Institute for Plant Breeding Research) for helpful discussions regarding confidence interval calculations, Daniel Horrer and Johanna Weirich (Max Planck Institute for Developmental Biology) for help with the screen, and the anonymous reviewers for helpful suggestions. This work was supported by FP7 Collaborative Project AENEAS (contract KBBE-2009-226477), a Deutsche Forschungsgemeinschaft SPP1530 grant (SCHN1257/1-1), a Gottfried Wilhelm Leibniz Award from the Deutsche Forschungsgemeinschaft, and the Max Planck Society.

SUPPORTING INFORMATION

Additional Supporting Information may be found in the online version of this article:

Figure S1. Original SHOREmap output applied on the whole-genome sample using 461,070 markers.

Figure S2. Effect of random sampling.

Figure S3. Effect of changes in the seed region size on the confidence interval size.

Figure S4. Effect of changes in the outlier filtering window size on the confidence interval size.

Figure S5. Original SHOREmap output applied to the enriched F_2 sample with 24 254 markers.

Figure S6. Original SHOREmap output applied to the enriched F_2 sample with 4375 markers and cDNAs ordered along the reference sequence of *B. rapa* as alignment targets.

Table S1. Bait design.

Table S2. Mutants.

Table S3. Oligonucleotides.

Table S4. Bait region selection criteria.

Table S5. SHOREmap command line calls.

Please note: As a service to our authors and readers, this journal provides supporting information supplied by the authors. Such materials are peer-reviewed and may be re-organized for online delivery, but are not copy-edited or typeset. Technical support issues arising from supporting information (other than missing files) should be addressed to the authors.

REFERENCES

Abe, M., Kobayashi, Y., Yamamoto, S. *et al.* (2005) FD, a bZIP protein mediating signals from the floral pathway integrator FT at the shoot apex. *Science*, **309**, 1052–1056.

Arabidopsis Genome Initiative (2000) Analysis of the genome sequence of the flowering plant *Arabidopsis thaliana*. *Nature*, **408**, 796–815.

Austin, R.S., Vidaurre, D., Stamatiou, G. *et al.* (2011) Next-generation mapping of Arabidopsis genes. *Plant J.* **67**, 715–725.

Baird, N.A., Etter, P.D., Atwood, T.S. *et al.* (2008) Rapid SNP discovery and genetic mapping using sequenced RAD markers. *PLoS ONE*, **3**, e3376.

Beilstein, M.A., Nagalingum, N.S., Clements, M.D., Manchester, S.R. and Mathews, S. (2010) Dated molecular phylogenies indicate a Miocene origin for *Arabidopsis thaliana*. *Proc. Natl Acad. Sci. USA*, **107**, 18724–18728.

Bigelow, H., Doitsidou, M., Sarin, S. and Hobert, O. (2009) MAQGene: software to facilitate *C. elegans* mutant genome sequence analysis. *Nat. Methods*, **6**, 549.

Blumenstiel, J.P., Noll, A.C., Griffiths, J.A. *et al.* (2009) Identification of EMS-induced mutations in *Drosophila melanogaster* by whole-genome sequencing. *Genetics*, **182**, 25–32.

Clough, S.J. and Bent, A.F. (1998) Floral dip: a simplified method for *Agrobacterium*-mediated transformation of *Arabidopsis thaliana*. *Plant J.* **16**, 735–743.

Ehrenreich, I.M., Torabi, N., Jia, Y. *et al.* (2010) Dissection of genetically complex traits with extremely large pools of yeast segregants. *Nature*, **464**, 1039–1042.

Elshire, R.J., Glaubitz, J.C., Sun, Q. *et al.* (2011) A robust, simple genotyping-by-sequencing (GBS) approach for high diversity species. *PLoS ONE*, **6**, e19379.

Etter, P.D., Preston, J.L., Bassham, S., Cresko, W.A. and Johnson, E.A. (2011) Local *de novo* assembly of RAD paired-end contigs using short sequencing reads. *PLoS ONE*, **6**, e18561.

Gnirke, A., Melnikov, A., Maguire, J. *et al.* (2009) Solution hybrid selection with ultra-long oligonucleotides for massively parallel targeted sequencing. *Nat. Biotechnol.* **27**, 182–189.

Kardailsky, I., Shukla, V.K., Ahn, J.H. *et al.* (1999) Activation tagging of the floral inducer FT. *Science*, **286**, 1962–1965.

Kobayashi, Y., Kaya, H., Goto, K., Iwabuchi, M. and Araki, T. (1999) A pair of related genes with antagonistic roles in mediating flowering signals. *Science*, **286**, 1960–1962.

Lee, H., Suh, S.S., Park, E. *et al.* (2000) The AGAMOUS-LIKE 20 MADS domain protein integrates floral inductive pathways in Arabidopsis. *Genes Dev.* **14**, 2366–2376.

Mathieu, J., Warthmann, N., Küttner, F. and Schmid, M. (2007) Export of FT Protein from Phloem Companion Cells Is Sufficient For Floral Induction in Arabidopsis. *Curr Biol* **17**, 1055–1060.

Mayer, K.F., Martis, M., Hedley, P.E. *et al.* (2011) Unlocking the barley genome by chromosomal and comparative genomics. *Plant Cell*, **23**, 1249–1263.

Michelmore, R.W., Paran, I. and Kesseli, R.V. (1991) Identification of markers linked to disease-resistance genes by bulked segregant analysis: a rapid method to detect markers in specific genomic regions by using segregating populations. *Proc. Natl Acad. Sci. USA*, **88**, 9828–9832.

Mokry, M., Nijman, I.J., van Dijken, A. *et al.* (2011) Identification of factors required for meristem function in Arabidopsis using a novel next generation sequencing fast forward genetics approach. *BMC Genomics*, **12**, 256.

Nijman, I.J., Mokry, M., van Boxtel, R. *et al.* (2010) Mutation discovery by targeted genomic enrichment of multiplexed barcoded samples. *Nat. Methods*, **7**, 913–915.

O'Neill, C.M. and Bancroft, I. (2000) Comparative physical mapping of segments of the genome of *Brassica oleracea* var. *alboglabra* that are homoeologous to sequenced regions of chromosomes 4 and 5 of *Arabidopsis thaliana*. *Plant J.* **23**, 233–243.

Onouchi, H., Igeño, M.I., Périlleux, C., Graves, K. and Coupland, G. (2000) Mutagenesis of plants overexpressing *CONSTANS* demonstrates novel interactions among Arabidopsis flowering-time genes. *Plant Cell*, **12**, 885–900.

Ossowski, S., Schneeberger, K., Clark, R.M. *et al.* (2008) Sequencing of natural strains of *Arabidopsis thaliana* with short reads. *Genome Res.* **18**, 2024–2033.

Parts, L., Cubillos, F.A., Warringer, J. *et al.* (2011) Revealing the genetic structure of a trait by sequencing a population under selection. *Genome Res.* **21**, 1131–1138.

Schneeberger, K., Ossowski, S., Lanz, C. *et al.* (2009a) SHOREmap: simultaneous mapping and mutation identification by deep sequencing. *Nat. Methods*, **6**, 550–551.

Schneeberger, K., Hagmann, J., Ossowski, S. *et al.* (2009b) Simultaneous alignment of short reads against multiple genomes. *Genome Biol.* **10**, R98.

Schneeberger, K., Ossowski, S., Ott, F. *et al.* (2011) Reference-guided assembly of four diverse *Arabidopsis thaliana* genomes. *Proc. Natl Acad. Sci. USA*, **108**, 10249–10254.

Turner, E.H., Lee, C., Ng, S.B., Nickerson, D.A. and Shendure, J. (2009) Massively parallel exon capture and library-free resequencing across 16 genomes. *Nat. Methods*, **6**, 315–316.

Turner, T.L., Stewart, A.D., Fields, A.T., Rice, W.R. and Tarone, A.M. (2011) Population-based resequencing of experimentally evolved populations reveals the genetic basis of body size variation in *Drosophila melanogaster*. *PLoS Genet.* **7**, e1001336.

Wang, X., Wang, H., Wang, J. *et al.* (2011) The genome of the mesopolyploid crop species *Brassica rapa*. *Nat. Genet.* **43**, 1035–1039.

Weigel, D. and Glazebrook, J. (2002) *Arabidopsis: A Laboratory Manual*. Cold Spring Harbor, NY: Cold Spring Harbor Laboratory Press.

Willing, E.M., Hoffmann, M., Klein, J.D., Weigel, D. and Dreyer, C. (2011) Paired-end RAD-seq for *de novo* assembly and marker design without available reference. *Bioinformatics*, **27**, 2187–2193.

Wu, F. and Tanksley, S. (2010) Chromosomal evolution in the plant family Solanaceae. *BMC Genomics*, **11**, 182.

Zuryn, S., Le Gras, S., Jamet, K. and Jarriault, S. (2010) A strategy for direct mapping and identification of mutations by whole genome sequencing. *Genetics*, **186**, 427–430.

Development 139, 4072-4082 (2012) doi:10.1242/dev.080879

Spatial control of flowering by DELLA proteins in *Arabidopsis thaliana*

Vinicius C. Galvão, Daniel Horrer*, Frank Küttner and Markus Schmid‡

SUMMARY

The transition from vegetative to reproductive development is a central event in the plant life cycle. To time the induction of flowering correctly, plants integrate environmental and endogenous signals such as photoperiod, temperature and hormonal status. The hormone gibberellic acid (GA) has long been known to regulate flowering. However, the spatial contribution of GA signaling in flowering time control is poorly understood. Here we have analyzed the effect of tissue-specific misexpression of wild-type and GA-insensitive (*della*Δ*17*) DELLA proteins on the floral transition in *Arabidopsis thaliana*. We demonstrate that under long days, GA affects the floral transition by promoting the expression of flowering time integrator genes such as *FLOWERING LOCUS T* (*FT*) and *TWIN SISTER OF FT* (*TSF*) in leaves independently of *CONSTANS* (*CO*) and *GIGANTEA* (*GI*). In addition, GA signaling promotes flowering independently of photoperiod through the regulation of *SQUAMOSA PROMOTER BINDING PROTEIN-LIKE* (*SPL*) genes in both the leaves and at the shoot meristem. Our data suggest that GA regulates flowering by controlling the spatial expression of floral regulatory genes throughout the plant in a day-length-specific manner.

KEY WORDS: Gibberellic acid, Flowering, DELLA, *Arabidopsis thaliana*

INTRODUCTION

Since its discovery in the 1930s, giberellic acid (GA) has been shown to affect such diverse biological processes as seed germination, root development, cell elongation, flower development and flowering time (Davies, 2004). However, only recently have we begun to understand the molecular mechanisms that underlie GA signaling. GA is perceived by its receptor, GID1, which undergoes conformational changes after binding to bioactive GA. These changes facilitate the interaction between GID1 and DELLA proteins, which ultimately results in their degradation (Fu et al., 2004; Griffiths et al., 2006; Willige et al., 2007; Murase et al., 2008). The DELLA proteins have been named after a conserved motif of five amino acids in their N-terminal region (Peng et al., 1997; Silverstone et al., 1998; Dill et al., 2001), which were later shown to be required for interaction with GID1 (Griffiths et al., 2006; Willige et al., 2007; Murase et al., 2008). Deletion of the DELLA motif confers dwarfism and dark green color, similar to mutants with impaired GA biosynthesis, such as *ga1-3*. However, in contrast to *ga1-3*, deletion of the DELLA domain cannot be fully rescued by exogenous GA (Koornneef and van der Veen, 1980; Koornneef et al., 1985; Peng et al., 1997).

The *Arabidopsis thaliana* genome contains five DELLA genes, *GIBBERELLIC ACID INSENSITIVE* (*GAI*), *REPRESSOR OF ga1-3* (*RGA*), *RGA-LIKE1* (*RGL1*), *RGL2* and *RGL3*, that exhibit partial functional redundancy (Dill and Sun, 2001; Lee et al., 2002; Bolle, 2004; Gallego-Bartolome et al., 2010). Gene expression analysis has demonstrated that hundreds of genes are differentially expressed in response to GA and that this response is DELLA-dependent (Ogawa et al., 2003; Willige et al., 2007). However, DELLA proteins exert their function mainly by regulating transcription factor activity through protein-protein interactions (Daviere et al., 2008; de Lucas et al., 2008; Feng et al., 2008).

The role of GA in regulating flowering was first studied by the application of GA to plants (Lang, 1957; Langridge, 1957). Only later, after the isolation of GA biosynthesis and signaling mutants, such as *ga1-3*, could the GA-mediated control of flowering be investigated in detail (Koornneef and van der Veen, 1980; Sun et al., 1992; Wilson et al., 1992). *ga1-3* mutants completely failed to flower when grown under short-day (SD) conditions, whereas flowering was only moderately delayed under long-day (LD) conditions (Wilson et al., 1992), suggesting that GA was not required to induce flowering under inductive photoperiod. However, more recent analyses strongly indicate that GA contributes to the regulation of flowering time in *A. thaliana* in response to LD conditions after all (Griffiths et al., 2006; Willige et al., 2007; Hisamatsu and King, 2008; Osnato et al., 2012; Porri et al., 2012).

The role of *FLOWERING LOCUS T* (*FT*) in mediating flowering in response to inductive photoperiod has well been documented. It is now widely accepted that the FT protein acts as a florigen and conveys the information to induce flowering from the leaves to the shoot meristem (Wigge et al., 2005; Corbesier et al., 2007; Jaeger and Wigge, 2007; Mathieu et al., 2007; Tamaki et al., 2007; Liu et al., 2012). At the shoot meristem, FT interacts with 14-3-3 proteins and the bZIP transcription factor FD to form a heterotrimeric complex that is thought to bind to the regulatory regions of target genes to trigger the transition to the reproductive phase (Abe et al., 2005; Wigge et al., 2005; Taoka et al., 2011).

Besides FT, the SQUAMOSA PROMOTER BINDING PROTEIN-LIKE (SPL) transcription factors have been shown to regulate flowering (Cardon et al., 1997; Wang et al., 2009; Yamaguchi et al., 2009). The *A. thaliana* genome contains 17 *SPL*-like genes, 11 of which are targets of microRNA156 (miR156) (Rhoades et al., 2002; Guo et al., 2008). The levels of mature

Max Planck Institute for Developmental Biology, Spemannstrasse 35, 72076 Tübingen, Germany.

*Present address: Institute of Plant Biology, University of Zürich, Zollikerstrasse 107, CH-8008 Zürich, Switzerland
‡Author for correspondence (markus.schmid@tuebingen.mpg.de)

Accepted 7 August 2012

miR156 decrease as a plant ages. As a consequence, *SPL* transcripts become more abundant, which ultimately induces flowering (Wang et al., 2009). The regulation of flowering by *SPLs* is in part due to the induction of miR172 (Wu et al., 2009). miR172 targets mRNAs of *APETALA2*-like (*AP2*-like) genes, which regulate flowering by directly binding to and repressing genes such as *FT* and *SUPPRESSOR OF OVEREXPRESSION OF CONSTANS 1* (*SOC1*) (Aukerman and Sakai, 2003; Schmid et al., 2003; Chen, 2004; Schwab et al., 2005; Mathieu et al., 2009; Yant et al., 2010).

In contrast to this detailed picture of the regulation of flowering by photoperiod and age, little is known about how the floral transition is regulated by GA. To address this question we carried out a comprehensive analysis of the regulation of flowering by DELLA proteins under both SD and LD conditions. Our results indicate that under LD conditions the DELLA proteins regulate the expression of flowering time genes in leaves and at the shoot meristem. By contrast, the effects of DELLA proteins on flowering under SD conditions seem to be limited to the shoot meristem.

MATERIALS AND METHODS

Plant material

Wild-type plants used in this work are of the Columbia (Col-0) and Landsberg erecta (L*er*) accessions. The mutants *ga1-3*, *rga-24*, *gai-t6*, *rga-t2*, *rgl1-1*, *rgl2-1*, *gai-1* and *sly1-10* are in L*er* background and have been described (Koornneef et al., 1985; Sun et al., 1992; Peng and Harberd, 1993; Peng et al., 1997; Silverstone et al., 1998; Lee et al., 2002; McGinnis et al., 2003; Achard et al., 2007). The triple *gid1a-c* mutant, *ft-10*, *tsf-1*, *pFT:GUS* and *p35S:MIM172* are in Col-0 background (Takada and Goto, 2003; Michaels et al., 2005; Yoo et al., 2005; Willige et al., 2007; Todesco et al., 2010). Genotypes were confirmed by PCR using published oligonucleotides (supplementary material Table S1).

Growth conditions and plant transformation

All plants were grown in chambers in controlled photoperiod at 16°C or 23°C, 65% humidity and a mixture of Cool White and Gro-Lux Wide Spectrum fluorescent lights, with a fluence rate of 125 to 175 μmol m^{-2} s^{-1}. LD conditions are defined as 16 hours light/8 hours dark and SD conditions as 8 hours light/16 hours dark.

Plant transformation was carried out as previously described (Clough and Bent, 1998). Transgenic T1 plants were raised on soil or MS medium supplemented with 0.1% glufosinate (BASTA) or 50 μg/ml kanamycin, respectively, after stratification for 4 days at 4°C in darkness. For germination of *gid1a-1 gid1b-1 gid1c-2* triple mutant, the seed coat was manually removed. *ga1-3* plants were germinated by treatment with 50 μM GA_3 in 0.1% agarose. GA_3 stock solutions were prepared in pure ethanol and working solutions containing 0.01% (v/v) Tween-20 (Sigma-Aldrich) were prepared in distilled water. After 3 days of incubation in darkness at 4°C, the seeds were washed at least ten times with distilled water to remove excess GA_3. Treatment of plants was performed by spraying with 50 μM GA_3.

Molecular cloning

All nucleotides and constructs used in this work are listed in supplementary material Tables S1 and S2. All constructs were confirmed by Sanger sequencing. For misexpression of *GA2ox8*, the open reading frame (ORF) was amplified from cDNA using Phusion High-Fidelity DNA Polymerase (New England Biolabs) and oligonucleotides G-31688 and G-31689. The fragment was purified and ligated into the Gateway-compatible vector pJLSmart to create pVG-412, and subsequently used for recombination into pGREEN-IIS destination vector (Mathieu et al., 2007) containing the *SUC2* promoter to create the construct pVG-417.

The complete ORFs of the five DELLA genes (*RGA*, *GAI*, *RGL1*, *RGL2*, *RGL3*) were amplified directly from *A. thaliana* genomic DNA with specific oligonucleotides. The amplified PCR products were cloned into Gateway-compatible vector pJLSmart using T4 DNA ligase (Fermentas) to create the entry vectors pVG-156, pVG-157, pVG-158, pVG-159 and pVG-160. The 17-amino-acid deletion in RGL1, RGL2 and RGL3 to create GA-insensitive DELLA was created by overlapping PCR. First, the two halves of the ORFs were amplified separately using the oligonucleotides G-25736/G-25731 and G-25732/G-25735 (*RGL1*), G-25739/G-25737 and G-25738/G-25740 (*RGL2*), and G-25743/G-25746 and G-25744/G-25745 (*RGL3*). The two fragments were fused in a second PCR using forward and reverse oligonucleotides G-25733/G-25734 (*RGL1*), G-25741/G-25742 (*RGL2*) and G-25747/G-25748 (*RGL3*). *GAI* and *RGA* deletions were amplified directly from genomic DNA of *rgaΔ17* and *gai-1*. The amplified fragments were ligated into pJLSmart using T4 DNA ligase to create the entry vectors pVG-104, pVG-105, pVG-118, pVG-119 and pVG-120. Expression vectors suitable for plant transformation were created by recombination into pGREEN-IIS plant binary destination vectors (Mathieu et al., 2007) containing the *SUC2*, *FD* and *CLV3* promoters, respectively (supplementary material Table S2).

Expression analysis

Total RNA was extracted using either the RNeasy Kit (Qiagen) or TRIZOL reagent (Invitrogen) according to the manufacturer's instructions. At least 600 ng total RNA was treated with DNase I and used for cDNA synthesis using oligo (dT) and the RevertAid First Strand cDNA Synthesis Kit (Fermentas). Quantitative real-time PCR (qPCR) was performed using the Platinum SYBR Green qPCR Supermix-UDG (Invitrogen) and specific oligonucleotides (supplementary material Table S1) on an MJR Opticon Continuous Fluorescence Detection System. Expression was normalized against *A. thaliana β-TUBULIN* or *ACTIN 2*, and expression differences were calculated using the ΔΔCT method. For each sample, material from a minimum of 15 seedlings was pooled per replicate and at least two biological and two technical replicates were used for the analysis. A minimum of 40 apical meristems was dissected for each biological replicate for RNA extraction.

Small RNA northern blots were performed using 2 μg total RNA resolved on a 17% polyacrylamide gel in denaturing conditions (7 M urea). The RNA was transferred to HyBond-N^+ membranes and hybridized with digoxigenin-labeled oligonucleotides (supplementary material Table S1). Probe labeling was carried out using the DIG Oligonucleotide 3′-End Labeling Kit, 2nd generation (Roche). microRNA quantitative PCR was performed as previously described (Chen et al., 2005).

GUS staining was performed as described (Blazquez et al., 1997) and pictures obtained using the Leica MZ FLIII microscope. Transcriptome analysis was performed using publicly available data downloaded from AtGenExpress (Schmid et al., 2005).

RESULTS

DELLA proteins repress flowering under LD photoperiod

Genetic analyses have shown that *DELLA* genes have partially overlapping function in controlling various aspects of plant development (Dill and Sun, 2001; Lee et al., 2002; Cheng et al., 2004; de Lucas et al., 2008; Feng et al., 2008); however, their relative contribution to the regulation of flowering under inductive photoperiod is still unclear. To address this question we first analyzed the effect of *della* gain- and loss-of-function mutations on flowering time. We observed that under LD conditions, the loss-of-function mutants *gai-t6* and *rga-24* flowered early with 9.9±0.8 and 9.9±0.5 leaves, respectively, compared with wild type, which produced 11.3±0.6 leaves ($P<0.00001$, unpaired *t*-test; Table 1). However, these single mutants still flowered later than wild-type plants treated with 50 μM GA_3, which produced 7.8±0.9 leaves. In agreement with the notion of functional redundancy among the *DELLA* genes, early flowering was enhanced in a *gai-t6 rga-24* double mutant and a *ga1-3 gai-t6 rga-t2 rgl1-1 rgl2-1* pentuple mutant, which produced 8.6±0.7 and 7.6±0.9 leaves, respectively ($P<0.00001$; Table 1 and supplementary material Fig. S1A,B). By contrast, the semi-dominant GA-insensitive *gai-1* allele flowered considerably late with about 16.8±1.0 leaves ($P<0.00001$; Table 1

Table 1. Flowering time of plants used in this study

Genotype	RL	CL	Total	Deviation	Range	*n*
Experiment 1						
Ler-1	8.3	3.0	11.3	0.6	10-12	17
ga1-3	10.9	2.9	13.7	0.8	13-15	7
gai-t6	7.0	2.9	9.9	0.8	8-11	25
rga-24	6.9	3.0	9.9	0.5	9-11	25
gai-t6 rga-24	5.7	2.9	8.6	0.7	7-10	25
ga1-3 gai-t6 rga-t2 rgl1-1 rgl2-1	4.5	3.1	7.6	0.9	6-9	20
Ler-1 (GA_3 50 μM)	5.2	2.6	7.8	0.9	7-9	10
gai-1	14.5	2.3	16.8	1.0	16-19	16
Experiment 2						
Col-0	11.1	3.0	14.1	1.0	12-16	22
Col-0 (GA_3 50 μM)	8.1	3.4	11.5	1.1	8-13	20
gid1b-1 gid1c-2	13.5	2.8	16.3	1.1	14-18	19
gid1a-1 gid1b-1 gid1c-2	n.a.	n.a.	n.a.	n.a.	n.a.	8
Experiment 3						
Col-0	10.1	2.7	12.8	1.8	9-16	29
pSUC2:RGA (T1)	15.1	3.2	18.3	3.3	10-23	26
pSUC2:rgaΔ17 (T1)	15.6	4.4	20.0	3.4	14-28	18
pSUC2:GAI (T1)	14.2	3.2	17.4	3.3	12-23	26
pSUC2:gaiΔ17 (T1)	12.3	2.8	15.1	1.8	13-18	25
pSUC2:RGL1 (T1)	15.1	4.0	19.1	2.9	12-23	27
pSUC2:rgl1Δ17 (T1)	14.5	3.8	18.3	3.2	12-23	18
pSUC2:RGL2 (T1)	14.1	3.8	17.9	3.9	12-23	28
pSUC2:rgl2Δ17 (T1)	17.2	5.1	22.3	1.8	12-33	30
pSUC2:RGL3 (T1)	15.0	3.9	18.9	4.0	13-23	33
pSUC2:rgl3Δ17 (T1)	18.1	4.2	22.3	4.5	14-30	27
Experiment 4						
Col-0	10.7	2.8	13.5	1.3	11-16	24
pFD:RGA (T1)	11.0	1.9	12.9	1.9	9-19	52
pFD:rgaΔ17 (T1)	29.4	0.3	29.7	8.0	14-52	*21*
pFD:GAI (T1)	11.6	2.0	13.6	2.5	9-20	*51*
pFD:gaiΔ17 (T1)	25.0	0.4	25.4	10.4	13-52	*49*
pFD:RGL1 (T1)	11.2	1.8	13.0	2.4	9-22	*51*
pFD:rgl1Δ17 (T1)	20.3	0.8	21.1	4.6	10-35	*55*
pFD:RGL2 (T1)	11.1	2.0	13.1	1.8	9-17	*37*
pFD:rgl2Δ17 (T1)	21.0	0.5	21.5	8.5	7-40	*46*
pFD:RGL3 (T1)	10.9	2.2	13.1	2.6	9-22	*39*
pFD:rgl3Δ17 (T1)	11.7	1.7	13.4	2.2	10-19	*26*
pCLV3:RGA (T1)	10.0	2.8	12.8	1.4	10-15	35
pCLV3:rgaΔ17 (T1)	19.7	8.1	27.8	10.1	11-46	44
pCLV3:GAI (T1)	11.1	2.8	13.9	1.5	9-17	48
pCLV3:gaiΔ17 (T1)	17.5	5.6	23.1	8.0	12-42	45
pCLV3:RGL1 (T1)	11.3	2.8	14.1	1.7	11-18	42
pCLV3:rgl1Δ17 (T1)	17.6	5.6	23.2	7.4	13-41	48
pCLV3:RGL2 (T1)	10.9	2.5	13.4	0.9	12-15	18
pCLV3:rgl2Δ17 (T1)	17.5	5.5	23.0	7.5	13-45	54
pCLV3:RGL3 (T1)	11.6	2.6	14.2	1.6	11-18	52
pCLV3:rgl3Δ17 (T1)	11.4	2.9	14.3	2.1	11-20	50
Experiment 5						
p35S:MIM172 (GA_3 50 μM; 23°C)	13.7	6.9	20.5	2.1	15-25	31
p35S:empty (GA_3 50 μM; 23°C)	8.4	2.9	11.3	0.9	9-13	33
p35S:MIM172 (mock; 23°C)	23.7	4.0	27.7	1.9	23-31	32
p35S:empty (mock; 23°C)	10.8	2.8	13.6	1.4	10-16	36
p35S:MIM172 (GA_3 50 μM; 16°C)	26.8	8.7	35.5	3.1	31-40	22
p35S:empty (GA_3 50 μM; 16°C)	13.0	7.3	20.3	2.3	17-24	24
p35S:MIM172 (mock; 16°C)	45.1	9.4	54.6	3.2	50-60	9
p35S:empty (mock; 16°C)	20.4	4.8	25.2	1.9	22-29	24

RL, rosette leaves; CL, cauline leaves; n.a., plants did not flower in the course of the experiment.

and supplementary material Fig. S1A,B). Similarly, and in agreement with a previous report (Willige et al., 2007), the *gid1a-c* triple mutant did not flower at all under our LD conditions. Presumably due to high functional redundancy among the GID1 receptors, flowering time was almost, but not completely, recovered ($P<0.00001$) in the *gid1b-1 gid1c-2* double mutant, which flowered with 16.3±1.1 leaves compared with 14.1±1.0 in wild-type plants (Table 1 and supplementary material Fig. S1A,C). Together, our results confirm that DELLA proteins act as repressors of flowering and that their GID1-mediated, GA-dependent degradation contributes to induction of flowering under LD conditions.

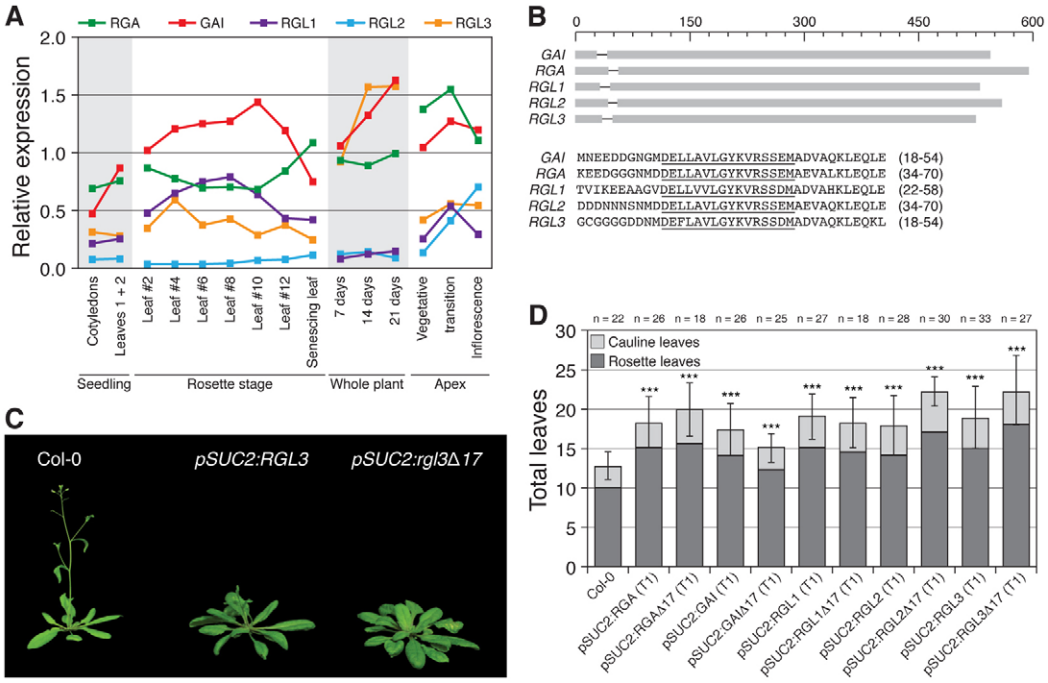

Fig. 1. Accumulation of DELLA proteins in vasculature delays flowering under LD conditions. (**A**) *DELLA* genes are expressed in *A. thaliana* leaves and at the shoot meristem throughout development [data from AtGenExpress atlas (Schmid et al., 2005)]. (**B**) GA-insensitive DELLA proteins were created by deleting 17 amino acids at the N-terminal region, corresponding to the deletion originally identified in the dominant *gai-1* allele. Underlined amino acids correspond to deleted residues in *della*Δ*17* mutants. (**C**) Expression of *RGL3* and *rgl3*Δ*17* in phloem companion cells delays flowering in LD conditions at 23°C. Shown are 30-day-old plants. (**D**) Flowering time of *pSUC2:DELLA* and *pSUC2:della*Δ*17* (T1) lines under LD conditions at 23°C. Transgenic plants (C,D) are in Col-0 background. Error bars indicate the standard deviation (s.d.) of total leaf number; n indicates the number of T1 plants analyzed. Significance was calculated using the unpaired Student's *t*-test: **P*<0.05, ***P*<0.01, ****P*<0.001.

DELLA proteins regulate flowering under LD conditions in the leaf vasculature

The control of flowering can be spatially divided into processes that occur in leaves, such as perception of photoperiod, and those that occur at the shoot meristem (Kobayashi and Weigel, 2007). The analysis of publicly available microarrays (Schmid et al., 2005) revealed a dynamic regulation of the five *DELLA* genes in different plant tissues, including the leaves and the shoot meristem (Fig. 1A), indicating that the DELLA proteins could affect flowering in either of those two tissues. To investigate their spatial contribution to the regulation of flowering we employed tissue-specific expression of wild-type (*GAI*, *RGA*, *RGL1*, *RGL2* and *RGL3*) and GA-insensitive versions (*gai*Δ*17*, *rga*Δ*17*, *rgl1*Δ*17*, *rgl2*Δ*17*, *rgl3*Δ*17*) of the *DELLA* cDNAs. The latter were created by introducing a 17-amino-acid deletion into the *DELLA* cDNAs, analogous to the one originally identified in the *gai-1* mutant (Fig. 1B) (Peng et al., 1997).

Transgenic T1 plants expressing *della*Δ*17* from the phloem companion cell (PCC)-specific *SUC2* promoter (Stadler and Sauer, 1996) exhibited the dark green color typically observed in GA-deficient mutants. We found that *pSUC2:rga*Δ*17*, *pSUC2:rgl1*Δ*17*, *pSUC2:rgl2*Δ*17* and *pSUC2:rgl3*Δ*17* delayed flowering more strongly than *pSUC2:GAI*Δ*17*, although late-flowering individuals were occasionally observed among the latter (*P*<0.00001; Fig. 1C,D; supplementary material Figs S2, S3). Furthermore, transgenic plants expressing full-length *DELLA* ORFs also displayed an intermediate dark green color and late-flowering phenotype (*P*<0.00001; Fig. 1C,D). In particular, *pSUC2:RGA* and *pSUC2:RGL1* flowered almost at the same time as *pSUC2:rga*Δ*17* and *pSUC2:rgl1*Δ*17* (Fig. 1C,D; supplementary material Figs S2, S3).

To ensure that also the endogenous DELLA proteins regulate flowering in the leaf PCCs, we expressed the GA catabolic enzyme GA2ox8 under control of the *SUC2* promoter (Stadler and Sauer, 1996; Olszewski et al., 2002; Rieu et al., 2008). The reasoning for this is that it would reduce the pool of bioactive GA, resulting in higher DELLA protein levels specifically in the PCCs. Indeed, transgenic T1 plants expressing *pSUC2:GA2ox8* displayed a dark green color and flowered later (14.1±1.5 rosette leaves) than control plants (10.4±0.8; *P*<0.00001; supplementary material Fig. S4). Taken together, these observations suggest that the DELLA proteins regulate flowering in response to GA under LD conditions in the leaf PCCs.

CO- and GI-independent regulation of *FT* by DELLA proteins in the vasculature

The *FT* gene has been shown to be specifically expressed in leaf vasculature in response to inductive photoperiod (Kobayashi and Weigel, 2007; Turck et al., 2008). To test if the late flowering observed in the *pSUC2:della*Δ*17* lines (Fig. 1C,D; supplementary material Figs S2, S3) was due to a reduction in *FT* expression, we introduced *pSUC2:rgl3*Δ*17* into a *pFT:GUS* reporter line (Takada and Goto, 2003). T2 plants derived from seven independent T1 lines that varied in their flowering time from wild-type-like to late flowering were analyzed and a clear anti-correlation between flowering time and expression of the endogenous *FT* gene was observed (Fig. 2A). *FT* expression was strongly reduced in late-flowering *pSUC2:rgl3*Δ*17* T2 lines, whereas lines flowering at the same time as the control plants had almost wild-type-like *FT* expression (Fig. 2A). Similarly, the

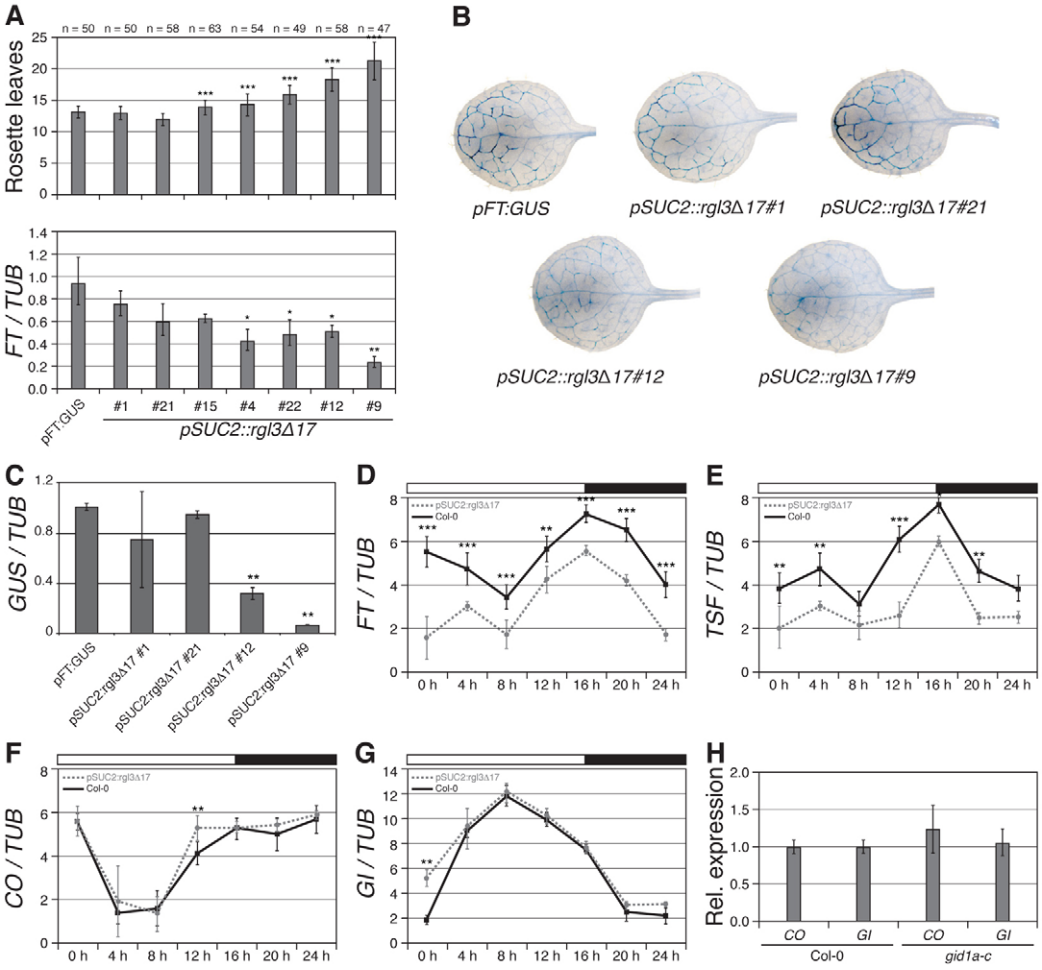

Fig. 2. DELLA proteins regulate *FT* and *TSF* expression under LD conditions. (**A-C**) Repression of *FT* by RGL3 was confirmed in *pSUC2:rgl3Δ17 pFT:GUS* (T2) plants by (A, bottom) quantitative RT-PCR of *FT*, (B) GUS staining, and (C) *GUS* quantitative RT-PCR. GUS staining represents the third leaf of 10-day-old transgenic plants at *zeitgeber* (ZT) 16 grown under LD conditions at 23°C. (**D-G**) Diurnal expression profile of *FT*, *TSF, CO* and *GI* in *pSUC2:rgl3Δ17* (T2). Plants were grown under SD conditions for 30 days and shifted to LD conditions for 5 days to induce flowering. Transgenic plants (A-G) are in Col-0 background. The aerial part of the plants was collected every 4 hours for 24 hours. Bars on the top indicate day (white) and night (black) phases. (**H**) Expression of *CO* and *GI* in 3-week-old triple *gid1a-c* mutant plants growing at 23°C under LD conditions. The error bars indicate the s.d. of rosette leaf number (A, top) and quantitative expression of at least two biological and two technical replicates each (A, bottom; C-H); n indicates the number of plants analyzed. Significance was calculated using the unpaired Student's *t*-test: **P*<0.05, ***P*<0.01, ****P*<0.001.

pFT:GUS reporter showed a much decreased expression and staining in the vasculature of late-flowering plants (Fig. 2B,C).

As *FT*, as well as its closest paralog *TWIN SISTER OF FT* (*TSF*), are under the control of the circadian clock, we analyzed the diurnal expression of these two genes in the late-flowering *pSUC2:rgl3Δ17* line. Quantitative analysis showed that both *FT* and *TSF* maintained their diurnal expression but at a reduced level (Fig. 2D,E). By contrast, expression of *GIGANTEA* (*GI*) and *CONSTANS* (*CO*), which act upstream of *FT*, was unchanged in *pSUC2:rgl3Δ17* and in the strong *gid1a-c* mutant (Fig. 2F,G,H). Together these results suggest that the DELLA proteins participate in the regulation of *FT* and *TSF* expression in PCCs and contribute to their regulation under LD conditions independently of *CO* and *GI*.

Regulation of *FT* and *TSF* by GA

To confirm that *FT* and *TSF* are regulated by GA, and to ensure that the effects we had observed in the *pSUC2:rgl3Δ17* line reflected normal DELLA function, we analyzed their expression in GA biosynthesis and signaling mutants. Results obtained in the strong GA biosynthesis mutant *ga1-3* had suggested that GA does not substantially contribute to the regulation of flowering time under LD conditions (Wilson et al., 1992). Consistent with this, *FT* and *TSF* were expressed normally in *ga1-3* under LD conditions (Fig. 3A). By contrast, expression of *FT* and *TSF* was reduced approximately twofold in the partially GA-insensitive *sly1-10* mutant, which accumulates higher levels of DELLA proteins (McGinnis et al., 2003) compared with wild type (Fig. 3A). Similarly, *FT* and *TSF* expression was reduced to ~30% in the non-flowering *gid1a-c* triple mutant compared with control plants (Fig. 3B).

In agreement with GA regulating *FT* independently of the photoperiod pathway, we also observed increased levels of *FT* in a diurnal timecourse in the early-flowering *ga1-3 gai-t6 rga-t2 rgl1-1 rgl2*-1 mutant compared with wild-type plants (Fig. 3C). Furthermore, *FT* was precociously expressed in leaves of the *ga1-3 gai-t6 rga-t2 rgl1-1 rgl2-1* mutant compared with L*er*-1. Expression of *FT* was comparable between the two genotypes 3

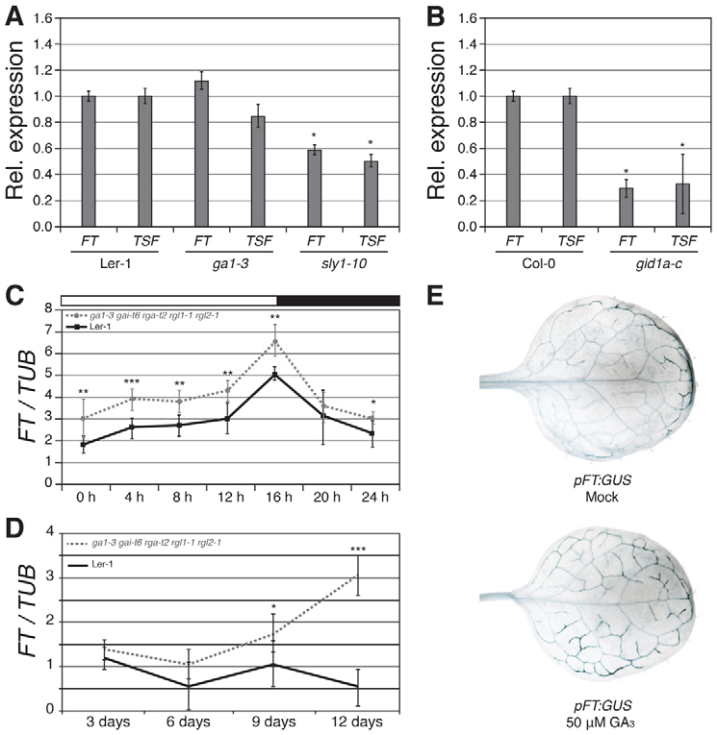

Fig. 3. GA regulates *FT* expression in the leaf vasculature. (**A**) Relative expression of *FT* and *TSF* at ZT 16 in seedlings grown for 14 days under LD conditions at 23°C. (**B**) Relative expression of *FT* and *TSF* in the triple *gid1a-c* mutant compared with wild-type plants. Plant material was collected 3 weeks after germination at ZT 16. (**C**) *FT* diurnal expression in leaves of 8- to 9-day-old *ga1-3 gai-t6 rga-t2 rgl1-1 rgl2-1* and Ler-1 plants grown under LD conditions at 23°C. (**D**) *FT* expression in leaves of *ga1-3 gai-t6 rga-t2 rgl1-1 rgl2-1* and Ler-1 plants 3, 6, 9 and 12 days after germination. Plants were grown under LD conditions at 23°C and cotyledons (day 3) and rosette leaves (days 6, 9 and 12) were harvested at ZT 15. (**E**) Increased GUS staining of *pFT:GUS* in response to exogenous GA_3. GUS staining represents the third rosette leaf of 12-day-old plants at ZT 16 grown under LD conditions at 23°C. Transgenic plants are in Col-0 background. Error bars for quantitative RT-PCR indicate s.d. of two biological and two technical replicates each. Significance was calculated using the unpaired Student's *t*-test: $*P<0.05$, $**P<0.01$, $***P<0.001$.

days after germination but gradually increased in the *ga1-3 gai-t6 rga-t2 rgl1-1 rgl2-1* mutant (Fig. 3D). To confirm that GA can promote *FT* expression even under LD conditions, plants containing the *pFT:GUS* reporter were treated with GA_3 or mock-treated every other day for 12 days. In contrast to mock-treated plants, in which the GUS staining was mostly restricted to the peripheral veins, GA_3-treated plants displayed a stronger and more dispersed GUS signal (Fig. 3E). This finding was corroborated by quantitative RT-PCR, which revealed a 2.5-fold increase in GUS expression in the GA_3-treated samples (supplementary material Fig. S5). Taken together, these results suggest that GA substantially promotes the expression of *FT* and *TSF* in PCCs and thus the induction of flowering even under LD conditions.

DELLA proteins repress flowering under LD conditions at the shoot meristem

Even though plants expressing *della*Δ*17* and *DELLA* cDNAs in the PCCs were clearly late flowering, these plants nevertheless flowered earlier than the triple *gid1a-c* mutant, suggesting that GA signaling in tissues other than the leaf vasculature contributes to the regulation of flowering. To investigate the contribution of DELLA proteins to flowering-time regulation at the shoot apex, we expressed the *della*Δ*17* and *DELLA* cDNAs under control of the meristem-specific *FD* (*pFD*) and the shoot stem cell niche-specific *CLAVATA3* (*pCLV3*) promoters (Fig. 4). Expression of *rga*Δ*17*, *gai*Δ*17*, *rgl1*Δ*17* and *rgl2*Δ*17* ($P<0.00001$), but not *rgl3*Δ*17* ($P>0.05$), at the shoot apex from either *pFD* or *pCLV3* delayed flowering even more strongly than observed in the *pSUC2* lines (Table 1; Fig. 4; supplementary material Figs S2, S3). In general, the delay in flowering was stronger in the *pFD:della*Δ*17* lines compared with the *CLV3* promoter lines, which is probably a consequence of the larger *FD* expression domain. By contrast, expression of the wild-type *DELLA* did not significantly affect flowering time ($P>0.05$; Table 1; Fig. 4B,C; supplementary material Figs S2, S3), suggesting that endogenous GA levels at the meristem are sufficiently high to target misexpressed DELLA proteins for degradation. Taken together, these results highlight the importance of DELLA degradation in promoting flowering at the shoot meristem downstream of the photoperiodic signal produced in leaves.

*della*Δ*17* delay flowering at the shoot meristem under SD conditions

To better understand the contribution of DELLA proteins in controlling the transition to flowering under non-inductive photoperiod, we scored flowering time in transgenic plants expressing *della*Δ*17* and wild-type *DELLA* in the PCCs (*pSUC2*) and at the shoot meristem (*pFD; pCLV3*) in SD conditions. We observed that expression of *rga*Δ*17*, *gai*Δ*17*, *rgl1*Δ*17* and *rgl2*Δ*17* at the shoot meristem caused plants to flower extremely late or not to flower at all even after 6 months of vegetative growth (supplementary material Figs S6, S7). As observed in LD conditions, expression of *rgl3*Δ*17* at the shoot meristem did not affect flowering. However, in contrast to what we had observed in LD conditions, misexpression of *della*Δ*17* and *DELLA* in the phloem companion cells just had a minor effect on flowering time under SD conditions (supplementary material Fig. S6).

DELLA proteins regulate *SPL* expression at the shoot meristem

SPL genes constitute a class of transcription factors that regulates diverse aspects of plant development at the shoot meristem, including the transition to flowering (Cardon et al., 1997; Wang et al., 2009; Jung et al., 2011; Kim et al., 2012). Interestingly, we observed a significant reduction of *SPL3*, *SPL4* and *SPL5* mRNA levels in dissected apices of LD-grown late-flowering *pFD:rgl2*Δ*17* plants compared with Col-0 (Fig. 5A). By contrast, *SPL9* and *SPL15* transcripts were downregulated only twofold, and expression of *SPL10* and *SPL11* remained nearly unchanged. Supporting the idea that *SPL3*, *SPL4*, *SPL5* and *SPL9*, but not *SPL11*, are targets of GA signaling, we observed reduced expression of these genes in the

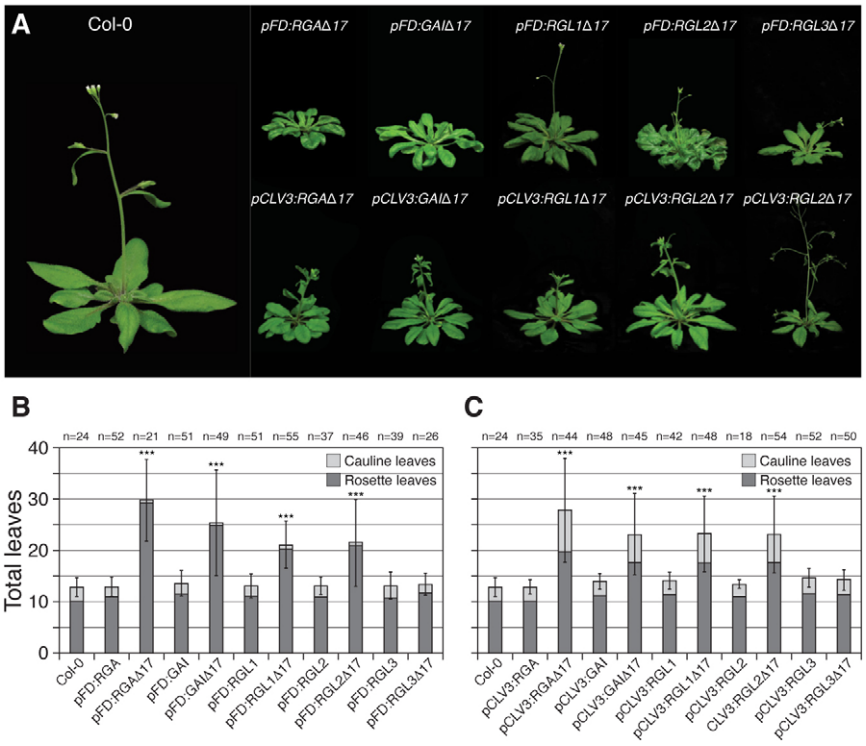

Fig. 4. Expression of *della*Δ*17* at the shoot meristem delays flowering under LD conditions. (**A**) Phenotypes and (**B**,**C**) flowering time of transgenic T1 plants expressing *della*Δ*17* and *DELLA* genes from the *FD* and *CLV3* promoters under LD conditions at 23°C. Transgenic plants are in Col-0 background. Shown are 28-day-old plants (Col-0 and *RGL3* lines) and 40-day-old plants (*GAI, RGA, RGL1, 2* lines). Error bars indicate the s.d. of total leaf number; n indicates the number of T1 plants analyzed. Significance was calculated using the unpaired Student's *t*-test: **P*<0.05, ***P*<0.01, ****P*<0.001.

gid1a-c triple mutant grown under LD conditions (Fig. 5B). In addition, *SPL3*, *SPL4* and *SPL5* were precociously expressed in dissected apices of the early-flowering *ga1-3 gai-t6 rga-t2 rgl1-1 rgl2-1* pentuple mutant compared with wild type (Fig. 5C,D,E). By contrast, expression of these genes remained at low levels in apices of the late-flowering *gai-1* mutant (Fig. 5C,D,E). Together these findings indicate that GA transcriptionally regulates these three important *SPL* genes at the shoot meristem.

A gene that has been shown to respond strongly to GA under SD conditions is the MADS-domain transcription factor SOC1 (Bonhomme et al., 2000; Moon et al., 2003; Jung et al., 2011). By contrast, *SOC1* expression was only moderately increased in apices of the *ga1-3 gai-t6 rga-t2 rgl1-1 rgl2-1* mutant compared with L*er*-1 plants (supplementary material Fig. S8). In addition, application of GA_3 in the strong photoperiod pathway mutant *ft-10 tsf-1* resulted in only very mild induction of *SOC1*. Together, these results indicate that *SOC1* is only a minor target of GA signaling at the shoot meristem under inductive photoperiod.

DELLA proteins regulate *SPL3* expression in leaves

SPL3 and FT have recently been shown to regulate each other's expression in a feedback loop in which SPL3 directly binds to and regulates *FT* in leaves, whereas FT seems to feed back onto *SPL3* expression (Jung et al., 2011; Kim et al., 2012). Interestingly, we observed elevated levels of *SPL3* in leaves of LD-grown *ga1-3 gai-t6 rga-t2 rgl1-1 rgl2-1* plants compared with L*er*-1 and *gai-1* mutant (Fig. 5F). This result suggests that, in addition to the shoot meristem, GA also controls *SPL3* expression in leaves.

p35S:MIM172 partially suppress acceleration of flowering in LD and SD conditions

It has recently been shown that at least one of the *MIR172* genes, *MIR172b*, is a direct target of SPL proteins (Wang et al., 2009; Wu et al., 2009; Yamaguchi et al., 2009). miR172 and its targets, a clade of six *AP2*-like transcription factors, are known regulators of flowering in both leaves and at the shoot meristem (Rhoades et al., 2002; Aukerman and Sakai, 2003; Schmid et al., 2003; Schwab et al., 2005; Mathieu et al., 2009; Yant et al., 2010). To test the possibility that the miR172/*AP2*-like module participates in the GA-mediated regulation of flowering, we analyzed the response of a late-flowering *p35S:MIM172* line, which displays artificially reduced levels of mature miR172 (Franco-Zorrilla et al., 2007; Todesco et al., 2010), to exogenous GA_3. We observed that the late flowering of *p35S:MIM172* could be overcome only partially by GA_3 treatment under LD conditions at both 16°C and 23°C (Fig. 6A,B; Table 1; supplementary material Fig. S9). At 16°C GA_3-treated control plants flowered with only 20.3±2.3 leaves, compared with 25.2±1.9 leaves produced by untreated plants. By contrast, GA_3-treated *p35S:MIM172* flowered much later with 35.5±3.1 compared with 54.6±3.2 leaves of untreated plants (Fig. 6A,B). A similar but weaker effect was observed in plants grown at 23°C (Fig. 6B; supplementary material Fig. S9A). In addition, *p35S:MIM172* also partially blocked the flower-promoting effect of GA in non-inductive SD conditions (supplementary material Fig. S9A,B). Taken together, these results suggest that GA regulates flowering, in part through the miR172/*AP2*-like module, or that the miR172/*AP2*-like genes and the GA pathway converge on the same targets.

Expression of *della*Δ*17* represses miR172

The partial suppression of the GA-mediated induction of flowering observed in the *p35S:MIM172* line suggested that *MIR172* itself could be regulated by GA. To test this possibility we analyzed miR172 levels by small RNA northern blot. Under SD conditions, we observed an increase in mature miR172 levels in the pentuple *ga1-3 gai-t6 rga-t2 rgl1-1 rgl2*-1 relative to *ga1-3*, indicating that DELLA proteins repress *MIR172* (Fig. 6C). By contrast, and in agreement with a previous report (Jung et al., 2011), the levels of mature miR156, which is genetically upstream of MIR172, were unchanged in *ga1-3 gai-t6 rga-t2 rgl1-1 rgl2-1* (Fig. 6D).

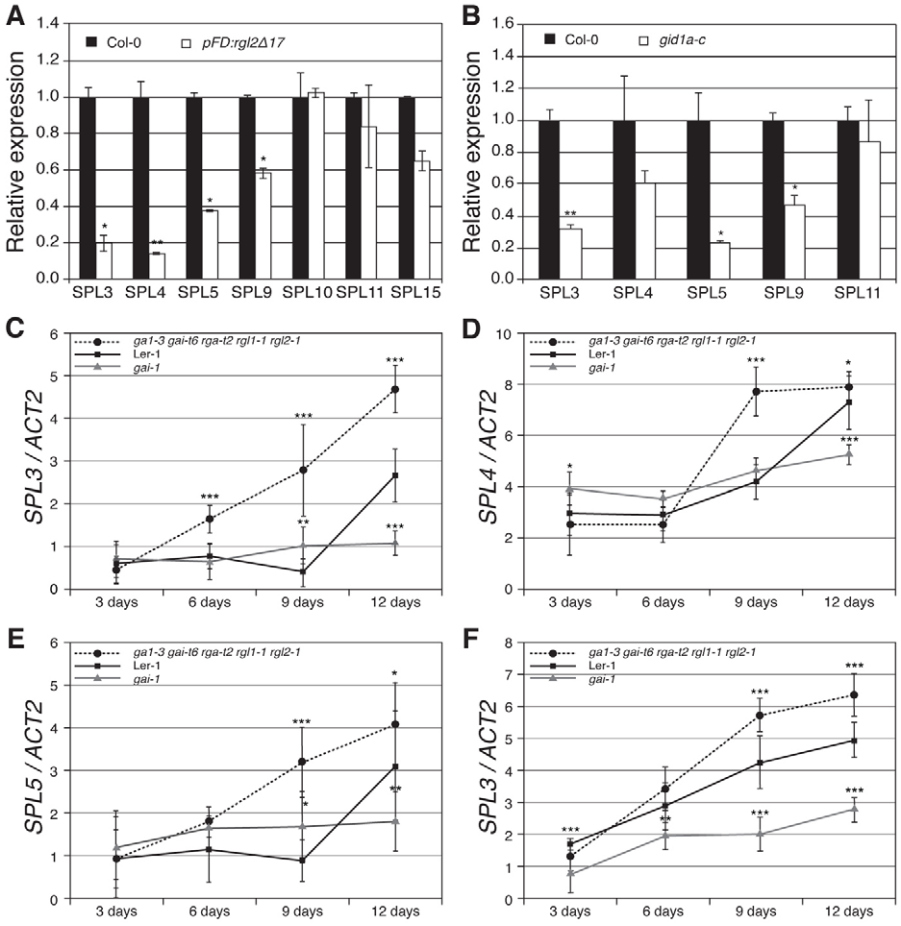

Fig. 5. GA regulates *SPL* expression at the shoot meristem and in leaves.
(**A**) Expression of *SPL* transcripts at the shoot meristem of *pFD:rgl2Δ17* plants. Apices of 12-day-old plants grown under LD 23°C were dissected at ZT 12-16. (**B**) Quantitative analysis of *SPL* gene expression in triple *gid1a-c* mutant grown under LD conditions compared with wild-type plants (ZT 16). (**C-E**) Expression of (C) *SPL3*, (D) *SPL4* and (E) *SPL5* in shoot meristem of L*er*-1, *gai-1,* and *ga1-3 gai-t6 rga-t2 rgl1-1 rgl2-1*. Apices (C-E) were dissected at ZT 12-16 3, 6, 9, and 12 days after germination from plants grown under LD conditions at 23°C. (**F**) *SPL3* expression in cotyledons (day 3) and true leaves (days 6, 9 and 12) of L*er*-1, *gai-1* and *ga1-3 gai-t6 rga-t2 rgl1-1 rgl2-1* harvested 3, 6, 9 and 12 days after germination at ZT 15. Error bars represent the s.d. of two biological and two technical replicates each. Significance was calculated using the unpaired Student's *t*-test: **P*<0.05, ***P*<0.01, ****P*<0.001.

Similar results were obtained in the late-flowering *pSUC2:rgl3Δ17* and *pFD:rgl2Δ17* lines. Quantitative analysis showed that the mature miR172 was moderately more abundant throughout the day in Col-0 plants grown under SD conditions for 30 days and shifted to LD conditions for 5 days to induce flowering when compared with *pSUC2:rgl3Δ17* plants (Fig. 6E). By contrast, the levels of miR156 were comparable between the two genotypes (Fig. 6F). Similarly, the level of miR172 was reduced in apices of *pFD:rgl2Δ17* compared with LD-grown Col-0 (Fig. 6G). Together, these results indicate that DELLA proteins regulate *MIR172* expression, which could therefore contribute to the GA-mediated control of flowering in both SD and LD conditions.

DISCUSSION

Arabidopsis thaliana controls the transition to reproductive development through a complex regulatory network that integrates environmental and endogenous signals to ensure the correct timing of flowering. The hormone GA has been shown to be essential for flowering under SD photoperiod (Wilson et al., 1992). However, its role in regulating flowering under LD conditions is less well understood. Here we demonstrate that the DELLA proteins, which are key components of GA signaling, contribute substantially to the regulation of flowering under LD conditions. In agreement with previous reports (Silverstone et al., 1997; Dill and Sun, 2001; Dill et al., 2004) we found that the loss of individual *DELLA* genes resulted in only a minor acceleration in flowering. By contrast, flowering was induced much earlier in higher order mutants. These results not only confirm the importance of the DELLA proteins during flowering in LD conditions but also suggest a certain degree of functional redundancy between the individual proteins. The extreme delay in flowering observed in LD-grown triple *gid1a-c* mutants, which is due to an increase in DELLA protein (Griffiths et al., 2006; Willige et al., 2007), further strengthens the notion that the accumulation of DELLA proteins contributes substantially to the regulation of flowering under inductive LD conditions.

In addition, expression of GA-insensitive DELLA proteins (*della*Δ*17*) in leaves and at the shoot apex consistently demonstrated that these proteins can act as floral repressors in different tissues throughout the plant. However, there are clear differences in the effectiveness of individual DELLA proteins in regulating flowering in different tissues. For example, we observed that RGL3 reproducibly delayed flowering only when expressed in leaves, but not at the shoot apex. This observation was not completely unexpected, as genetic and molecular analysis of DELLA mutants had previously demonstrated some functional specificity of DELLA proteins, despite their generally high functional redundancy (Dill and Sun, 2001; King et al., 2001; Lee et al., 2002; Piskurewicz et al., 2009; Gallego-Bartolome et al., 2010).

Interestingly, the delay in flowering observed in *pSUC2:rgl3Δ17* plants was clearly correlated with a reduction in *FT* expression in the PCCs in the leaves, suggesting that at least part of the effect of DELLA proteins on flowering time in LD conditions is through the regulation of *FT*. In agreement with this we observed increased *pFT:GUS* expression in response to GA_3 application specifically in the leaf vasculature and not in other tissues. In addition, the reduction of *FT* expression most likely accounts at least in part for

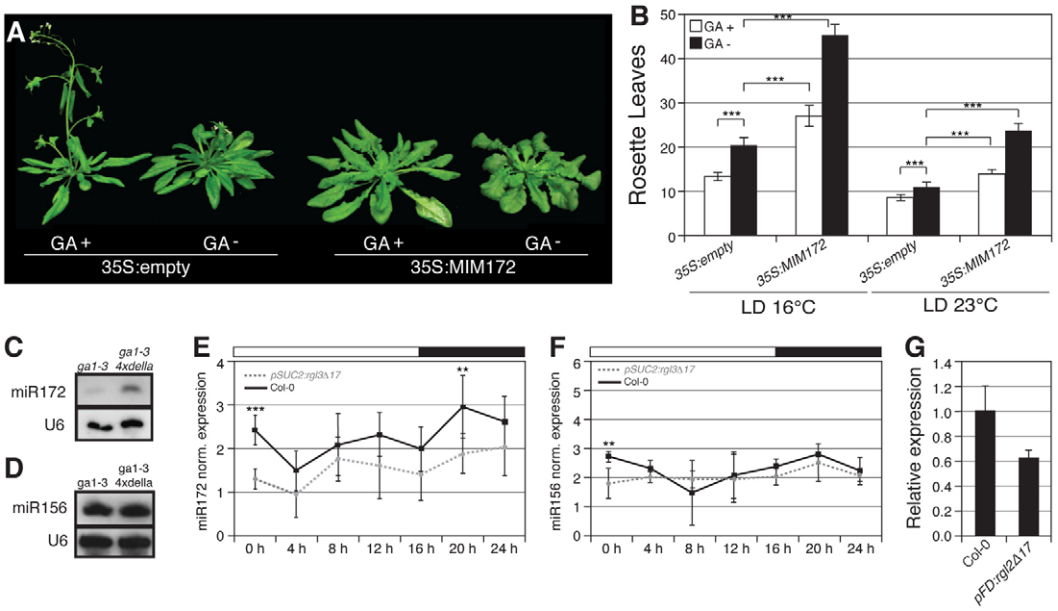

Fig. 6. GA controls flowering at least partially through miR172. (**A**,**B**) *p35S:MIM172* overexpression partially suppresses the inductive effect of exogenously applied GA on flowering under LD conditions at 16°C (A,B) or 23°C (B). GA_3 treatments were performed every third day throughout vegetative growth until the plants had started to flower. 35-day-old plants are shown. (**C**,**D**) Small RNA northern blot of miR172 (C) and miR156 (D) in *ga1-3* and *ga1-3 gai-t6 rga-t2 rgl1-1 rgl2-1* (labeled *ga1-3 4xdella*) mutants grown under SD conditions (ZT 8). Samples were collected 25 days after germination. (**E**,**F**) Diurnal expression of mature miR172 (E) and miR156 (F) in *pSUC2:rgl3Δ17* (T2). Plants were grown at 23°C for 30 days under SD conditions and shifted to 23°C LD conditions to induce flowering. Samples were harvested 5 days after the shift from SD to LD conditions every 4 hours for 24 hours. (**G**) Quantification of mature miR172 in dissected apices of 12-day-old Col-0 and *pFD:rgl2Δ17* plants harvested at ZT 12-16. Transgenic plants are in Col-0 background. Error bars indicate s.d. of rosette leaf number (B) and of two biological and two technical replicates each for quantitative PCR of small RNAs (E-G). Significance was calculated using the unpaired Student's *t*-test: **P*<0.05, ***P*<0.01, ****P*<0.001.

the late flowering of the *gid1a-c* mutant, which displays elevated levels of the DELLA proteins. Further evidence that the DELLA proteins repress *FT* comes from the observation that the early flowering *ga1-3 gai-t6 rga-t2 rgl1-1 rgl2-1* mutant exhibits increased *FT* expression. By contrast, the targeted reduction of bioactive GAs in the PCCs by the misexpression of the catabolic enzyme GA2ox8 significantly delayed flowering. Taken together, our data strongly indicate that DELLA protein accumulation contributes to the regulation of *FT* in the PCCs under LD conditions. However, DELLA-mediated GA signaling is only one of several inputs that converge on *FT*, which probably explains why mutations in the *DELLA* genes result in only a minor delay in flowering under LD conditions.

Although the delay in flowering we observed in response to misexpression of GA-insensitive DELLA proteins in the PCCs was to be expected based on the phenotypes of dominant DELLA mutants such as *gai-1*, it was surprising to see that transgenic plants expressing full-length DELLA proteins were also late-flowering. One possible explanation for this finding is that in the misexpression lines, DELLA proteins accumulate to such high levels that they can no longer be efficiently degraded even in the presence of GA, as has been previously demonstrated for GAI (Fleck and Harberd, 2002).

By contrast, when expressed at the shoot meristem only the GA-insensitive *della*Δ*17*, and not the full-length DELLA proteins, delayed flowering efficiently. It has been previously shown that bioactive GA accumulates at the shoot meristem before the transition to flowering (Eriksson et al., 2006). Assuming that other factors, such as the GID1 receptors or downstream components, are not limiting at the shoot meristem, this would result in a locally increased capability to degrade DELLA proteins, which might explain why meristem-specific expression of DELLA proteins at the meristem has little effect on flowering. Alternatively, the promoters used in this study (*pFD*, *pCLV3*) might be too weak to drive the expression of DELLA proteins beyond the capacity of the endogenous GA-signaling machinery to degrade (Lee et al., 2002).

It has previously been shown that GA signaling controls flowering at the shoot meristem specifically under SD conditions (Blazquez et al., 1998; Blazquez and Weigel, 2000; Moon et al., 2003; Achard et al., 2004). By contrast, the finding that *pFD:della*Δ*17* and *pCLV3:della*Δ*17* lines displayed pronounced late flowering, as well as a recent report describing the effects of *GA2ox7* misexpression on flowering (Porri et al., 2012), indicate that the accumulation of DELLA proteins at the shoot meristem contributes to the induction of flowering under LD conditions after all. GA positively regulates *SOC1* expression through DELLA proteins under non-inductive SD conditions (Moon et al., 2003). However, we and others (Porri et al., 2012) have observed only a mild effect of GA on *SOC1* expression under LD conditions. This is in stark contrast to the strong effect of GA under SD conditions and suggests that under LD conditions GA signaling controls flowering at the shoot meristem predominantly downstream of the photoperiodic pathway and *SOC1*.

Recently, Wang and colleagues proposed the existence of an endogenous microRNA-regulated pathway that ensures that plants eventually make the transition to flowering even under a non-inductive photoperiod (Wang et al., 2009). This pathway relies on the gradual increase of *SPL* transcripts in response to the decrease of miR156 level during *A. thaliana* development. The increase in SPL protein level would ultimately lead to the activation of floral

regulators and transition to flowering (Wang et al., 2009; Yamaguchi et al., 2009). The observation that *SPL9* and miR156 level remains unchanged in the *ga1-3* mutant when treated with exogenous GA leads to the conclusion that the *SPL*/miR156 module constitutes a pathway that regulates flowering under SD conditions independently of GA (Wang et al., 2009). Indeed, in our experiments and in agreement with previous work (Jung et al., 2011) miR156 levels remained unchanged in response to GA. However, the expression of the miR156-targets *SPL3*, *SPL4* and *SPL5* is significantly altered at the shoot meristem in response to GA, indicating that GA contributes to the regulation of the floral transition by modulating *SPL* gene expression independently of miR156 under both SD and LD conditions.

In contrast to miR156, there is at least circumstantial evidence for a role of yet another microRNA, miR172, in GA-mediated control of flowering. Plants with artificially reduced miR172 levels were still responsive to treatment with exogenous GA but did not completely recover the early flowering phenotype observed in control plants. One explanation for this behavior could be that the miR172 targets, a clade of *AP2*-like transcription factors that function as floral repressors (Aukerman and Sakai, 2003; Mathieu et al., 2009; Yant et al., 2010), were expressed too highly in the MIM172 lines for exogenous GA to compensate. In this scenario GA and miR172 would act in parallel signaling pathways that converge on the same targets. However, the observation that miR172 levels were elevated in *ga1-3 gai-t6 rga-t2 rgl1-1 rgl2-1* and reduced in *pSUC2:rgl3Δ17* suggests that DELLA proteins act at least partially through the miR172/*AP2*-like module.

In contrast to the results observed in LD conditions, regulation of flowering under SD photoperiod seems to be mostly restricted to the shoot meristem. Plants expressing *della*Δ*17* proteins from the *FD* or *CLV3* promoters under SD conditions in many cases completely failed to flower, whereas the expression of these proteins in leaves of SD-grown plants seems to have little or no effect. Interestingly, although GAI, RGA, RGL1 and RGL2 seem to be able to repress flowering in SD conditions when ectopically expressed at the shoot meristem, the *gai-t6 rga-24* double mutant has been reported to rescue the non-flowering phenotype of *ga1-3* in SD (Dill and Sun, 2001), suggesting that these two DELLA proteins are crucial for repressing flowering at the shoot meristem under a non-inductive photoperiod. Taken together, our results demonstrate that under LD conditions GA promotes flowering through the degradation of DELLA proteins in different parts of the plant, whereas its effect under a non-inductive photoperiod seems to be mostly restricted to the shoot meristem.

Acknowledgements
We thank the European Stock Centre for seeds, Dr Nicholas Harberd for *ga1-3 gai-t6 rga-t2 rgl1-1 rgl2-1* mutant, Dr Claus Schwechheimer for *gid1a-c* mutant, Dr Marco Todesco and Dr Ignacio Rubio-Somoza for *p35S:MIM172* and *p35S:empty* lines, Dr Koji Goto for *pFT:GUS* line, Dr Rüdiger Simon for a plasmid with *CLV3* regulatory sequences, Johanna Weirich for technical support, and Dr Levi Yant for critical comments on the manuscript.

Funding
Work in the Schmid laboratory on the regulation on flowering time is supported by the Max Planck Institute for Developmental Biology and grants from the Deutsche Forschungsgemeinschaft (DFG) [SCHM 1560/5-1].

Competing interests statement
The authors declare no competing financial interests.

Supplementary material
Supplementary material available online at
http://dev.biologists.org/lookup/suppl/doi:10.1242/dev.080879/-/DC1

References

Abe, M., Kobayashi, Y., Yamamoto, S., Daimon, Y., Yamaguchi, A., Ikeda, Y., Ichinoki, H., Notaguchi, M., Goto, K. and Araki, T. (2005). FD, a bZIP protein mediating signals from the floral pathway integrator FT at the shoot apex. *Science* **309**, 1052-1056.
Achard, P., Herr, A., Baulcombe, D. C. and Harberd, N. P. (2004). Modulation of floral development by a gibberellin-regulated microRNA. *Development* **131**, 3357-3365.
Achard, P., Liao, L. L., Jiang, C. F., Desnos, T., Bartlett, J., Fu, X. D. and Harberd, N. P. (2007). DELLAs contribute to plant photomorphogenesis. *Plant Physiol.* **143**, 1163-1172.
Achard, P., Gusti, A., Cheminant, S., Alioua, M., Dhondt, S., Coppens, F., Beemster, G. T. S. and Genschik, P. (2009). Gibberellin signaling controls cell proliferation rate in Arabidopsis. *Curr. Biol.* **19**, 1188-1193.
Aukerman, M. J. and Sakai, H. (2003). Regulation of flowering time and floral organ identity by a microRNA and its APETALA2-like target genes. *Plant Cell* **15**, 2730-2741.
Blazquez, M. and Weigel, D. (2000). Integration of floral inductive signals in Arabidopsis. *Nature* **404**, 889-892.
Blazquez, M. A., Green, R., Nilsson, O., Sussman, M. R. and Weigel, D. (1998). Gibberellins promote flowering of Arabidopsis by activating the LEAFY promoter. *Plant Cell* **10**, 791-800.
Blazquez, M. A., Soowal, L. N., Lee, I. and Weigel, D. (1997). LEAFY expression and flower initiation in Arabidopsis. *Development* **124**, 3835-3844.
Bolle, C. (2004). The role of GRAS proteins in plant signal transduction and development. *Planta* **218**, 683-692.
Bonhomme, F., Kurz, B., Melzer, S., Bernier, G. and Jacqmard, A. (2000). Cytokinin and gibberellin activate SaMADS A, a gene apparently involved in regulation of the floral transition in Sinapis alba. *Plant J.* **24**, 103-111.
Cardon, G. H., Hohmann, S., Nettesheim, K., Saedler, H. and Huijser, P. (1997). Functional analysis of the Arabidopsis thaliana SBP-box gene SPL3: a novel gene involved in the floral transition. *Plant J.* **12**, 367-377.
Chen, C., Ridzon, D. A., Broomer, A. J., Zhou, Z., Lee, D. H., Nguyen, J. T., Barbisin, M., Xu, N. L., Mahuvakar, V. R., Andersen, M. R. et al. (2005). Real-time quantification of microRNAs by stem-loop RT-PCR. *Nucleic Acids Res.* **33**, e179.
Chen, X. M. (2004). A microRNA as a translational repressor of APETALA2 in Arabidopsis flower development. *Science* **303**, 2022-2025.
Cheng, H., Qin, L., Lee, S., Fu, X., Richards, D. E., Cao, D., Luo, D., Harberd, N. P. and Peng, J. (2004). Gibberellin regulates Arabidopsis floral development via suppression of DELLA protein function. *Development* **131**, 1055-1064.
Clough, S. J. and Bent, A. F. (1998). Floral dip: a simplified method for Agrobacterium-mediated transformation of Arabidopsis thaliana. *Plant J.* **16**, 735-743.
Corbesier, L., Vincent, C., Jang, S. H., Fornara, F., Fan, Q. Z., Searle, I., Giakountis, A., Farrona, S., Gissot, L., Turnbull, C. et al. (2007). FT protein movement contributes to long-distance signaling in floral induction of Arabidopsis. *Science* **316**, 1030-1033.
Daviere, J. M., de Lucas, M. and Prat, S. (2008). Transcriptional factor interaction: a central step in DELLA function. *Curr. Opin. Genet. Dev.* **18**, 295-303.
Davies, P. J. (2004). *Plant Hormones: Biosynthesis, Signal Transduction, Action!* (3rd edn). Dordrecht, The Netherlands: Springer.
de Lucas, M., Daviere, J. M., Rodriguez-Falcon, M., Pontin, M., Iglesias-Pedraz, J. M., Lorrain, S., Fankhauser, C., Blazquez, M. A., Titarenko, E. and Prat, S. (2008). A molecular framework for light and gibberellin control of cell elongation. *Nature* **451**, 480-484.
Dill, A. and Sun, T. (2001). Synergistic derepression of gibberellin signaling by removing RGA and GAI function in Arabidopsis thaliana. *Genetics* **159**, 777-785.
Dill, A., Jung, H. S. and Sun, T. P. (2001). The DELLA motif is essential for gibberellin-induced degradation of RGA. *Proc. Natl. Acad. Sci. USA* **98**, 14162-14167.
Dill, A., Thomas, S. G., Hu, J., Steber, C. M. and Sun, T. P. (2004). The Arabidopsis F-box protein SLEEPY1 targets gibberellin signaling repressors for gibberellin-induced degradation. *Plant Cell* **16**, 1392-1405.
Eriksson, S., Bohlenius, H., Moritz, T. and Nilsson, O. (2006). GA4 is the active gibberellin in the regulation of LEAFY transcription and Arabidopsis floral initiation. *Plant Cell* **18**, 2172-2181.
Feng, S., Martinez, C., Gusmaroli, G., Wang, Y., Zhou, J., Wang, F., Chen, L., Yu, L., Iglesias-Pedraz, J. M., Kircher, S. et al. (2008). Coordinated regulation of Arabidopsis thaliana development by light and gibberellins. *Nature* **451**, 475-479.
Fleck, B. and Harberd, N. P. (2002). Evidence that the Arabidopsis nuclear gibberellin signalling protein GAI is not destabilised by gibberellin. *Plant J.* **32**, 935-947.
Franco-Zorrilla, J. M., Valli, A., Todesco, M., Mateos, I., Puga, M. I., Rubio-Somoza, I., Leyva, A., Weigel, D., Garcia, J. A. and Paz-Ares, J. (2007). Target mimicry provides a new mechanism for regulation of microRNA activity. *Nat. Genet.* **39**, 1033-1037.

Fu, X. D., Richards, D. E., Fleck, B., Xie, D. X., Burton, N. and Harberd, N. P. (2004). The Arabidopsis mutant sleepy1(gar2-1) protein promotes plant growth by increasing the affinity of the SCFSLY1 E3 ubiquitin ligase for DELLA protein substrates. *Plant Cell* **16**, 1406-1418.
Gallego-Bartolome, J., Minguet, E. G., Marin, J. A., Prat, S., Blazquez, M. A. and Alabadi, D. (2010). Transcriptional diversification and functional conservation between DELLA proteins in Arabidopsis. *Mol. Biol. Evol.* **27**, 1247-1256.
Griffiths, J., Murase, K., Rieu, I., Zentella, R., Zhang, Z. L., Powers, S. J., Gong, F., Phillips, A. L., Hedden, P., Sun, T. P. et al. (2006). Genetic characterization and functional analysis of the GID1 gibberellin receptors in Arabidopsis. *Plant Cell* **18**, 3399-3414.
Guo, A. Y., Zhu, Q. H., Gu, X. C., Ge, S., Yang, J. and Luo, J. C. (2008). Genome-wide identification and evolutionary analysis of the plant specific SBP-box transcription factor family. *Gene* **418**, 1-8.
Hisamatsu, T. and King, R. W. (2008). The nature of floral signals in Arabidopsis. II. Roles for FLOWERING LOCUS T (FT) and gibberellin. *J. Exp. Bot.* **59**, 3821-3819.
Jaeger, K. E. and Wigge, P. A. (2007). FT protein acts as a long-range signal in Arabidopsis. *Curr. Biol.* **17**, 1050-1054.
Jung, J. H., Ju, Y., Seo, P. J., Lee, J. H. and Park, C. M. (2011). The SOC1-SPL module integrates photoperiod and gibberellic acid signals to control flowering time in Arabidopsis. *Plant J.* **69**, 577-588.
Kim, J. J., Lee, J. H., Kim, W., Jung, H. S., Huijser, P. and Ahn, J. H. (2012). The microRNA156-SQUAMOSA PROMOTER BINDING PROTEIN-LIKE3 module regulates ambient temperature-responsive flowering via FLOWERING LOCUS T in Arabidopsis. *Plant Physiol.* **159**, 461-478.
King, K. E., Moritz, T. and Harberd, N. P. (2001). Gibberellins are not required for normal stem growth in Arabidopsis thaliana in the absence of GAI and RGA. *Genetics* **159**, 767-776.
Kobayashi, Y. and Weigel, D. (2007). Move on up, it's time for change-mobile signals controlling photoperiod-dependent flowering. *Genes Dev.* **21**, 2371-2384.
Koornneef, M. and van der Veen, J. (1980). Induction and analysis of gibberellin sensitive mutants in Arabidopsis thaliana (L) Heynh. *Theor. Appl. Genet.* **58**, 257-263.
Koornneef, M., Elgersma, A., Hanhart, C. J., Vanloenenmartinet, E. P., Vanrijn, L. and Zeevaart, J. A. D. (1985). A gibberellin insensitive mutant of Arabidopsis thaliana. *Physiologia Plantarum* **65**, 33-39.
Lang, A. (1957). The effect of gibberellin upon flower formation. *Proc. Natl. Acad. Sci. USA* **43**, 709-717.
Langridge, J. (1957). Effect of day-length and gibberellic acid on the flowering of Arabidopsis. *Nature* **180**, 36-37.
Lee, S., Cheng, H., King, K. E., Wang, W., He, Y., Hussain, A., Lo, J., Harberd, N. P. and Peng, J. (2002). Gibberellin regulates Arabidopsis seed germination via RGL2, a GAI/RGA-like gene whose expression is up-regulated following imbibition. *Genes Dev.* **16**, 646-658.
Liu, L., Liu, C., Hou, X., Xi, W., Shen, L., Tao, Z., Wang, Y. and Yu, H. (2012). FTIP1 is an essential regulator required for florigen transport. *PLoS Biol.* **10**, e1001313.
Mathieu, J., Warthmann, N., Kuttner, F. and Schmid, M. (2007). Export of FT protein from phloem companion cells is sufficient for floral induction in Arabidopsis. *Curr. Biol.* **17**, 1055-1060.
Mathieu, J., Yant, L. J., Murdter, F., Kuttner, F. and Schmid, M. (2009). Repression of flowering by the miR172 target SMZ. *PLoS Biol.* **7**, e1000148.
McGinnis, K. M., Thomas, S. G., Soule, J. D., Strader, L. C., Zale, J. M., Sun, T. P. and Steber, C. M. (2003). The Arabidopsis SLEEPY1 gene encodes a putative F-box subunit of an SCF E3 ubiquitin ligase. *Plant Cell* **15**, 1120-1130.
Michaels, S. D., Himelblau, E., Kim, S. Y., Schomburg, F. M. and Amasino, R. M. (2005). Integration of flowering signals in winter-annual Arabidopsis. *Plant Physiol.* **137**, 149-156.
Moon, J., Suh, S.-S., Lee, H., Choi, K.-R., Hong, C. B., Paek, N.-C., Kim, S.-G. and Lee, I. (2003). The SOC1 MADS-box gene integrates vernalization and gibberellin signals for flowering in Arabidopsis. *Plant J.* **35**, 613-623.
Murase, K., Hirano, Y., Sun, T. P. and Hakoshima, T. (2008). Gibberellin-induced DELLA recognition by the gibberellin receptor GID1. *Nature* **456**, 459-463.
Ogawa, M., Hanada, A., Yamauchi, Y., Kuwahara, A., Kamiya, Y. and Yamaguchi, S. (2003). Gibberellin biosynthesis and response during Arabidopsis seed germination. *Plant Cell* **15**, 1591-1604.
Olszewski, N., Sun, T. P. and Gubler, F. (2002). Gibberellin signaling: biosynthesis, catabolism, and response pathways. *Plant Cell* **14 Suppl.**, S61-S80.
Osnato, M., Castillejo, C., Matias-Hernandez, L. and Pelaz, S. (2012). TEMPRANILLO genes link photoperiod and gibberellin pathways to control flowering in Arabidopsis. *Nat. Commun.* **3**, 808.
Peng, J. R. and Harberd, N. P. (1993). Derivative alleles of the Arabidopsis gibberellin-insensitive (Gai) mutation confer a wild-type phenotype. *Plant Cell* **5**, 351-360.
Peng, J. R., Carol, P., Richards, D. E., King, K. E., Cowling, R. J., Murphy, G. P. and Harberd, N. P. (1997). The Arabidopsis GAI gene defines a signaling pathway that negatively regulates gibberellin responses. *Genes Dev.* **11**, 3194-3205.
Piskurewicz, U., Tureckova, V., Lacombe, E. and Lopez-Molina, L. (2009). Far-red light inhibits germination through DELLA-dependent stimulation of ABA synthesis and ABI3 activity. *EMBO J.* **28**, 2259-2271.
Porri, A., Torti, S., Romera-Branchat, M. and Coupland, G. (2012). Spatially distinct regulatory roles for gibberellins in the promotion of flowering of Arabidopsis under long photoperiods. *Development* **139**, 2198-2209.
Rhoades, M. W., Reinhart, B. J., Lim, L. P., Burge, C. B., Bartel, B. and Bartel, D. P. (2002). Prediction of plant microRNA targets. *Cell* **110**, 513-520.
Rieu, I., Eriksson, S., Powers, S. J., Gong, F., Griffiths, J., Woolley, L., Benlloch, R., Nilsson, O., Thomas, S. G., Hedden, P. et al. (2008). Genetic analysis reveals that C(19)-GA 2-oxidation is a major gibberellin inactivation pathway in Arabidopsis. *Plant Cell* **20**, 2420-2436.
Schmid, M., Uhlenhaut, N. H., Godard, F., Demar, M., Bressan, R., Weigel, D. and Lohmann, J. U. (2003). Dissection of floral induction pathways using global expression analysis. *Development* **130**, 6001-6012.
Schmid, M., Davison, T. S., Henz, S. R., Pape, U. J., Demar, M., Vingron, M., Scholkopf, B., Weigel, D. and Lohmann, J. U. (2005). A gene expression map of *Arabidopsis thaliana* development. *Nat. Genet.* **37**, 501-506.
Schwab, R., Palatnik, J. F., Riester, M., Schommer, C., Schmid, M. and Weigel, D. (2005). Specific effects of microRNAs on the plant transcriptome. *Dev. Cell* **8**, 517-527.
Silverstone, A. L., Mak, P. Y., Martinez, E. C. and Sun, T. P. (1997). The new RGA locus encodes a negative regulator of gibberellin response in Arabidopsis thaliana. *Genetics* **146**, 1087-1099.
Silverstone, A. L., Ciampaglio, C. N. and Sun, T. P. (1998). The Arabidopsis RGA gene encodes a transcriptional regulator repressing the gibberellin signal transduction pathway. *Plant Cell* **10**, 155-169.
Stadler, R. and Sauer, N. (1996). The Arabidopsis thaliana AtSUC2 gene is specifically expressed in companion cells. *Botanica Acta* **109**, 299-306.
Sun, T. P., Goodman, H. M. and Ausubel, F. M. (1992). Cloning the Arabidopsis Ga1 locus by genomic subtraction. *Plant Cell* **4**, 119-128.
Takada, S. and Goto, K. (2003). Terminal flower2, an Arabidopsis homolog of heterochromatin protein1, counteracts the activation of flowering locus T by constans in the vascular tissues of leaves to regulate flowering time. *Plant Cell* **15**, 2856-2865.
Tamaki, S., Matsuo, S., Wong, H. L., Yokoi, S. and Shimamoto, K. (2007). Hd3a protein is a mobile flowering signal in rice. *Science* **316**, 1033-1036.
Taoka, K., Ohki, I., Tsuji, H., Furuita, K., Hayashi, K., Yanase, T., Yamaguchi, M., Nakashima, C., Purwestri, Y. A., Tamaki, S. et al. (2011). 14-3-3 proteins act as intracellular receptors for rice Hd3a florigen. *Nature* **476**, 332-335.
Todesco, M., Rubio-Somoza, I., Paz-Ares, J. and Weigel, D. (2010). A collection of target mimics for comprehensive analysis of microRNA function in Arabidopsis thaliana. *PLoS Genet.* **6**, e1001031.
Turck, F., Fornara, F. and Coupland, G. (2008). Regulation and identity of florigen: FLOWERING LOCUS T moves center stage. *Annu. Rev. Plant Biol.* **59**, 573-594.
Wang, J. W., Czech, B. and Weigel, D. (2009). miR156-regulated SPL transcription factors define an endogenous flowering pathway in Arabidopsis thaliana. *Cell* **138**, 738-749.
Wigge, P. A., Kim, M. C., Jaeger, K. E., Busch, W., Schmid, M., Lohmann, J. U. and Weigel, D. (2005). Integration of spatial and temporal information during floral induction in Arabidopsis. *Science* **309**, 1056-1059.
Willige, B. C., Ghosh, S., Nill, C., Zourelidou, M., Dohmann, E. M., Maier, A. and Schwechheimer, C. (2007). The DELLA domain of GA INSENSITIVE mediates the interaction with the GA INSENSITIVE DWARF1A gibberellin receptor of Arabidopsis. *Plant Cell* **19**, 1209-1220.
Wilson, R. N., Heckman, J. W. and Sommerville, C. R. (1992). Gibberellin is required for flowering in Arabidopsis thaliana under short days. *Plant Physiol.* **100**, 403-408.
Wu, G., Park, M. Y., Conway, S. R., Wang, J. W., Weigel, D. and Poethig, R. S. (2009). The sequential action of miR156 and miR172 regulates developmental timing in Arabidopsis. *Cell* **138**, 750-759.
Yamaguchi, A., Wu, M. F., Yang, L., Wu, G., Poethig, R. S. and Wagner, D. (2009). The MicroRNA-regulated SBP-Box transcription factor SPL3 is a direct upstream activator of LEAFY, FRUITFULL, and APETALA1. *Dev. Cell* **17**, 268-278.
Yant, L., Mathieu, J., Dinh, T. T., Ott, F., Lanz, C., Wollmann, H., Chen, X. and Schmid, M. (2010). Orchestration of the floral transition and floral development in Arabidopsis by the bifunctional transcription factor APETALA2. *Plant Cell* **22**, 2156-2170.
Yoo, S. K., Chung, K. S., Kim, J., Lee, J. H., Hong, S. M., Yoo, S. J., Yoo, S. Y., Lee, J. S. and Ahn, J. H. (2005). CONSTANS activates SUPPRESSOR OF OVEREXPRESSION OF CONSTANS 1 through FLOWERING LOCUS T to promote flowering in Arabidopsis. *Plant Physiol.* **139**, 770-778.

The Plant Cell, Vol. 24: 3320–3332, August 2012, www.plantcell.org

Gibberellin Regulates the *Arabidopsis* Floral Transition through miR156-Targeted SQUAMOSA PROMOTER BINDING–LIKE Transcription Factors[W]

Sha Yu,[a,b,1] Vinicius C. Galvão,[c,1] Yan-Chun Zhang,[a] Daniel Horrer,[c,2] Tian-Qi Zhang,[a,b] Yan-Hong Hao,[d] Yu-Qi Feng,[d] Shui Wang,[a] Markus Schmid,[c] and Jia-Wei Wang[a,3]

[a] National Key Laboratory of Plant Genetics, Institute of Plant Physiology and Ecology, Shanghai Institutes for Biological Sciences, Shanghai 200032, China

[b] Graduate School of Chinese Academy of Sciences, Beijing 100049, China

[c] Department of Molecular Biology, Max Planck Institute for Developmental Biology, Tuebingen D-72076, Germany

[d] Key Laboratory of Analytical Chemistry for Biology and Medicine (Ministry of Education), Department of Chemistry, Wuhan University, Wuhan 430072, China

Gibberellin (GA), a diterpene hormone, plays diverse roles in plant growth and development, including seed germination, stem elongation, and flowering time. Although it is known that GA accelerates flowering through degradation of transcription repressors, DELLAs, the underlying mechanism is poorly understood. We show here that DELLA directly binds to microRNA156 (miR156)-targeted SQUAMOSA PROMOTER BINDING–LIKE (SPL) transcription factors, which promote flowering by activating miR172 and MADS box genes. The interaction between DELLA and SPL interferes with SPL transcriptional activity and consequently delays floral transition through inactivating miR172 in leaves and MADS box genes at shoot apex under long-day conditions or through repressing MADS box genes at the shoot apex under short-day conditions. Our results elucidate the molecular mechanism by which GA controls flowering and provide the missing link between DELLA and MADS box genes.

INTRODUCTION

The shoot apical meristem (SAM) of plants continuously produces lateral organs. Based on the identity and morphological traits of the lateral organs, the life cycle of a plant can be divided into two major phases: vegetative and reproductive. The SAM produces leaves during the vegetative phase, whereas it gives rise to flowers in the reproductive phase (Poethig, 2003). The switch from vegetative to reproductive growth, also known as the floral transition, is controlled by both endogenous and exogenous cues, such as age, temperature, photoperiod, and hormones. Molecular and genetic analyses have revealed that the multiple floral inductive cues are integrated via a set of floral-promoting MADS box genes, including *APETALA1* (*AP1*), *SUPPRESSOR OF OVEREXPRESSION OF CO1* (*SOC1*), *FRUITFULL* (*FUL*), and plant-specific transcription factor *LEAFY* (*LFY*) (Amasino, 2010; Lee and Lee, 2010; Srikanth and Schmid, 2011).

In *Arabidopsis thaliana*, the onset of flowering is accelerated by long-day conditions and delayed by short-day conditions. Seasonal changes in daylength are perceived in leaves and transduced to CONSTANS (CO), which activates the expression of *FLOWERING LOCUS T* (*FT*) in the vascular tissues of the leaves (Samach et al., 2000; An et al., 2004; Kobayashi and Weigel, 2007). The FT protein, as the output of the photoperiodic cue, moves from the leaves to the shoot apex, where it binds to the 14-3-3 protein and the transcription factor FD to activate the expression of MADS box genes (Abe et al., 2005; Wigge et al., 2005; Corbesier et al., 2007; Jaeger and Wigge, 2007; Lin et al., 2007; Mathieu et al., 2007; Taoka et al., 2011). In addition to being activated by CO, the expression of *FT* is negatively regulated by other transcriptional regulators, such as *FLOWERING LOCUS C* (*FLC*), *SHORT VEGETATIVE PHASE* (*SVP*), and *TEMPRANILLO* (*TEM*) (Searle et al., 2006; Castillejo and Pelaz, 2008; Li et al., 2008).

Under noninductive short-day conditions, two pathways play critical roles in flowering: one is dependent on the biosynthesis of the plant hormone gibberellin (GA) (Mutasa-Göttgens and Hedden, 2009); another is mediated by microRNA156 (miR156), which targets a group of transcription factors called SQUAMOSA PROMOTER BINDING–LIKEs (SPLs) (Cardon et al., 1999; Rhoades et al., 2002).

The miR156–SPL interaction constitutes an evolutionarily conserved, endogenous cue for both vegetative phase transition and flowering (Huijser and Schmid, 2011). The age-dependent decrease in miR156 results in an increase in SPLs that promote juvenile to adult phase transition and flowering through activation of miR172, MADS box genes, and *LFY* (Wang et al., 2009; Wu et al., 2009; Yamaguchi et al., 2009). Interestingly, SPLs not

[1] These authors contributed equally to this work.

[2] Current address: Institute of Plant Biology, University of Zürich, CH-8008 Zurich, Switzerland.

[3] Address correspondence to jwwang@sibs.ac.cn.

The author responsible for distribution of materials integral to the findings presented in this article in accordance with the policy described in the Instructions for Authors (www.plantcell.org) is: Jia-Wei Wang (jwwang@sibs.ac.cn).

[W] Online version contains Web-only data.

www.plantcell.org/cgi/doi/10.1105/tpc.112.101014

only act as the upstream activators of the floral-promoting MADS box genes but also serve as their downstream targets. The expression of three miR156-targeted *SPLs*, namely *SPL3*, *SPL4*, and *SPL5*, is highly induced by photoperiod (Schmid et al., 2003). More recently, *SPL3* has been shown to be directly regulated by SOC1 (Jung et al., 2012), and the transcript level of *SPL4* is reduced in the SAM of the *soc1 ful* double mutant (Torti et al., 2012). This interlocking feed-forward loop might contribute to a rapid and irreversible transition from vegetative to reproductive development.

GA is essential for floral induction in short-day conditions, because the plants that harbor the mutation in a GA biosynthetic gene, such as *GA1*, fail to flower (Wilson et al., 1992). In long-day conditions, the effect of GA on flowering is less pronounced. However, the analyses of the GA receptor mutants indicate that GA also plays an important role in flowering in long-day conditions (Griffiths et al., 2006). Recent studies have demonstrated that the GA response is mediated by the ubiquitin-proteasome pathway (Harberd, 2003; Schwechheimer and Willige, 2009). By binding to a nuclear receptor, GIBBERELLIN INSENSITIVE DWARF1 (GID1), GAs regulate gene expression by promoting the degradation of the transcriptional regulator DELLA proteins, including REPRESSOR OF GA1-3 1 (RGA), GA INSENSITIVE (GAI), RGA-LIKE1 (RGL1), and RGL2 (Murase et al., 2008). The degradation of DELLA proteins is mediated by 17 amino acids, called the DELLA motif (Dill et al., 2001). The *Arabidopsis gai*-1 mutant, which carries a deletion of the DELLA motif, is insensitive to GA-induced proteolysis and delays flowering (Peng

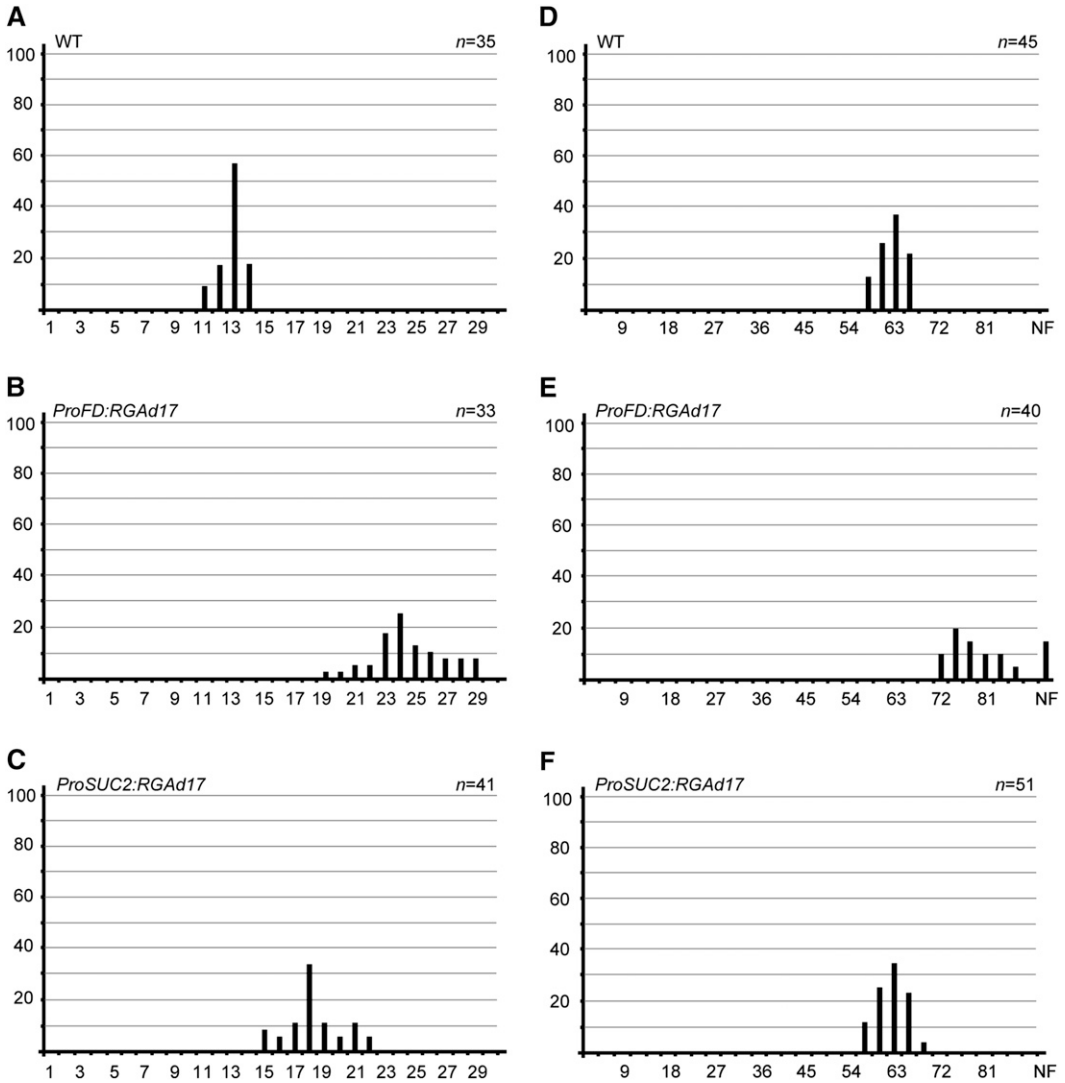

Figure 1. RGA Represses Flowering Both in Leaves and at Shoot Apices.

Flowering time of wild-type (WT), *ProSUC2:RGAd17*, and *ProFD:RGAd17* plants under long-day (**[A]** to **[C]**) or short-day conditions (**[D]** to **[F]**). Flowering frequency of T1 transgenic lines is shown as a histogram, with the *y* axis indicating percentage of plants that flower with a given number of leaves. The *x* axis indicates the number of leaves. NF, never flowering.

et al., 1997; Dill et al., 2001). Although it is known that GA promotes flowering through activating MADS box genes and *LFY* (Blazquez et al., 1998; Moon et al., 2003; Eriksson et al., 2006; Achard et al., 2007), the underlying mechanism is largely elusive. Interestingly, several studies have revealed that DELLA exerts its biological functions through interacting with other transcription factors. For example, DELLA regulates hypocotyl elongation by interacting with PHYTOCHOME INTERACTING FACTORs (PIFs) (de Lucas et al., 2008), contributes to plant defense by interacting with JASMONATE ZIM-DOMAIN (JAZ) (Hou et al., 2010; Yang et al., 2012), and participates in secondary metabolism by interacting with MYC2 (Hong et al., 2012).

Here, we demonstrate the existence of crosstalk between GA and miR156 age pathways. DELLA regulates flowering partially through a direct interaction with miR156-targeted SPL transcription factors. The DELLA–SPL interaction inhibits SPL transcriptional activation of MADS box genes and miR172.

RESULTS

RGA Represses Flowering both in Leaves and at Shoot Apices

Under normal conditions, DELLAs are subjected to GA-induced proteolysis. To reveal the role of GA in flowering, we expressed *RGAd17*, the GA-insensitive form of *RGA* (Dill et al., 2001), from its own upstream regulatory sequence (*ProRGA*:*RGAd17*). *ProRGA*:*RGAd17* phenocopied the GA-deficient mutant, developed small dark green leaves, and delayed flowering (see Supplemental Figure 1 online). Both phloem and SAM have been shown to play critical roles in the floral induction. To understand where RGA regulates flowering, we generated transgenic plants in which *RGAd17* was expressed from either a phloem-specific promoter, *SUC2* (Truernit and Sauer, 1995), or a meristem-specific promoter, *FD* (Abe et al., 2005).

In long-day conditions, the wild-type plants began to flower with ~12 leaves. Both *ProSUC2*:*RGAd17* and *ProFD*:*RGAd17* exhibited a late flowering phenotype, producing more than 20 leaves at the time of bolting (Figures 1A to 1C). In short-day conditions, the flowering of the wild type was greatly delayed, because of the absence of photoperiodic input (Figure 1D). *ProSUC2*:*RGAd17* plants flowered nearly at the same time as the wild type, whereas *ProFD*:*RGAd17* severely blocked the floral transition (Figures 1E and 1F). Six out of 40 T1 *ProFD*:*RGAd17* plants failed to flower. Taken together, these results indicate that RGA regulates flowering via two distinct mechanisms: it suppresses flowering both in the leaves and at the shoot apices in long-day conditions and delays flowering at the shoot apices in short-day conditions.

RGA Represses Flowering through *FT* and miR172 in Leaves under Long-Day Conditions

To assess whether the late flowering phenotype of *ProSUC2*:*RGAd17* in long-day conditions was caused by a low amount of *FT*, we performed quantitative real-time PCR. To facilitate the expression analyses, we chose one representative T3 line of *ProFD*:*RGAd17* and *ProSUC2*:*RGAd17*. Both of these flowered late under long-day or short-day conditions (see Supplemental Figure 2 online).

The leaves of wild-type, *ProFD*:*RGAd17*, and *ProSUC2*:*RGAd17* plants were collected at zeitgeber time 16, when *FT* shows the highest expression level (Kobayashi et al., 1999). Compared with wild-type and *ProFD*:*RGAd17* plants, the transcript level of *FT* was markedly less in *ProSUC2*:*RGAd17* (Figure 2A), indicating that RGA is able to repress *FT* in the vascular tissue of the leaves. In agreement with this finding, it has been shown that GA was able to induce *FT* expression in long-day conditions (Hisamatsu and King, 2008; Porri et al., 2012).

Recent studies have demonstrated that miR172, which is activated by miR156-targeted SPLs, targets *AP2*-like transcription factors that negatively control *FT* expression in leaves (Mathieu et al., 2009; Yant et al., 2010). Overexpression of *SCHLAFMUTZE* (*SMZ*) or *SCHNARCHZAPFEN* (*SNZ*), two miR172-targed AP2-like

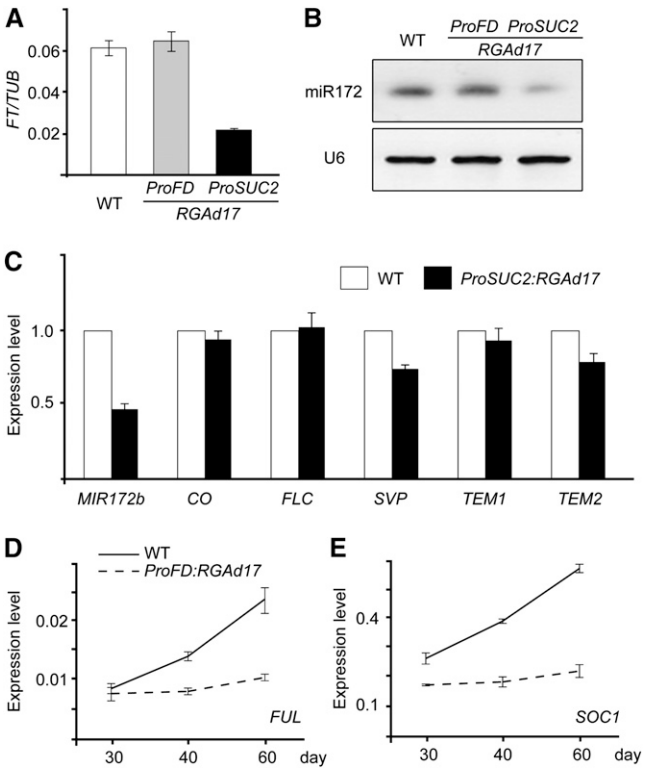

Figure 2. RGA Represses Flowering through *FT* and MADS Box Genes.

(A) Expression of *FT* normalized to β-*TUBULIN-2* (*TUB*) in the wild type (WT) and plants expressing *RGAd17* under the *FD* or *SUC2* promoters.
(B) Expression of miR172 by small RNA gel blot. The amount of U6 was monitored as loading control.
(C) Expression of *MIR172b* and *FT* regulators.
The leaves of wild-type and *ProSUC2*:*RGAd17* plants were used for expression analyses by quantitative real-time–PCR. Plants were grown in long-day conditions for 14 d, and the leaves were harvested at zeitgeber time 16. Expression was normalized to that of β-*TUBULIN-2*. Expression in the wild type was set as 1 for each gene. Two biological replicates were performed with similar results. Error bars represent ±SE (n = 3).
(D) and **(E)** Expression of *FUL* **(D)** and *SOC1* **(E)**. The shoot apices of short-day–grown wild-type and *ProFD*:*RGAd17* plants were harvested at different time points and subjected to quantitative real-time PCR analyses. Error bars represent ±SE (n = 3).

genes, results in a decrease in *FT* expression and a late flowering phenotype in long-day conditions (Mathieu et al., 2009). To test whether DELLA represses *FT* through the SPL-miR172-AP2 module, we analyzed the level of miR172. Compared with wild-type and *ProFD:RGAd17* plants, the level of mature miR172 was much lower in the leaves of *ProSUC2:RGAd17* plants (Figure 2B). Consistent with this, the accumulation of the primary transcript of *MIR172b*, one of the five coding genes of miR172, was accordingly less (Figure 2C).

We then examined the expression of miR172-targeted AP2-like genes, including *AP2*, *SMZ*, *SNZ*, *TARGET OF EAT1* (*TOE1*), *TOE2*, and *TOE3* (Rhoades et al., 2002). The transcript levels of all these genes except those of *SMZ* were not greatly changed (see Supplemental Figure 3 online), which is probably because miR172 controls its targeted genes mainly through the translational inhibition (Aukerman and Sakai, 2003; Chen, 2004; Schwab et al., 2005).

In addition to the miR172-AP2 module, the expression of *FT* is regulated by other transcriptional regulators, such as *CO*, *FLC*, *SVP*, and *TEM* (Searle et al., 2006; Castillejo and Pelaz, 2008; Li et al., 2008). The expression of these genes was not significantly altered in *ProSUC2:RGAd17* in comparison with wild-type and *ProFD:RGAd17* plants (Figure 2C).

To confirm that RGA suppresses flowering through the miR172-AP2-FT module in leaves, we expressed *MIR172a* or *FT* from the *SUC2* promoter in wild-type and *ProSUC2:RGAd17* plants. Both *ProSUC2:FT* and *ProSUC2:MIR172a* flowered earlier than the wild type and were sufficient to suppress the late flowering phenotype of *ProSUC2:RGAd17* under long-day conditions (Figure 3; see Supplemental Figure 4 online).

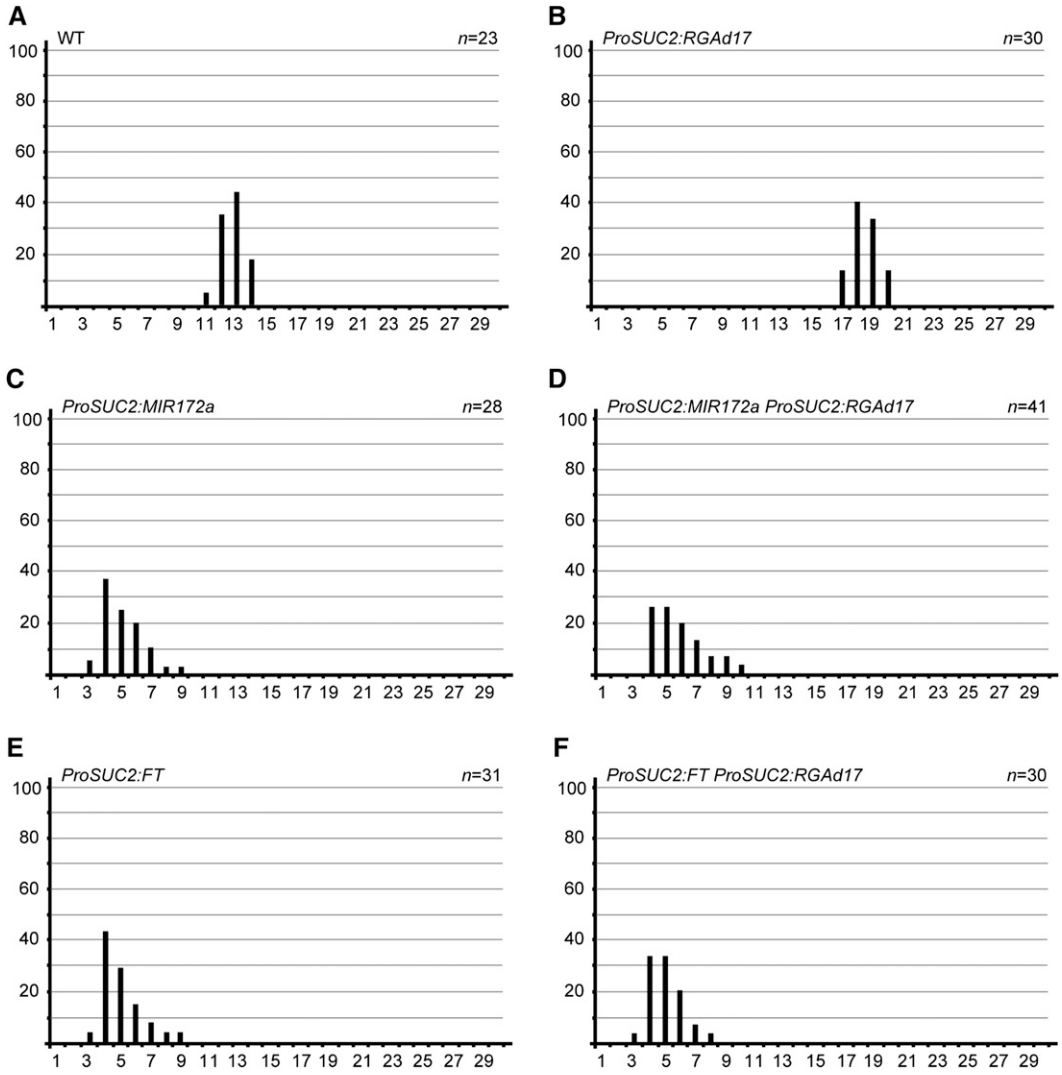

Figure 3. RGA Represses Flowering through miR172-AP2-FT in Leaves.

Flowering time of wild-type (WT), *ProSUC2:RGAd17*, *ProSUC2:MIR172a*, *ProSUC2:FT*, *ProSUC2:RGAd17 ProSUC2:MIR172a*, and *ProSUC2:RGAd17 ProSUC2:FT* plants under long-day conditions. Flowering frequency of T1 transgenic lines is shown as a histogram, with the *y* axis indicating percentage of plants that flower with a given number of leaves. The *x* axis indicates the number of leaves.

RGA Represses Flowering through MADS Box Genes at Shoot Apex

We have shown that *ProFD:RGAd17* delays flowering at the shoot apex under both long-day and short-day conditions (Figure 1). At the shoot apex, the transition from the vegetative to the reproductive phase is executed by the MADS box genes, such as *FUL* and *SOC1*. We extracted the RNAs from the shoot apices of wild-type and *ProFD:RGAd17* plants of different ages in short-day conditions. In 20-d-old seedlings, *FUL* and *SOC1* transcripts accumulated to a similar level in *ProFD:RGAd17* plants as in the wild type (Figures 2D and 2E). As the plants grew, the expression of *FUL* and *SOC1* was gradually increased in the wild type. However, we did not observe the same increase in both genes in *ProFD:RGAd17* plants (Figures 2D and 2E). Under long-day conditions, the expression of *FUL* and *SOC1* was also decreased in *ProFD:RGAd17* in comparison with the wild type (see Supplemental Figure 5 online). These results indicate that RGA blocks the activation of MADS box genes at the shoot apices. Consistent with this, it has been shown that the activation of *SOC1* is attenuated in the *ga1-3* mutant and that overexpression of *SOC1* rescues the flowering phenotype of the *ga1-3* plants in short-day conditions (Moon et al., 2003).

Overexpression of miR156 Reduces the GA Response in Flowering

To understand the genetic interaction between GA and miR156, we studied the GA response of the wild type, the miR156 overexpression line (*Pro35S:MIR156*), in which miR156 was expressed from the *35S* promoter (Schwab et al., 2005), and the miR156 target mimicry line (*Pro35S:MIM156*), which reduces miR156 activity (Franco-Zorrilla et al., 2007; Wang et al., 2008; Todesco et al., 2010). miR156 has been shown to affect leaf initiation rate (Wang et al., 2008); therefore, we measured the flowering time by counting both the number of leaves and the number of days until the plants started to flower.

Under long day conditions, 5-d-old seedlings were sprayed once with 50 μM of gibberellic acid (GA_3). The photoperiod pathway plays a predominant role in long-day conditions; therefore, the flowering response to GA was largely masked (see Supplemental Figure 6 online). We performed the same GA treatment assay under short-day conditions. As shown in Figure 4, application of GA_3 was sufficient to accelerate flowering in the wild-type plants. The number of leaves or days was accordingly decreased by 33 or 19%, respectively (Figures 4A to 4C). By contrast, *Pro35S:MIR156* significantly reduced GA sensitivity. The GA_3-treated *Pro35S:MIR156* plants flowered almost as late as the mock-treated plants (Figures 4A and 4B; see Supplemental Figure 7 online). We only observed 4.4% reduction in the number of days and 3.7% reduction in the number of leaves (Figure 4C).

To understand whether the change in GA response of *Pro35S:MIR156* plants under short-day conditions is caused by a reduction in MADS box genes, we analyzed the expression of *SOC1* and *FUL*. We sprayed 50-d-old short-day–grown plants with 50 μM of GA_3, and their shoot apices were collected after 6 h. The expression of *SOC1* and *FUL* was elevated in the GA_3-treated wild-type plants but not in *Pro35S:MIR156* plants (Figures 4D and 4E).

Expression of *SPL* and *DELLA*

In the *Arabidopsis* genome, miR156-targeted *SPLs* can be divided into two groups, represented by *SPL3* and *SPL9* (Guo et al., 2008; Xing et al., 2010). To determine whether RGA regulates the transcription of *SPL*s, we analyzed the mRNAs of *SPL3* and *SPL9* in wild-type and *Pro35S:RGAd17* plants at different time points in short-day conditions. There was no significant change in *SPL9* transcript levels between wild-type and *Pro35S:RGAd17* plants (Figure 5A). *SPL3* exhibited a distinct expression pattern: its mRNAs gradually increased in wild-type plants but increased less in *Pro35S:RGAd17* plants (Figure 5B). In agreement with this finding, a recent report has shown that *SPL3* level was repressed by paclobutrazol (PAC), a GA biosynthesis inhibitor (Jung et al., 2012). Compared with the wild type, the expression of *DELLAs*, including *RGA*, *RGL1*, and *GAI*, was not greatly altered in either *Pro35S:MIR156* or *Pro35S:MIM156* plants (Figure 5C).

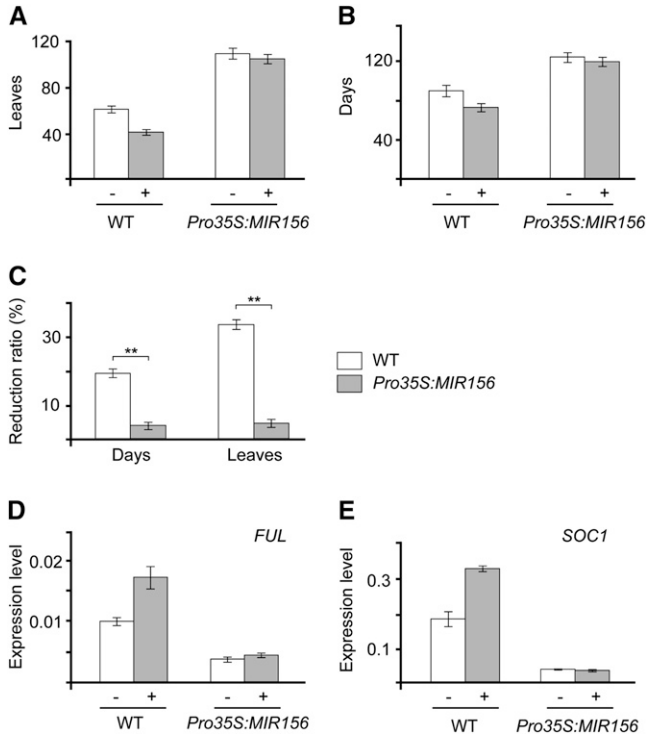

Figure 4. *Pro35S:MIR156* Reduces the GA Response.

(A) and **(B)** GA response of wild-type (WT) and *Pro35S:MIR156* plants under short-day conditions. We sprayed 7-d-old seedlings with 50 μM of GA_3 (+) or ethanol (mock, −). The number of leaves **(A)** and the days to flowering **(B)** were counted.

(C) The reduction ratio in response to GA. The reduction ratio was calculated as (number of leaves/days [mock] − number of leaves/days [GA_3] / number of leaves/days [mock]). **, Student's *t* test, $P < 0.01$.

(D) and **(E)** Expression of *SOC1* and *FUL* in 50-d-old GA_3-treated wild-type and *Pro35S:MIR156* plants in short-day conditions. The shoot apices were collected 6 h after treatment. Error bars represent ±SE ($n = 3$).

Expression of GA Biosynthetic and Catabolic Genes

To understand whether SPL affects GA biosynthesis, we monitored the expression of several GA biosynthetic genes that are highly expressed in leaves, including *GA2-oxidase-1* (*GA2ox-1*), *GA2ox-2*, *GA2ox-6*, *GA3-oxidase-1* (*GA3ox-1*), *GA20-oxidase-1* (*GA20ox-1*), and *GA20ox-2*. GA3ox and GA20ox are responsible for the biosynthesis of bioactive GA_4, whereas GA2ox catalyzes the deactivation of GA_4 by oxidation (Figure 6A) (Eriksson et al., 2006; Yamaguchi, 2008). Compared with the wild type, the expression of the genes encoding *GA2ox-1*, *GA3ox-1*, *GA20ox-1*, and *GA20ox-2* was not changed in either *Pro35S*:*MIR156* or *Pro35S*:*MIM156* plants. The transcript levels of *GA2ox-2* and *GA2ox-6* were moderately decreased in *Pro35S*:*MIM156* and increased in *Pro35S*:*MIR156* plants (Figure 6B). To test whether the change in *GA2ox* expression results in an increase in bioactive GA, we measured the content of GAs, including GA_4, GA_{53}, and GA_{12}. As shown in Figure 6C, *Pro35S*:*MIM156* and *Pro35S*:*MIR156* plants accumulated the same amount of GA_4, one of the bioactive forms of GA, as wild-type plants (Figure 6C).

Genetic Interaction between Age and GA Pathway

To further elucidate the genetic interaction between DELLA and SPL, we overexpressed miR156 in the *della* pentuple mutant (Landsberg *erecta* [L*er*] background) (Feng et al., 2008). The *della* mutant flowered earlier than the wild type (L*er*) under long-day conditions. Overexpression of *MIR156* resulted in a delay of flowering in both the wild type (L*er*) and *della* mutant background (Figures 7A and 7B; see Supplemental Figure 8 online).

SPL9 and SPL15 play a dominant role within miR156-targeted SPLs. The *spl9 spl15* double mutant shows a similar but weak phenotype as the miR156 overexpression line (Schwarz et al., 2008; Wang et al., 2008). Under long-day conditions, *ProSPL9*:*rSPL9* plants, where the miR156-resistant form of *SPL9* (*rSPL9*) was expressed under its own regulatory sequence (Wang et al., 2008), promoted flowering in long-day conditions (Figure 7C). We crossed *ProSPL9*:*rSPL9* to *ProRGA*:*RGAd17*. *ProSPL9*:*rSPL9 ProRGA*:*RGAd17* plants developed the same small dark green leaves as *Pro35S*:*RGAd17* and flowered earlier than *ProRGA*:*RGAd17* (Figure 7C; see Supplemental Figure 9 online). Taken together, our genetic and expression analyses indicate that miR156-targeted SPLs are essential for the floral induction by GAs and that DELLA represses flowering partially through miR156-targeted SPLs.

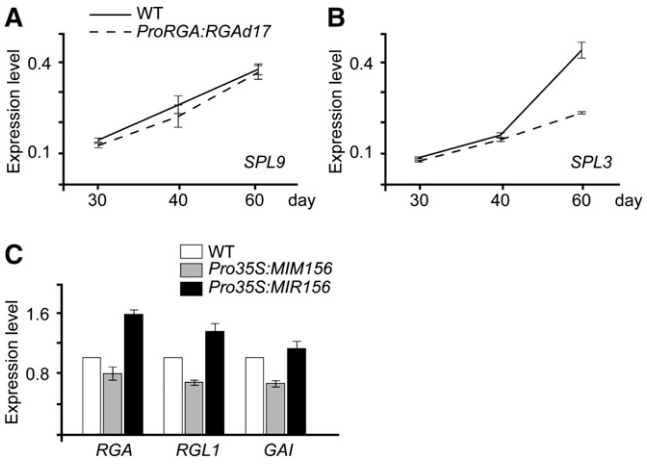

Figure 5. Expression of *SPLs* and *DELLAs*.

(A) and **(B)** Expression of *SPL3* **(A)** and *SPL9* **(B)** in wild-type (WT) and *ProRGA*:*RGAd17* plants. Error bars represent ±SE (n = 3). The shoot apices of short-day–grown plants were harvested at different time points.
(C) Expression of *DELLAs* in wild-type, *Pro35S*:*MIM156*, and *Pro35S*:*MIR156* plants. We used 20-d-old plants grown in short-day conditions for expression analyses. Error bars represent ±SE (n = 3).

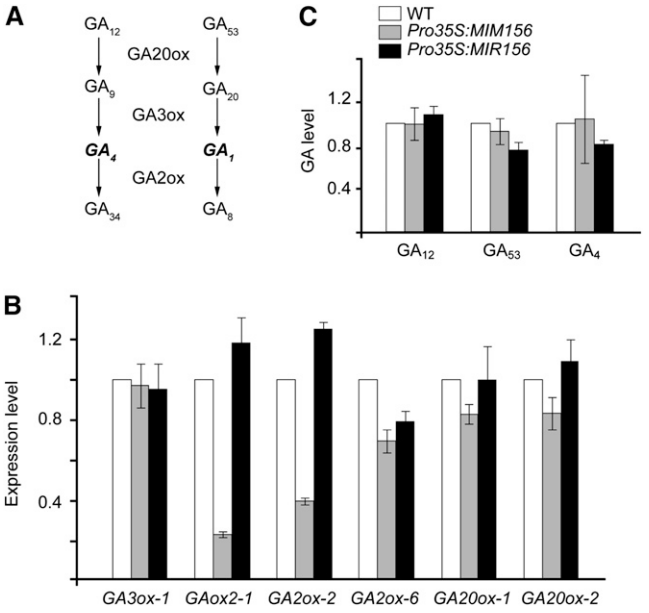

Figure 6. Expression of GA Biosynthetic and Catabolic Genes.

(A) GA biosynthetic and catabolic pathway. The bioactive forms of GA are labeled in bold italic.
(B) Expression of *GA3ox*, *GA20ox*, and *GA2ox* in 15-d-old plants grown in short-day conditions. Error bars represent ±SE (n = 3).
(C) GA measurement. The level in the wild type (WT) was set to 1. Error bars represent ±SE (n = 3).

RGA Binds Directly to SPLs

Because of lack of a canonical DNA binding domain, DELLA regulates plant development and physiology by interacting with other transcription factors, such as PIFs, SCL3, MYC2, and JAZ (de Lucas et al., 2008; Feng et al., 2008; Hou et al., 2010; Zhang et al., 2011; Hong et al., 2012; Yang et al., 2012). Given the fact that both SPLs and RGA regulate the floral transition through the same downstream targets, such as miR172, *FUL*, and *SOC1* (Wang et al., 2009; Wu et al., 2009), we suspected that RGA might directly bind to SPL. To test this hypothesis, we performed yeast two-hybrid assays. A strong interaction was observed when RGA was fused to GAL4 activation domain and SPL9 was fused to GAL4 DNA binding domain (BD) (Figure 8A). This interaction was compromised when the C-terminal domain of SPL9 was deleted

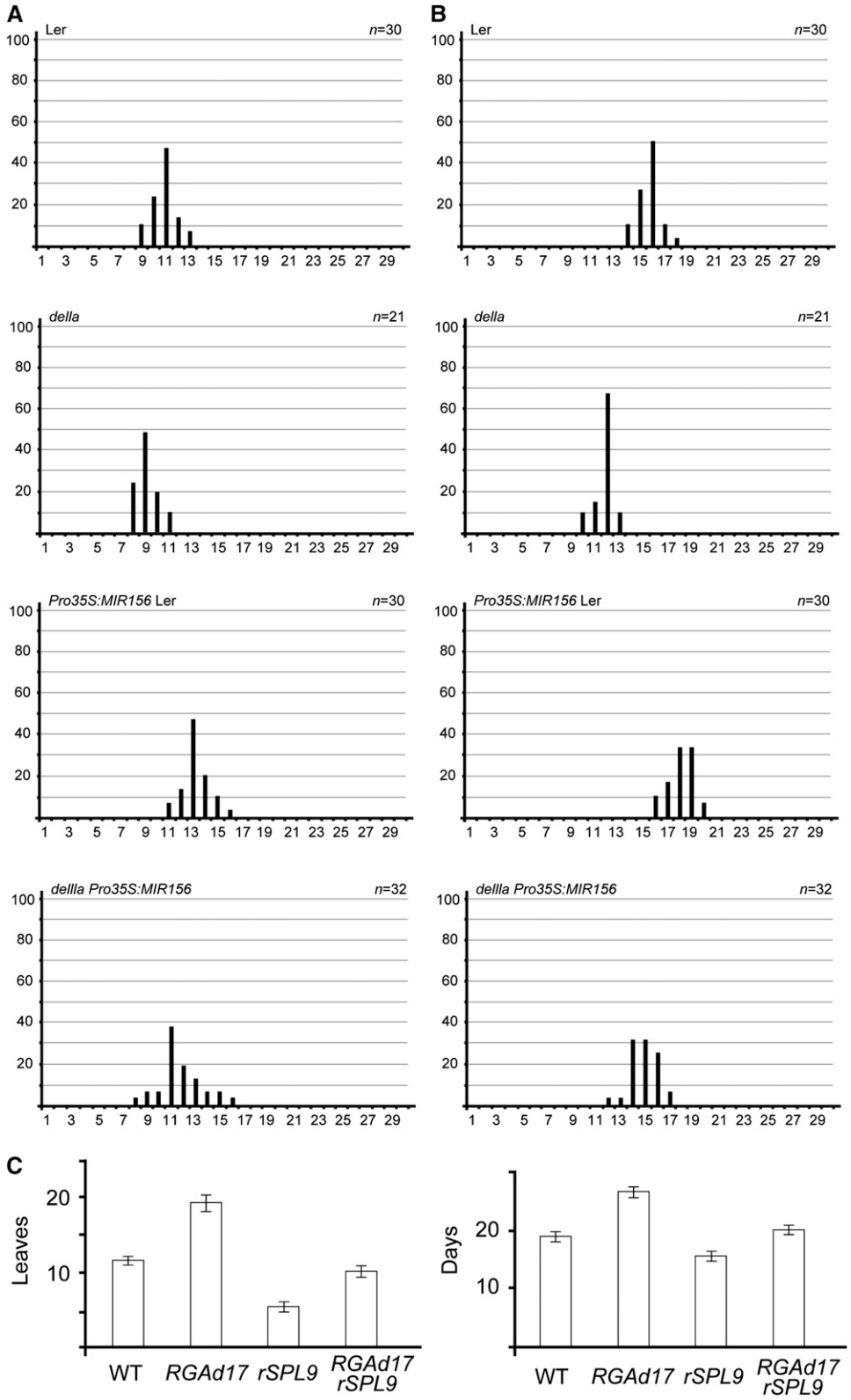

Figure 7. Genetic Interaction between GA and miR156.

(A) and **(B)** Flowering time of *della* and *della Pro35S*:*MIR156* under long-day conditions. The *x* axis indicates the number of leaves **(A)** or the number of days **(B)**. Flowering frequency of *della* homozygous plants and T1 *della Pro35S*:*MIR156* transgenic lines are shown as a histogram, with the *y* axis indicating percentage of plants that flower with a given number of leaves.

(C) Flowering time of wild-type (WT), *ProRGA*::*RGAd17*, *ProSPL9*:*rSPL9*, *and ProRGA*:*RGAd17 ProSPL9*:*rSPL9* plants under long-day conditions. Homozygous *ProRGA*:*RGAd17*, *ProSPL9*:*rSPL9*, and *ProRGA*:*RGAd17 ProSPL9*:*rSPL9* plants were used for flowering time measurements.

(SPL9dC) (Figure 8B). Consistent with this finding, an SPL3 mutant that only harbors the SBP DNA binding domain also failed to interact with RGA (Gandikota et al., 2007) (Figure 8B), suggesting that the C-terminal domain of SPL9 is responsible for its interaction with RGA. Yeast two-hybrid assays further demonstrated the widespread interactions between DELLAs and miR156-targeted SPLs (see Supplemental Figure 10 online).

To examine the interaction between SPL9 and RGA in vivo, we used a bimolecular fluorescence complementation (BiFC) assay in *Nicotiana benthamiana* (Chen et al., 2008). rSPL9 was in-frame fused to the N-terminal half of firefly luciferase (LUC) (rSPL9-LUC^n), and RGA was fused to the C-terminal half of LUC (LUC^c-RGA). Luminescence was detected when the leaves were infiltrated with LUC^c-rSPL9/RGA-LUC^n, but not in those infiltrated with LUC^c-rSPL9/LUC^n or LUC^c/RGA-LUC^n (Figure 8C).

To further confirm the direct interaction between SPL9 and RGA, we performed a coimmunoprecipitation (CoIP) experiment using an *N. benthamiana* transient expression assay. Hemagglutinin (HA)-tagged RGAd17 and green fluorescent protein (GFP)-tagged rSPL9 were transiently expressed in the leaves of *N. benthamiana*. Protein extract of RGAd17-3xHA or RGAd17-3xHA GFP-rSPL9 was immunoprecipitated by the antibody against SPL9. In the immunoprecipitation fraction, RGAd17-3xHA was readily detected in the sample of RGAd17-3xHA GFP-rSPL9 but not in that of RGAd17-3xHA (Figure 8D).

Interaction between DELLA and SPL Interferes with SPL Transcriptional Activity

To understand whether DELLA interferes with SPL transcriptional activity, we examined the expression of *SOC1* and *MIR172b* in *ProSPL9:rSPL9 ProRGA:RGAd17* plants. Consistent with previous reports (Wang et al., 2009; Wu et al., 2009), the expression of *SOC1* and *MIR172b* was upregulated in *ProSPL9:rSPL9* in comparison with the wild type (Figure 9A). If DELLA interferes with the transcriptional activity of SPL, one would expect that the activation of *SOC1* and *MIR172b* by SPL would be compromised by the increased level of RGA. Indeed, the transcripts of *SOC1* and *MIR172b* accumulated to the same level in *ProSPL9:rSPL9 ProRGA:RGAd17* as in the wild type (Figure 9A).

Next, we studied the sensitivity of wild-type, *ProSPL9:rSPL9*, *Pro35S:MIR156* plants to PAC. To verify the treatment efficiency, we examined the expression of *NOD26-LIKE INTRINSIC PROTEIN* (*NOD26*, At4g19030) and *LIPID TRANSFER PROTEIN3* (*LTP3*, At5g59320), both of which are the direct targets of the DELLA-PIF3 module (de Lucas et al., 2008; Feng et al., 2008). After 2 d of the treatment with PAC, the expression of *NOD26* and *LTP3* was greatly decreased (see Supplemental Figure 11 online). We observed a similar reduction in *SOC1* and *MIR172b* transcripts in the PAC-treated wild-type plants, whereas the expression of both genes was insensitive to PAC in *ProSPL9:rSPL9* and *Pro35S:MIR156* plants (Figures 9B and 9C).

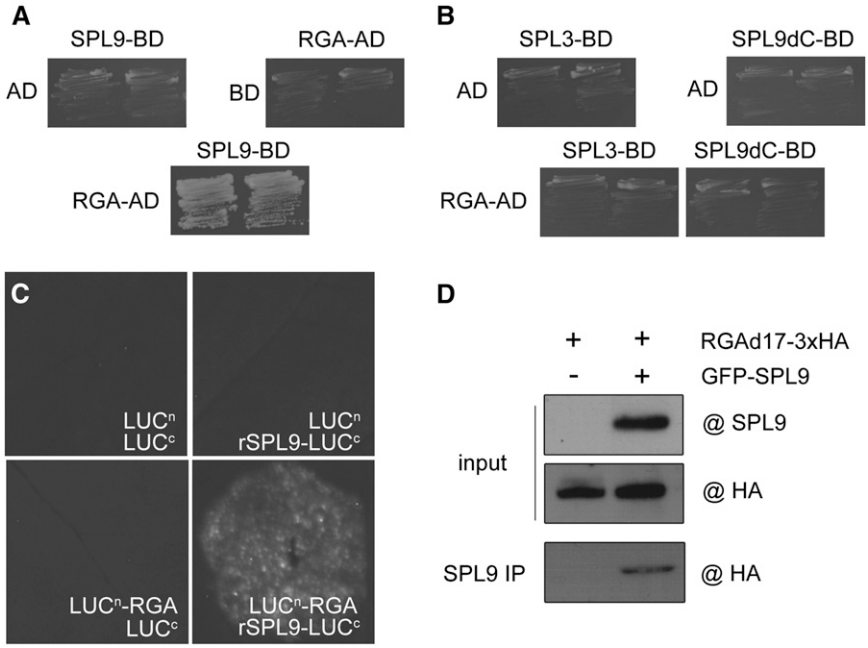

Figure 8. RGA Directly Interacts with SPL9.

(A) Yeast two-hybrid assay. SPL9 was fused to GAL4 BD and RGA to GAL4 activation domain. Interactions were examined on SD/-Leu/-Trp/-His plates supplemented with 15 mM of 3-amino-1,2,4-triazole. Two independent clones are shown.

(B) SPL9 binds to RGA through its C-terminal. SPL3 and SPL9dC were fused to BD.

(C) BiFC analyses. *N. benthamiana* leaves were infiltrated with agrobacteria. The combinations of LUC^c-rSPL9 with LUC^n and LUC^c with RGA-LUC^n were used as negative controls.

(D) CoIP analyses. Soluble protein extract was immunoprecipitated with anti-SPL9 antibody. RGAd17-3xHA proteins were detected by immunoblot with anti-HA antibody.

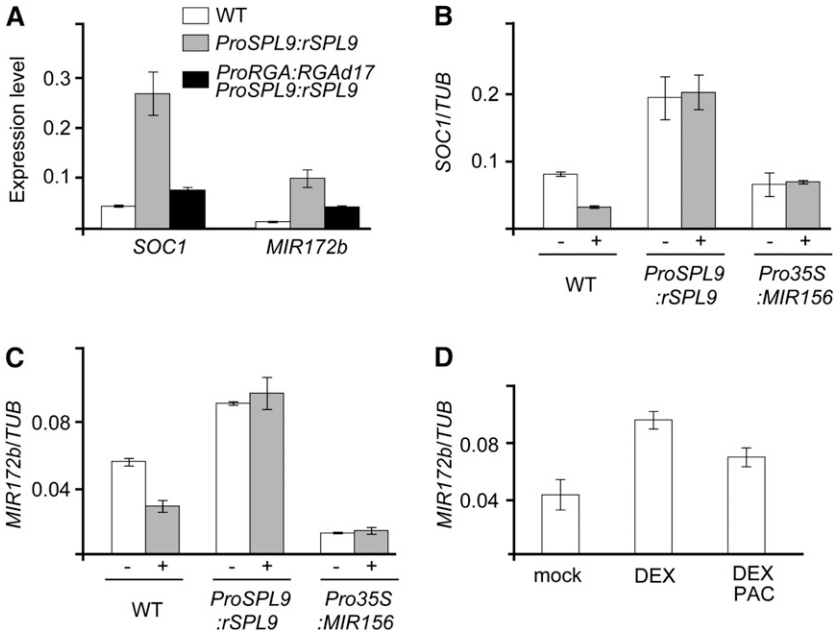

Figure 9. RGA Impairs the Activation of miR172 and *SOC1* through SPL9.

(A) RGA interferes with the activation of *SOC1* and *MIR172b*. We analyzed 30-d-old short-day–grown wild-type (WT), *ProSPL9:rSPL9*, and *ProRGA:RGAd17 ProSPL9:rSPL9* plants. Error bars represent ±SE (n = 3).

(B) and **(C)** Expression of *SOC1* **(B)** and *MIR172b* **(C)** in the PAC-treated wild-type, *ProSPL9:rSPL9*, and *Pro35S:MIR156* plants. We collected 20-d-old short-day–grown seedlings 2 d after treatment. Error bars represent ±SE (n = 3).

(D) Inducible expression of *MIR172b*. We sprayed 10-d-old long-day–grown *ProSPL9:rSPL9-GR* seedlings with DEX, DEX + PAC, or ethanol (mock) for 12 h. Error bars represent ±SE (n = 3).

To further confirm these results, we used an inducible system in which *rSPL9* fused to the rat glucocorticoid receptor (GR) was expressed under its regulatory sequence (*ProSPL9:rSPL9-GR*) (Wang et al., 2009). Treatment with the GR ligand dexamethasone (DEX) resulted in a threefold increase in *MIR172b* transcripts after 12 h (Figure 9D). By contrast, we only observed a 1.5-fold induction in *MIR172b* when 50 μM of PAC was coapplied. Taken together, these observations indicate that a high level of RGA impairs the activation of MADS box genes and miR172 through SPL.

DISCUSSION

Integration of Flowering Time Pathways

Forward and reverse genetics have identified five flowering pathways in *Arabidopsis*, including photoperiod, vernalization, GA, autonomous, and age pathways (Amasino, 2010; Srikanth and Schmid, 2011). Elucidation of how these pathways are integrated is of great importance in understanding how plants flower in response to diverse developmental and environmental signals. Previous results have shown that vernalization and autonomous pathways converge at *FLC*, which encodes a MADS box–type flowering repressor (Simpson, 2004). Interestingly, FLC could also inactivate *FT* in leaves, providing a molecular link between vernalization and photoperiod pathways (Searle et al., 2006).

The age pathway is governed by miR156, the level of which gradually decreases as age increases (Wu and Poethig, 2006; Wang et al., 2009). The integration between photoperiod and age pathway has been extensively studied. In leaves, miR156-SPL acts in parallel with CO, both of which are positive regulators of *FT*. SPL promotes flowering through the miR172-AP2-FT signaling cascade (Mathieu et al., 2009; Wang et al., 2009; Yant et al., 2010). At the shoot apex, the photoperiod pathway acts upstream of SPL. The FT–14-3-3–FD complex activates the expression of *SPL3* and *SPL4* (Jung et al., 2012).

Our results reveal that age and GA pathways are integrated through a direct physical interaction between SPL and DELLA. The binding of DELLA to SPLs attenuates SPL transcriptional activities toward FT and MADS box genes, subsequently blocking the floral transition. It will be interesting to see how the age pathway is integrated into vernalization and autonomous pathways. Indeed, a recent study in *Arabis alpina*, a perennial herb, has revealed that the vernalization response of this perennial plant is age-dependent (Wang et al., 2011). Given the fact that the transcript level of *FLC* is not altered in either *Pro35S:MIM156* or *Pro35S:MIR156 Arabidopsis* plants (Wang et al., 2009), it is unlikely that the age pathway regulates vernalization through modulating *FLC* expression.

DELLA Represses Flowering via Distinct Mechanisms

Our results demonstrate that DELLA regulates flowering via two distinct mechanisms (see Supplemental Figure 12 online). Under short-day conditions, miR156-targeted SPLs play a major role in

flowering by activating MADS box genes at the shoot apex. DELLAs delay the floral transition through interfering with the transcriptional activities of SPL. Under long-day conditions, in addition to a similar role at the shoot apex, the interaction between DELLA and SPL leads to a decrease of miR172. As a result, the increased level of AP2-like transcription factors represses flowering through inactivating *FT*.

Pro35S:MIR156 still responds to GA; therefore, additional flowering targets of DELLA must exist. Indeed, a recent report has shown that simultaneous inactivation of two GA-responsive GATA transcription factors, GATA, NITRATE-INDUCIBLE, CARBON-METABOLISM INVOLVED (GNC) and GNC-LIKE/CYTOKININ-RESPONSIVE GATA FACTOR1 (GNL), partially rescues the flowering defect of *ga1-3* plants in short-day conditions (Richter et al., 2010). Another potential flowering target of DELLA is *SVP*, which encodes a MADS box–type floral repressor. The expression of *SVP* is reduced in the GA-treated plants and increased in a GA-deficient mutant (Li et al., 2008). Moreover, because the level of *SPL3* was decreased in the shoot apices of *ProFD:RGAd17* plants, we could not exclude the possibility that DELLA controls flowering through modulating the expression of *SPLs*. Indeed, a recent study has suggested that GA could promote flowering through SPL3 (Porri et al., 2012).

DELLA and SPL in Vegetative Phase Transition

In addition to a role in flowering, GA is essential for the expression of adult phase traits (Chien and Sussex, 1996; Poethig, 2003). In *Arabidopsis*, juvenile leaves only develop trichomes on their adaxial (upper) sides, whereas adult leaves produce trichomes on their adaxial and abaxial (lower) sides. The GA-deficient mutant delays the appearance of abaxial trichomes, whereas exogenous application of GA accelerates the formation of abaxial trichomes (Telfer et al., 1997).

miR156-targeted SPLs exert a similar role as that of GA in vegetative phase transition. The SPL level is correlated with abaxial trichome production (Wu and Poethig, 2006; Wu et al., 2009). DELLA directly binds to SPL; therefore, it is plausible that GA could promote abaxial trichome formation through releasing the inhibition of DELLA on SPL. However, a recent study has shown that application of GA_3 induces abaxial trichome formation in the miR156 overexpression line, suggesting that GA is able to promote abaxial trichome formation independent of SPL (Schwarz et al., 2008). Whether GA regulates the display of adult vegetative phase traits through SPL awaits further investigation.

METHODS

Plant Materials

Arabidopsis thaliana plants, ecotypes Columbia and L*er*, and *Nicotiana benthamiana* were grown at 21°C in long days (16-h light/8-h dark) or short days (8-h light/16-h dark). *Pro35S:MIR156*, *Pro35S:MIM156*, *ProSPL9:rSPL9*, and *ProSPL9:rSPL9-GR* have been described elsewhere (Wang et al., 2008; Wang et al., 2009). The *della* mutant (N16298) was ordered from the Nottingham Arabidopsis Stock Centre (www.*Arabidopsis*.info). For GA and PAC treatment, 50 μM of GA_3 (Sigma-Aldrich) and 50 μM of PAC were used. For DEX induction experiment, 10 μM of DEX or 10 μM of DEX plus 50 μM of PAC was used.

Constructs and Plant Transformation

For RGAd17 constructs, *RGAd17* was cloned into the binary constructs behind the *RGA*, *SUC2*, or *FD* promoter (Wang et al., 2008). For *FT* and *MIR172a* constructs, the coding region of *FT* and a 410-bp fragment harboring the stem loop of *MIR172a* was PCR amplified and cloned into the binary construct behind the *pSUC2* promoter. For yeast two-hybrid constructs, the cDNAs of *SPL2*, *SPL3*, *SPL9*, *SPL9dC*, *SPL10*, and *SPL11* were PCR amplified and cloned into pGBKT7 or pGADT7 (Clontech). *RGA* was cloned into pGADT7. The pGBKT7 series of *GAI*, *RGA*, *RGL1*, *RGL2*, and *RGL3* constructs was generated as described in de Lucas et al. (2008). BiFC constructs were generated as described elsewhere (Chen et al., 2008; Gou et al., 2011). For CoIP constructs, *RGAd17* and *rSPL9* was PCR amplified and cloned into the binary constructs with 3xHA or GFP tag. The oligonucleotide primers for these constructs are given in Supplemental Table 1 online. The constructs were delivered into *Agrobacterium tumefaciens* strain GV3101 (pMP90) by the freeze-thaw method. Transgenic plants were generated by the floral dipping method (Clough and Bent, 1998) and were screened with 0.05% glufosinate (Basta) on soil or 50 μg/mL of hygromycin on one-half–strength Murashige and Skoog plate.

Flowering Time Measurement and Expression Analyses

Flowering time was measured by counting the total number of leaves (rosette and cauline leaves) and the number of days to flower (when the floral buds are visible).

Total RNA was extracted with TRIzol reagent (Invitrogen). A total of 1 μg of total RNA was DNase I–treated and used for cDNA synthesis with oligo (dT) primer and RevertAid reverse transcriptase (Fermentas). Quantitative real-time–PCR was performed with SYBR-Green PCR Mastermix (TaKaRa), and amplification was real-time monitored on Mastercycler Realplex^2 (Eppendorf). Quantitative real-time PCR primers for *FT*, *MIR172b*, *SOC1*, *FUL*, *SPL3*, *SPL9*, and *TUB* have been described elsewhere (Wang et al., 2009; Wu et al., 2009). Other oligonucleotide primers are given in Supplemental Table 1 online.

Yeast Two-Hybrid Assay

Plasmids were transformed into yeast strain AH109 (Clontech) by the lithium chloride–polyethyleneglycol method according to the manufacturer's manual (Clontech). The transformants were selected on SD/-Leu/-Trp plates. The interactions were tested on SD/-Leu/-Trp/-His plate with 3-amino-1,2,4,-triazole (Figures 8A and 8B) or SD/-Ade/-Leu/-Trp/-His plate (see Supplemental Figure 10B online). At least 10 individual clones were analyzed.

BiFC Analysis

BiFC assays were performed as described in Gou et al. (2011). *A. tumefaciens* was resuspended in infiltration buffer at OD_{600} = 0.8. *Pro35S:P19-HA* (Papp et al., 2003) was coinfiltrated to inhibit gene silencing. A total of 1 mM of luciferin was infiltrated before LUC activity was monitored after 3 d.

CoIP Analysis

SPL9 antibody was raised against the peptide QHQYLNPPWVFKDNC, corresponding to the residues 299 to 312 of SPL9 (Willget Biotech). Agrobacteria-infiltrated *N. benthamiana* leaves were used for CoIP analyses. The soluble proteins were extracted in the extraction buffer (100 mM of Tris-HCl, 5 mM of EDTA, 100 mM of NaCl, 0.2% Nonidet P-40, 1.0% Triton X-100, pH 7.5). Immunoprecipitation was performed with anti-SPL9 antibody. RGAd17-3xHA fusion proteins were detected by immunoblot with anti-HA-horseradish peroxidase antibody (Roche).

GA Measurement

We harvested 2.0-g 40-d-old short-day–grown plants. Extraction and measurement of GA was performed according to a published protocol (Qi et al., 2011).

Accession Numbers

Sequence data from this article can be found in the Arabidopsis Genome Initiative or GenBank/EMBL databases under the following accession numbers: AP2 (At4g36920); CO (At5g15840); FLC (At5g10140); FUL (At5g60910); FT (At1g65480); GAI (At1g14920); GA20ox-1 (At4g25420); GA20ox-2 (At5g51810); GA2ox-1 (At1g78440); GA2ox-2 (At1g30040); GA2ox-6 (At1g02400); GA3ox-1 (At1g15550); MIR172a (At2g28056); MIR172b (At5g04275); RGA (At2g01570); RGL1 (At1g66350); RGL2 (At3g03450); RGL3 (At5g17490); SOC1 (At2g45660); SPL2 (At5g43270); SPL3 (At2g33810); SPL9 (At2g42200); SPL10 (At1g27370); SPL11 (At1g27360); TEM1 (At1g25560); TEM2 (At1g68840); TOE1 (At2g28550); TOE2 (At5g60120); TOE3 (At5g67180); TUB (At5g62690); SMZ (At2g39250); SNZ (At3g54990); SVP (At2g22540).

Supplemental Data

The following materials are available in the online version of this article.

Supplemental Figure 1. Phenotype of *ProRGA*:*RGAd17* Plants under Long-Day Conditions.

Supplemental Figure 2. Flowering Time of the Wild Type, *ProSUC2*:*RGAd17*, and *ProFD*:*RGAd17*.

Supplemental Figure 3. Expression of miR172 Targets.

Supplemental Figure 4. Flowering Time of ProSUC2:MIR172a ProSUC2:RGAd17 and ProSUC2:FT ProSUC2:RGAd17.

Supplemental Figure 5. Expression of *SOC1* and *FUL* at the Shoot Apex in Long-Day Conditions.

Supplemental Figure 6. GA Response in Long-Day Conditions.

Supplemental Figure 7. GA Response of the Wild Type and *Pro35S*:*MIR156* in Short-Day Conditions.

Supplemental Figure 8. Phenotype of *della Pro35S*:*MIR156* Double Mutant.

Supplemental Figure 9. Phenotype of *ProRGA*::*RGAd17 ProSPL9*::*rSPL9* Double Mutant.

Supplemental Figure 10. Interaction between DELLAs and SPLs in Yeast.

Supplemental Figure 11. Expression of *NOD26* and *LTP3* in Response to PAC.

Supplemental Figure 12. A Model for Integration of GA and miR156 Pathway.

Supplemental Table 1. Oligonucleotide Primer Sequences.

ACKNOWLEDGMENTS

We thank Xiao-Ya Chen and Detlef Weigel for their generous scientific support. This article was supported by the National Natural Science Foundation of China (31222029), Recruitment Program of Global Expects (China), and initiation grants from the National Key Laboratory of Plant Genetics, Shanghai Institute of Plant Physiology, and Shanghai Institutes for Biological Sciences to J.-W.W. and by grants from National Nature Science Foundation (91017013 and 31070327) to Q.-Y.F. Work in the Schmid lab on the regulation on flowering time is supported by the Max Planck Institute for Developmental Biology and by grants from the Deutsche Forschungsgemeinschaft.

AUTHOR CONTRIBUTIONS

J.-W.W. and M.S. designed the research. S.Y., V.C.G., Y.-C.Z., D.H., T.-Q.Z., Y.-H.H., and J.-W.W. performed the experiments. Y.-Q.F., M.S., and J.-W.W. analyzed the data. S.W. and J.-W.W. wrote the article.

Received May 29, 2012; revised August 1, 2012; accepted August 6, 2012; published August 31, 2012.

REFERENCES

Abe, M., Kobayashi, Y., Yamamoto, S., Daimon, Y., Yamaguchi, A., Ikeda, Y., Ichinoki, H., Notaguchi, M., Goto, K., and Araki, T. (2005). FD, a bZIP protein mediating signals from the floral pathway integrator FT at the shoot apex. Science **309:** 1052–1056.

Achard, P., Baghour, M., Chapple, A., Hedden, P., Van Der Straeten, D., Genschik, P., Moritz, T., and Harberd, N.P. (2007). The plant stress hormone ethylene controls floral transition via DELLA-dependent regulation of floral meristem-identity genes. Proc. Natl. Acad. Sci. USA **104:** 6484–6489.

Amasino, R. (2010). Seasonal and developmental timing of flowering. Plant J. **61:** 1001–1013.

An, H., Roussot, C., Suárez-López, P., Corbesier, L., Vincent, C., Piñeiro, M., Hepworth, S., Mouradov, A., Justin, S., Turnbull, C., and Coupland, G. (2004). CONSTANS acts in the phloem to regulate a systemic signal that induces photoperiodic flowering of *Arabidopsis*. Development **131:** 3615–3626.

Aukerman, M.J., and Sakai, H. (2003). Regulation of flowering time and floral organ identity by a MicroRNA and its APETALA2-like target genes. Plant Cell **15:** 2730–2741.

Blazquez, M.A., Green, R., Nilsson, O., Sussman, M.R., and Weigel, D. (1998). Gibberellins promote flowering of *Arabidopsis* by activating the LEAFY promoter. Plant Cell **10:** 791–800.

Cardon, G., Höhmann, S., Klein, J., Nettesheim, K., Saedler, H., and Huijser, P. (1999). Molecular characterisation of the *Arabidopsis* SBP-box genes. Gene **237:** 91–104.

Castillejo, C., and Pelaz, S. (2008). The balance between CONSTANS and TEMPRANILLO activities determines FT expression to trigger flowering. Curr. Biol. **18:** 1338–1343.

Chen, H., Zou, Y., Shang, Y., Lin, H., Wang, Y., Cai, R., Tang, X., and Zhou, J.M. (2008). Firefly luciferase complementation imaging assay for protein-protein interactions in plants. Plant Physiol. **146:** 368–376.

Chen, X. (2004). A microRNA as a translational repressor of APETALA2 in *Arabidopsis* flower development. Science **303:** 2022–2025.

Chien, J.C., and Sussex, I.M. (1996). Differential regulation of trichome formation on the adaxial and abaxial leaf surfaces by gibberellins and photoperiod in Arabidopsis thaliana (L.) Heynh. Plant Physiol. **111:** 1321–1328.

Clough, S.J., and Bent, A.F. (1998). Floral dip: A simplified method for *Agrobacterium*-mediated transformation of *Arabidopsis thaliana*. Plant J. **16:** 735–743.

Corbesier, L., Vincent, C., Jang, S., Fornara, F., Fan, Q., Searle, I., Giakountis, A., Farrona, S., Gissot, L., Turnbull, C., and Coupland, G. (2007). FT protein movement contributes to long-distance signaling in floral induction of *Arabidopsis*. Science **316:** 1030–1033.

de Lucas, M., Davière, J.M., Rodríguez-Falcón, M., Pontin, M., Iglesias-Pedraz, J.M., Lorrain, S., Fankhauser, C., Blázquez, M.A., Titarenko, E., and Prat, S. (2008). A molecular framework for light and gibberellin control of cell elongation. Nature **451:** 480–484.

Dill, A., Jung, H.S., and Sun, T.P. (2001). The DELLA motif is essential for gibberellin-induced degradation of RGA. Proc. Natl. Acad. Sci. USA **98:** 14162–14167.

Eriksson, S., Böhlenius, H., Moritz, T., and Nilsson, O. (2006). GA4 is the active gibberellin in the regulation of LEAFY transcription and *Arabidopsis* floral initiation. Plant Cell **18:** 2172–2181.

Feng, S., et al. (2008). Coordinated regulation of *Arabidopsis thaliana* development by light and gibberellins. Nature **451:** 475–479.

Franco-Zorrilla, J.M., Valli, A., Todesco, M., Mateos, I., Puga, M.I., Rubio-Somoza, I., Leyva, A., Weigel, D., García, J.A., and Paz-Ares, J. (2007). Target mimicry provides a new mechanism for regulation of microRNA activity. Nat. Genet. **39:** 1033–1037.

Gandikota, M., Birkenbihl, R.P., Höhmann, S., Cardon, G.H., Saedler, H., and Huijser, P. (2007). The miRNA156/157 recognition element in the 3′ UTR of the *Arabidopsis* SBP box gene SPL3 prevents early flowering by translational inhibition in seedlings. Plant J. **49:** 683–693.

Gou, J.Y., Felippes, F.F., Liu, C.J., Weigel, D., and Wang, J.W. (2011). Negative regulation of anthocyanin biosynthesis in *Arabidopsis* by a miR156-targeted SPL transcription factor. Plant Cell **23:** 1512–1522.

Griffiths, J., Murase, K., Rieu, I., Zentella, R., Zhang, Z.L., Powers, S.J., Gong, F., Phillips, A.L., Hedden, P., Sun, T.P., and Thomas, S.G. (2006). Genetic characterization and functional analysis of the GID1 gibberellin receptors in *Arabidopsis*. Plant Cell **18:** 3399–3414.

Guo, A.Y., Zhu, Q.H., Gu, X., Ge, S., Yang, J., and Luo, J. (2008). Genome-wide identification and evolutionary analysis of the plant specific SBP-box transcription factor family. Gene **418:** 1–8.

Harberd, N.P. (2003). Botany. Relieving DELLA restraint. Science **299:** 1853–1854.

Hisamatsu, T., and King, R.W. (2008). The nature of floral signals in *Arabidopsis*. II. Roles for FLOWERING LOCUS T (FT) and gibberellin. J. Exp. Bot. **59:** 3821–3829.

Hong, G.J., Xue, X.Y., Mao, Y.B., Wang, L.J., and Chen, X.Y. (2012). *Arabidopsis* MYC2 interacts with DELLA proteins in regulating sesquiterpene synthase gene expression. Plant Cell **24:** 2635–2648.

Hou, X., Lee, L.Y., Xia, K., Yan, Y., and Yu, H. (2010). DELLAs modulate jasmonate signaling via competitive binding to JAZs. Dev. Cell **19:** 884–894.

Huijser, P., and Schmid, M. (2011). The control of developmental phase transitions in plants. Development **138:** 4117–4129.

Jaeger, K.E., and Wigge, P.A. (2007). FT protein acts as a long-range signal in *Arabidopsis*. Curr. Biol. **17:** 1050–1054.

Jung, J.H., Ju, Y., Seo, P.J., Lee, J.H., and Park, C.M. (2012). The SOC1-SPL module integrates photoperiod and gibberellic acid signals to control flowering time in *Arabidopsis*. Plant J. **69:** 577–588.

Kobayashi, Y., Kaya, H., Goto, K., Iwabuchi, M., and Araki, T. (1999). A pair of related genes with antagonistic roles in mediating flowering signals. Science **286:** 1960–1962.

Kobayashi, Y., and Weigel, D. (2007). Move on up, it's time for change—mobile signals controlling photoperiod-dependent flowering. Genes Dev. **21:** 2371–2384.

Lee, J., and Lee, I. (2010). Regulation and function of SOC1, a flowering pathway integrator. J. Exp. Bot. **61:** 2247–2254.

Li, D., Liu, C., Shen, L., Wu, Y., Chen, H., Robertson, M., Helliwell, C.A., Ito, T., Meyerowitz, E., and Yu, H. (2008). A repressor complex governs the integration of flowering signals in *Arabidopsis*. Dev. Cell **15:** 110–120.

Lin, M.K., Belanger, H., Lee, Y.J., Varkonyi-Gasic, E., Taoka, K., Miura, E., Xoconostle-Cázares, B., Gendler, K., Jorgensen, R.A., Phinney, B., Lough, T.J., and Lucas, W.J. (2007). FLOWERING LOCUS T protein may act as the long-distance florigenic signal in the cucurbits. Plant Cell **19:** 1488–1506.

Mathieu, J., Warthmann, N., Küttner, F., and Schmid, M. (2007). Export of FT protein from phloem companion cells is sufficient for floral induction in *Arabidopsis*. Curr. Biol. **17:** 1055–1060.

Mathieu, J., Yant, L.J., Mürdter, F., Küttner, F., and Schmid, M. (2009). Repression of flowering by the miR172 target SMZ. PLoS Biol. **7:** e1000148.

Moon, J., Suh, S.S., Lee, H., Choi, K.R., Hong, C.B., Paek, N.C., Kim, S.G., and Lee, I. (2003). The SOC1 MADS-box gene integrates vernalization and gibberellin signals for flowering in *Arabidopsis*. Plant J. **35:** 613–623.

Murase, K., Hirano, Y., Sun, T.P., and Hakoshima, T. (2008). Gibberellin-induced DELLA recognition by the gibberellin receptor GID1. Nature **456:** 459–463.

Mutasa-Göttgens, E., and Hedden, P. (2009). Gibberellin as a factor in floral regulatory networks. J. Exp. Bot. **60:** 1979–1989.

Papp, I., Mette, M.F., Aufsatz, W., Daxinger, L., Ray, A., van der Winden, J., Matzke, M., and Matzke, A.J. (2003). Evidence for nuclear processing of plant micro RNA and short interfering RNA precursors. Plant Physiol. **132:** 1382–1390.

Peng, J., Carol, P., Richards, D.E., King, K.E., Cowling, R.J., Murphy, G.P., and Harberd, N.P. (1997). The *Arabidopsis* GAI gene defines a signaling pathway that negatively regulates gibberellin responses. Genes Dev. **11:** 3194–3205.

Poethig, R.S. (2003). Phase change and the regulation of developmental timing in plants. Science **301:** 334–336.

Porri, A., Torti, S., Romera-Branchat, M., and Coupland, G. (2012). Spatially distinct regulatory roles for gibberellins in the promotion of flowering of *Arabidopsis* under long photoperiods. Development **139:** 2198–2209.

Qi, W., Sun, F., Wang, Q., Chen, M., Huang, Y., Feng, Y.Q., Luo, X., and Yang, J. (2011). Rice ethylene-response AP2/ERF factor OsEATB restricts internode elongation by down-regulating a gibberellin biosynthetic gene. Plant Physiol. **157:** 216–228.

Rhoades, M.W., Reinhart, B.J., Lim, L.P., Burge, C.B., Bartel, B., and Bartel, D.P. (2002). Prediction of plant microRNA targets. Cell **110:** 513–520.

Richter, R., Behringer, C., Müller, I.K., and Schwechheimer, C. (2010). The GATA-type transcription factors GNC and GNL/CGA1 repress gibberellin signaling downstream from DELLA proteins and PHYTOCHROME-INTERACTING FACTORS. Genes Dev. **24:** 2093–2104.

Samach, A., Onouchi, H., Gold, S.E., Ditta, G.S., Schwarz-Sommer, Z., Yanofsky, M.F., and Coupland, G. (2000). Distinct roles of CONSTANS target genes in reproductive development of *Arabidopsis*. Science **288:** 1613–1616.

Schmid, M., Uhlenhaut, N.H., Godard, F., Demar, M., Bressan, R., Weigel, D., and Lohmann, J.U. (2003). Dissection of floral induction pathways using global expression analysis. Development **130:** 6001–6012.

Schwab, R., Palatnik, J.F., Riester, M., Schommer, C., Schmid, M., and Weigel, D. (2005). Specific effects of microRNAs on the plant transcriptome. Dev. Cell **8:** 517–527.

Schwarz, S., Grande, A.V., Bujdoso, N., Saedler, H., and Huijser, P. (2008). The microRNA regulated SBP-box genes SPL9 and SPL15 control shoot maturation in *Arabidopsis*. Plant Mol. Biol. **67:** 183–195.

Schwechheimer, C., and Willige, B.C. (2009). Shedding light on gibberellic acid signalling. Curr. Opin. Plant Biol. **12:** 57–62.

Searle, I., He, Y., Turck, F., Vincent, C., Fornara, F., Kröber, S., Amasino, R.A., and Coupland, G. (2006). The transcription factor FLC confers a flowering response to vernalization by repressing meristem competence and systemic signaling in *Arabidopsis*. Genes Dev. **20:** 898–912.

Simpson, G.G. (2004). The autonomous pathway: Epigenetic and post-transcriptional gene regulation in the control of *Arabidopsis* flowering time. Curr. Opin. Plant Biol. **7:** 570–574.

Srikanth, A., and Schmid, M. (2011). Regulation of flowering time: All roads lead to Rome. Cell. Mol. Life Sci. **68:** 2013–2037.

Taoka, K., et al. (2011). 14-3-3 proteins act as intracellular receptors for rice Hd3a florigen. Nature **476:** 332–335.

Telfer, A., Bollman, K.M., and Poethig, R.S. (1997). Phase change and the regulation of trichome distribution in *Arabidopsis thaliana*. Development **124:** 645–654.

Todesco, M., Rubio-Somoza, I., Paz-Ares, J., and Weigel, D. (2010). A collection of target mimics for comprehensive analysis of microRNA function in *Arabidopsis thaliana*. PLoS Genet. **6:** e1001031.

Torti, S., Fornara, F., Vincent, C., Andrés, F., Nordström, K., Göbel, U., Knoll, D., Schoof, H., and Coupland, G. (2012). Analysis of the *Arabidopsis* shoot meristem transcriptome during floral transition identifies distinct regulatory patterns and a leucine-rich repeat protein that promotes flowering. Plant Cell **24:** 444–462.

Truernit, E., and Sauer, N. (1995). The promoter of the *Arabidopsis thaliana* SUC2 sucrose-H+ symporter gene directs expression of beta-glucuronidase to the phloem: Evidence for phloem loading and unloading by SUC2. Planta **196:** 564–570.

Wang, J.W., Czech, B., and Weigel, D. (2009). miR156-regulated SPL transcription factors define an endogenous flowering pathway in *Arabidopsis thaliana*. Cell **138:** 738–749.

Wang, J.W., Schwab, R., Czech, B., Mica, E., and Weigel, D. (2008). Dual effects of miR156-targeted SPL genes and CYP78A5/KLUH on plastochron length and organ size in *Arabidopsis thaliana*. Plant Cell **20:** 1231–1243.

Wang, R., Albani, M.C., Vincent, C., Bergonzi, S., Luan, M., Bai, Y., Kiefer, C., Castillo, R., and Coupland, G. (2011). Aa TFL1 confers an age-dependent response to vernalization in perennial *Arabis alpina*. Plant Cell **23:** 1307–1321.

Wigge, P.A., Kim, M.C., Jaeger, K.E., Busch, W., Schmid, M., Lohmann, J.U., and Weigel, D. (2005). Integration of spatial and temporal information during floral induction in *Arabidopsis*. Science **309:** 1056–1059.

Wilson, R.N., Heckman, J.W., and Somerville, C.R. (1992). Gibberellin is required for flowering in Arabidopsis thaliana under short days. Plant Physiol. **100:** 403–408.

Wu, G., Park, M.Y., Conway, S.R., Wang, J.W., Weigel, D., and Poethig, R.S. (2009). The sequential action of miR156 and miR172 regulates developmental timing in *Arabidopsis*. Cell **138:** 750–759.

Wu, G., and Poethig, R.S. (2006). Temporal regulation of shoot development in *Arabidopsis thaliana* by miR156 and its target SPL3. Development **133:** 3539–3547.

Xing, S., Salinas, M., Höhmann, S., Berndtgen, R., and Huijser, P. (2010). miR156-targeted and nontargeted SBP-box transcription factors act in concert to secure male fertility in *Arabidopsis*. Plant Cell **22:** 3935–3950.

Yamaguchi, A., Wu, M.F., Yang, L., Wu, G., Poethig, R.S., and Wagner, D. (2009). The microRNA-regulated SBP-Box transcription factor SPL3 is a direct upstream activator of LEAFY, FRUITFULL, and APETALA1. Dev. Cell **17:** 268–278.

Yamaguchi, S. (2008). Gibberellin metabolism and its regulation. Annu. Rev. Plant Biol. **59:** 225–251.

Yang, D.L., et al. (2012). Plant hormone jasmonate prioritizes defense over growth by interfering with gibberellin signaling cascade. Proc. Natl. Acad. Sci. USA **109:** E1192–E1200.

Yant, L., Mathieu, J., Dinh, T.T., Ott, F., Lanz, C., Wollmann, H., Chen, X., and Schmid, M. (2010). Orchestration of the floral transition and floral development in *Arabidopsis* by the bifunctional transcription factor APETALA2. Plant Cell **22:** 2156–2170.

Zhang, Z.L., Ogawa, M., Fleet, C.M., Zentella, R., Hu, J., Heo, J.O., Lim, J., Kamiya, Y., Yamaguchi, S., and Sun, T.P. (2011). Scarecrow-like 3 promotes gibberellin signaling by antagonizing master growth repressor DELLA in *Arabidopsis*. Proc. Natl. Acad. Sci. USA **108:** 2160–2165.